ARKIV FÖR KEMI Band 17 nr 10

Communicated 26 October 1960 by Arne Ölander and Ole Lamm

Some measurements on energy loss of 2.8 MeV electrons in light elements and chemical compounds

By Torbjörn Westermark

With 13 figures in the text

SUMMARY

Measurements have been made of the average energy loss, most probable energy loss and straggling properties of 2.8 MeV electrons in the elements Li, Be, $C_{graphite}$, Na, Al, Si and K and the chemical compounds LiH, H_2O, D_2O, benzene, toluene, heptane and methanol. Techniques and comparisons with theory are described. It is concluded from the studies on the elements that the theory for stopping power and the experiments agree within one or two percent. A systematic trend indicates some uncertainty with regard to the inclusion of radiation losses in the theoretical estimates in the narrow geometry used. It has proved possible to approximate the low-energy tail of the energy loss curve by means of an exponential function. Straggling leads to broader distributions than those predicted by theory. Reactor graphite shows a large straggling, apparently due to its porosity.

The results for organic liquids and water agree within 1.5 % with the theoretical calculations. Light and heavy water show the same energy loss per length unit within 0.5 %, as expected theoretically. Much work was performed on lithium hydride. The absorbers composed of this substance were produced in a hydraulic press giving 6 tons/cm² and were handled in a dry atmosphere. The final figure for the stopping power relative to beryllium was 1.176 ± 0.011. This has been compared with Brandt's theory for the stopping power of LiH. Using a certain assumption for calculating the density correction, a value for the mean excitation potential $I_{LiH} = 42.5 \pm 4.5$ eV has been obtained. This is near Brandt's estimate for the collective excitation model and X-ray data and quantum mechanical calculations of the electron distribution in solid LiH.

I. Introduction

The study of the energy loss and range properties of fast charged particles is of considerable interest both from a fundamental and an applied point of view. The theory has been developed to a considerable extent (Bohr, Bethe, Bloch and others, see [1]) and has been subject to many investigations. However, very few studies have been devoted to the energy loss properties of electrons of a few MeV, in spite of the fact that excessive corrections due to bremsstrahlung and scattering effects are thereby avoided. There have, in particular, been very few experimental studies devoted to the properties describing the *material* in relation to the fast electrons.

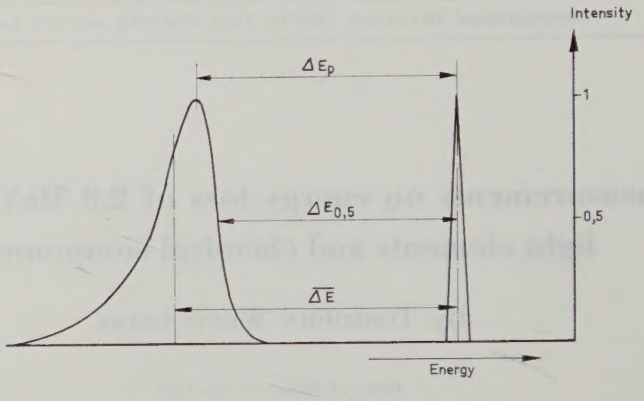

Fig. 1. General picture of various energy loss properties.

Theory predicts very interesting effects concerning the energy loss due to chemical valence effects. Early statements about such effects [2] in the absorption of beta radiation turned out later to be largely in error [3]. The changes due to the chemical valence have been found to be very small and so very precise experiments are needed in general. These changes should be largest for light elements and compounds and thus substances with as large a fraction of valency electrons as possible should be selected for the least difficult approach. *Lithium hydride* is the most outstanding case in this connection among the condensed substances [4].

The present paper will describe the first part of a study of material properties related to the loss of energy of electrons in the MeV region. It will be limited to a fixed energy, 2.8 MeV, to a test of the stopping theory for light elements and to an investigation of the chemical valence effects by means of the study of lithium hydride and some other chemical compounds and light elements. The electron source was a 5 MeV betatron and the energy-resolving device a double-focusing magnetic spectrometer of 90° sector type. They are described elsewhere [1, 5, 8], as is also the equipment for recording the energy loss spectra of one substance relative to a standard [6].

II. Basis of the comparison of the experiments with theory

1. *Scope*

Energy loss studies, such as those to be reported below, yield the following primary information: the average energy loss, $\Delta\bar{E}$; the most probable energy loss, ΔE_p; and the half-width of the energy loss curve, Γ. These properties are obtained on a relative scale, i.e. the energy loss of one substance under study relative to that of the standard. The energy loss of the standard is either obtained from independent measurements or by relying upon theory. The latter course has been adopted here. Similarly the straggling parameter, Γ, is obtained relative to either $\Delta\bar{E}$ or ΔE_p. Fig. 1 gives an idea of the magnitudes of these properties.

In addition to these properties, the energy loss at the upper half-intensity point, as introduced by Goldwasser, Mills and Hanson [7], has been measured. Further data describing an experiment are the actual primary energy and its energy distribution

as recorded by the instruments (half-width of the curve). In addition, the material under study may have a cover of some thin protecting film or cell windows in the case of liquids. The substance under investigation is, of course, characterized by its atomic number and atomic weight, density, state of aggregation, chemical state, purity, mass per unit area, porosity, etc.

The comparison of the experimental results thus obtained with theory is of great importance since any detectable deviations from theory would be of great interest. The comparison with theory is mainly straightforward but, in some respects, certain alternative interpretations do actually exist. The theory itself has been reviewed by several authors [8–13] fairly recently and need not be repeated here. In the following we shall briefly state the theory which has been used for comparison with experiments.

2. *Energy loss expression*

As is well known, a fast charged particle transfers momentum to the orbital electrons of the matter traversed. The momentum transfer to nuclei is negligible in this connection. The theory involves the summing of all kinds of energy transfers ranging from electronic excitation and ionization up to maximum energy transfer which is very large for electrons (half the kinetic energy). The quantum mechanical theory, due to Bethe [10], is considered to be the most exact one. In the case of electrons, relativistic effects, spin and indistinguishability considerations have to be taken into account (Møller). The exact expression for the average energy loss, according to this theory, gives for negative electrons [13]

$$-\frac{1}{\varrho}\frac{d\bar{E}}{dx}=a\left[\ln\frac{m_0 c^2\beta^2 E_0}{2I^2(1-\beta^2)}-(2\sqrt{1-\beta^2}-1+\beta^2)\ln 2+1-\beta^2+\frac{1}{8}(1-\sqrt{1-\beta^2})^2-\delta\right], \tag{1}$$

where

$$a=\frac{2\pi N_A e^4\cdot Z}{m_0 c^2\beta^2 A}. \tag{1 a}$$

In Sternheimers' notation $a=A/\beta^2$. Sternheimers' A will be avoided in the following to avoid confusion with the atomic weight A. The other notations have their usual meaning:

$\frac{d\bar{E}}{dx}$, average energy loss in MeV per cm length of matter;

$\frac{d\bar{E}}{dm_s}$, average energy loss per unit mass per unit area in

$$\frac{\text{MeV}\cdot\text{cm}^2}{g}\quad(\varrho\,dx=m_s)$$

(this property is often called the mass stopping power);

ϱ, density in g/cm^3;
m_0c^2, rest mass energy of the electron;
β, particle velocity in fraction of light velocity;
E_0, kinetic energy of electron;

δ, density correction (see below);
I, mean excitation potential of the absorber material (eV);
N_A, Avogadro–Loschmidts number;
e, electronic charge; and
Z, atomic number of the absorber.

For a given electron energy E_0, (1) reduces to

$$-\frac{d\bar{E}}{dm_s} = a\,(B - 2\ln I - \delta). \tag{2}$$

Besides the Z/A factor in (1a), the mean excitation potential and the density correction are the only properties describing the matter traversed at a fixed energy. The experiments to be described will apply for a certain fixed energy.

The experiments were performed at a mean energy of 2.8 MeV and accordingly the numerical calculations based on (1) will apply to this energy. Table 1 summarizes the numerical data used. It includes data useful for the calculation of the density effect and other corrections.

Table 1. Numerical data for 2.8 MeV electrons.

(p is the momentum, m the mass at E.)

$\beta^2 = 0.9762$	$\ln\frac{p}{m_0 c} = 1.857$
$\frac{m}{m_0} = 6.480$	For 2.8 Mev, B in (2) is 30.92

It should be noted that the average energy loss as given by (1) has a flat minimum (roughly at 2 m_0c^2) and then slowly rises again (due to the relativistic term). Fig. 2 gives some examples of this behaviour. The δ-correction, to be discussed below, contributes to a reduction of the relativistic rise. Experimentally, the energy loss minimum means that an energy loss experiment in this region is rather insensitive to the primary energy of the particle studied. The energy loss itself covers a finite energy region but the slow change with energy means that, provided the loss is not too large, the result can be assigned to the mean value of the primary energy and the energy loss spectrum to a very good approximation. For relative stopping powers related to some standard,

i.e. where
$$\bar{s} = \left(\frac{\Delta\bar{E}}{m_s}\right)_{\text{sub}} \Big/ \left(\frac{\Delta\bar{E}}{m_s}\right)_{\text{stand}}, \tag{3}$$

this is also true (and even more insensitive). Minor changes in E_0 due to the absorber thickness need therefore seldom be considered.

Another effect of the ionization minimum is the relative insensitivity with respect to energy of the response of detectors such as the ionization chamber used here.

3. *The average excitation potential*

The average excitation potential I present in the energy loss formula (1) is the main property describing the material in its relation to the stopping of charged particles. From Bethe's theory, I is obtained from

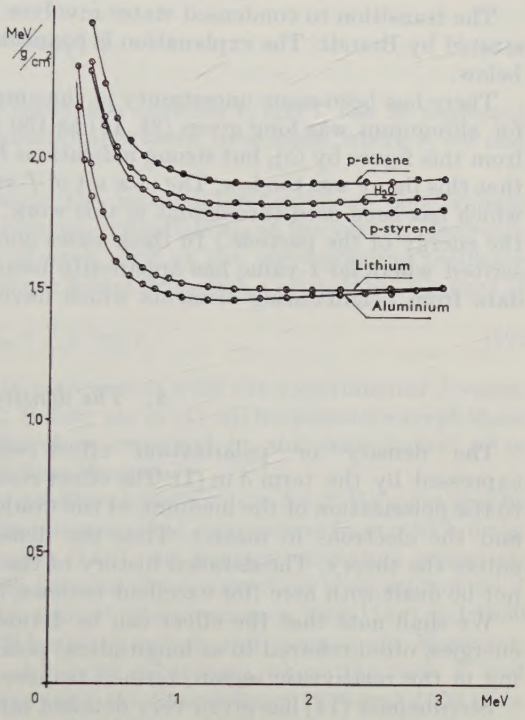

Fig. 2. $d\bar{E}/dm_g$ as a function of electron energy as compiled from Nelms' tables [13]. Measurements presented in this paper have been made near 2.8 MeV.

$$\ln I = \Sigma f_i \ln h\nu_i, \tag{4}$$

where $\Sigma f_i = 1$.

f_i are the oscillator strengths corresponding to the transition of $h\nu_i$. The summing should take into account all transition possibilities.

(4) can be nearly exactly evaluated for gases such as H, He and H_2 and perhaps other light elements and compounds for which all excitation possibilities are known either from exact theory or from optical transition data. In principle, (4) in conjunction with (1) can be regarded as an exact expression, but difficulties arise when heavier elements than those mentioned or condensed states and chemical compounds are considered. Approximate estimates of (4) have been made using ionization potential energies including X-ray data for the inner shells but this "optical approach" (in the words of Brandt [4]) has to be supported by empirical determinations of I.

Statistical models of the atoms have been used with some success ("the statistical approach") [4]. Bloch [20] showed that I should be proportional to the atomic number

$$I = I_0 \cdot Z, \tag{5}$$

I_0 being of the order of the Rydberg energy (13.5 eV). Determinations of I by means of fast protons and other particles showed that I_0 decreased with Z [16]. Brandt showed this trend to be understandable by using the more refined Thomas–Fermi–Dirac model [15], which yields

$$I = K_0 \cdot Z(1 + k_0 Z^{-2/3}). \tag{5a}$$

The transition to condensed states involves large changes in I as has been demonstrated by Brandt. The explanation is connected with the "density" effect described below.

There has been some uncertainty in the empirical determination of I. The I value for aluminium was long given [21, 16] as 150 eV and other I-values were calculated from this figure by (5), but strong indications from several groups [17, 18, 19] showed that this figure was too low. The new set of I-values is based on 166 eV for aluminium, which has been used throughout in this work. (The new I-values are independent of the energy of the particle.) In those cases encountered in the experiments to be described where no I-value has apparently been published, we have used interpolated data from neighbouring elements which have been studied by using (5).

4. *The density effect*

The "density" or "polarization" effect reduces the energy loss in a way that is expressed by the term δ in (1). The effect results as is known from the shielding, due to the polarization of the medium, of the Coulomb force between the charged particle and the electrons in matter. Thus the density and polarizability of the medium enters the theory. The detailed history of the investigation of the density effect will not be dealt with here (for excellent reviews, see [11, 8]).

We shall note that the effect can be divided into two effects, one present at low energies, often referred to as longitudinal polarization, and the other rapidly increasing in the relativistic region, termed transversal polarization.

Sternheimer [14] has given very detailed information concerning the (total) density effect and has given a method of calculation which takes into account the dispersion properties of matter in a fairly complete manner.

In some of our experiments, we have used absorbers for which no calculations have been presented by Sternheimer. In these cases we have used his method giving

$$\delta = \sum_i f_i \ln \frac{l_i^2 + l^2}{l_i^2} - l^2 (1 - \beta^2), \tag{6}$$

f_i, as above, is the oscillator strength for the ith transition of frequency ν_i.

l is obtained as the solution of the equation

$$\frac{1}{\beta^2} - 1 = \sum_i \frac{f_i}{\tilde{\nu}_i^2 + l^2}. \tag{7}$$

The $\tilde{\nu}_i$ are the transition energies in units of the plasma energy $h\nu_p$ where

$$\nu_p = \sqrt{\frac{n e^2}{\pi m_0}}, \tag{8}$$

n being the (total) number of electrons/cm^3. The l_i are given by

$$l_i = \sqrt{\tilde{\nu}_i^2 + f_i}. \tag{9}$$

In these units, I is

$$I = h\nu_p \prod_i l_i^{f_i}. \tag{4a}$$

According to Sternheimer [14c] the difference between $\bar{\nu}_i$ and l_i can be neglected for all transitions except for the conduction electrons in a metal where $\bar{\nu}_i = 0$ and $l_i = \sqrt{f_i}$.

We have followed Sternheimer also in the method for finding an approximate figure for δ, viz. by using the known ionization potentials $h\nu_i$ of the various electronic shells and the occupational numbers of each shell as the corresponding oscillator strengths, f_i. The geometric mean frequency found from such a procedure by means of

$$\log \nu_m = \sum f_i \log \nu_i \tag{10}$$

has been found to yield too low $h\nu_m$ in comparison with the experimental I-value. Often the difference is more than 25 %. Before use in (1), all frequencies except those for conduction electrons [14c] were therefore corrected by the same factor, ϱ, to yield $I = h\nu'_m$ where ν'_m is the corrected mean frequency.

In many cases, we have been able to use Sternheimer's data for δ. He gives graphs of δ as a function of p/m_0c and also simple analytical expressions from which δ can be found. Since Sternheimer's 1952 paper [14a], the average excitation potentials have been revised as stated above and, because the δ-correction is dependent on I as described above, they have also to be revised. Sternheimer in 1956 [14c] and 1959 [14d] has made such a revision himself for some metals and compounds. Moreover, Nelms has prepared graphs [13] for additional substances where the new I- and δ-values were apparently used. We have used the Sternheimer 1956 and 1959 data and Nelms data for $E = 2.80$ MeV for our calculations which are presented in Appendix I (cf. also sections V and VI of this paper).

It is seen that the δ-correction involves certain uncertainties and that it is made semi-empirically. It should be noted that, in the empirical determination of I, the influence of I on δ must be taken into account. Often the various influences counteract each other and thus limit the precision with which I can be determined experimentally. This is true not only for relativistic particles but also for slower ones because part of the counteracting effect resides in the zero-energy polarization term [15].

The density effect eliminates I under extreme relativistic conditions [10] and, in such a case, the electronic density is the only property describing the matter traversed (except a). Hence a periodic dependence of $(1/n)(dE/dx)$ was predicted [22].

5. *Chemical compounds*

For mixtures or chemical compounds in the ideal case, an additivity law exists:

$$\frac{d\bar{E}}{dm_s} = \sum_i x_i \frac{d\bar{E}}{dm_s}, \tag{11}$$

x_i being the weight percentages of the constituent atoms. For H_2O, as an example, we get

$$\frac{dE}{dm_s} = \frac{2}{18}\left(\frac{dE}{dm_s}\right)_H + \frac{16}{18}\left(\frac{dE}{dm_s}\right)_0. \tag{11a}$$

Theory predicts the additivity rule, or Bragg's law, to be exactly true only for a dilute gas, termed nicely by Brandt the "Bragg gas" and suggested to be a rational reference state for comparisons [12].

If the calculations involve mean excitation potentials, we have for the additive case [28 and others]

$$\ln I_{\text{cpd}} = \frac{a \cdot Z_A \ln I_A + b Z_B \cdot \ln I_B}{a Z_A + b Z_B}, \tag{4 b}$$

where I_{cpd} is the effective mean excitation potential of the compound and I_A and I_B the mean excitation potentials for the constituent atoms A and B. Z_A and Z_B are the atomic numbers respectively and a and b the number of atoms A and B constituting the compound. This general formula, of course, applies to any compound or mixture provided the additivity rule holds and provided appropriate terms for all constituent atoms are included.

As soon as we form a chemical compound from the constituents, the I value will be *a priori* changed and if, further, a condensed state is formed the density effect will set in. Even at low velocities, the zero-energy polarization is present and *a priori* violates the Bragg law [12]. At relativistic velocities, further changes should occur and Bragg's law should only hold, say, for a two-component system, if a fortuitous matching of the δ-figures occurs over the range in question. On the other hand, these interesting effects are hidden behind a logarithmic function and so the stopping powers would be affected only to a minor extent, thus necessitating precise measurements for the deviation to be detected.

As has already been stated, LiH might be the best example for testing these interesting valence effects which have been predicted in some detail by Brandt in this case [4].

Changes in the transition frequencies should have an influence on the atomic stopping power for various valence states. Hydrogen and carbon in, say, aliphatic or aromatic states are expected to differ. The influence on I can be inferred from optical dispersion data as suggested by the present author [3]. The easier excitation of π-electrons in aromatic systems (which corresponds to the near ultra-violet absorption of such compounds and a large dispersion effect on the molecular refraction properties) would be expected to decrease I in comparison with, say, the aliphatic case.

Brandt worked out the theory of the valence effects much more completely [15] and took the effect in question into account by introducing the atomic polarizability in the full expression which also included the zero-energy polarization effect. It then turned out, according to Brandt, that this effect often counteracts the influence on I and even reverses the effect on stopping power. This, for example, is the case for hydrogen as is seen in Table 2.

It is seen from this table that the existence of interesting chemical effects can be demonstrated provided sufficiently precise measurements can be made to detect them.

The early literature contains statements concerning the large medium and chemical valence effects on the stopping of beta [2] and alpha rays [23]. The influence on the latter has now been shown to be of very small proportions [24, 25] and the abnormal beta absorption effects stated were to a large extent caused by neglecting the abnormal Z/A factor for hydrogen. If the correct factor is taken into account, the abnormalities disappear almost completely as shown by the present author [3]. A small residual

Table 2. Calculated mean excitation potentials of light elements, compiled from W. Brandt, ref. [12].

Based on $I_{Al} = 165$ eV as reference value and on equation (5 *a*) with $K_0 = 8.2$ eV and $k_0 = 0.70$ and on methods due to Brandt [15].

Element	Valence state	I_{val} (eV)	Element	Valence state	I_{val} (eV)
H	Atomic	14	O	Atomic	77
	Molecular	18		Molecular	78
	Aliphatic	16		–O–	98
	Aromatic	19		O=	77
Li	Atomic	33	F	Atomic	86
	Metallic	38		Bound	87
Be	Atomic	42	Al	Atomic	120
	Metallic	60		Metallic	164
C	Atomic	60	P	Atomic	137
	Molecular (graphite)	71		Bound	147
	Aliphatic	80	S	Atomic	144
	Aromatic	71		Bound	171
N	Atomic	68	Cl	Atomic	154
	Molecular	78		Bound	183
	Amines, nitrates	73			
	In ring	90			

effect could be taken as an argument for an influence due to the polarizability of the aromatic compounds (Fig. 1, in [3]) but, later, it was shown by the author [26] that, by means of more realistic assumptions concerning the relative absorption power of carbon relative to hydrogen, the effect could be made to disappear completely and thus these results can be taken as arguments for additivity within the precision claimed rather than for the existence of chemical valence effects. Results obtained in connection with the practical measurements on hydrogen in hydrocarbons and other compounds [27] showed strict additivity within their very high precision. (On the other hand, the use of a conventional ionization chamber will in itself counteract any valence effects because an increased energy loss yields an average *increase* in the specific ionization in this energy region [26].)

The only real experimental attack on the valence effects yet made seems to be that of Thompson using 340 MeV protons [28]. Using very careful procedures, Thompson succeeded in performing very accurate stopping-power measurements and obtained different I-values for different valence states (cf. Table I in [15]). In some cases, Brandt's theoretical estimates agreed with the experimental results but in other cases such as hydrogen they did not. Further studies must therefore be awaited.

6. *Straggling effects*

As is well known, the energy loss curve is considerably broadened due to the different fates of different penetrating particles. Williams and Landau have treated this effect theoretically [29, 30]. The final result is given as the half-width of the

energy loss curve in terms of the property S_0:

$$\Gamma = 3.98\, S_0, \tag{12}$$

where S_0 is simply $a \cdot m_s$. Landau gave a mathematical expression for the characteristic shape of the straggling curve. Later Blunck and Leisegang [31] made a more refined calculation and took into account the larger energy transfers (of the order of S_0 and larger) and arrived at a broader curve. For a comparison with theory, the property b^2 has to be evaluated for each case under study:

$$b^2 = \frac{\bar{w}\, q\, Z^{4/3}}{S_0^2}, \tag{13}$$

where $\bar{w}$ is the average energy loss in the foil and q an energy of the order of 20 eV. The half-width corresponding to a certain b^2 was taken from a graph given by Birkhoff [8] or the curves due to Blunck and Westphal [23] taking radiation into account. The widths found were larger than Landau's.

Recently Hines [32] has stated that neither Landau's treatment nor Blunck and Leisegang's is exact. He predicted that for electrons the broadening is even larger than that given by Blunck and Leisegang. (For heavy particles, it is narrower.) The present author has obtained straggling data as a by-product from his results and has given some comparisons with the theories mentioned (see below).

7. *The most probable energy loss*

The most probable energy loss is the energy difference between the peak of the primary line and the maximum of the energy loss spectrum. Landau has given a theoretical expression for this energy loss [30]. We quote the formula in the form given by Sternheimer

$$\Delta E_p = a \cdot m_s \left[\ln \frac{m_0 c^2 \cdot 10^6}{I^2} + 2 \ln \frac{p}{m_0 c} + \ln \frac{a \cdot m_s}{\beta^2} + 1.37 - \delta \right]. \tag{14}$$

Specializing for 2.8 MeV (data of Table 1) we find

$$\Delta E_p = a \cdot m_s \left(25.14 + \ln \frac{a}{\beta^2} + \ln 1000\, m_s - 2 \ln I - \delta \right). \tag{14 a}$$

Again, for a given energy, the properties of interest describing the material are I and δ. The foil thickness occurs in the bracket and so the energy loss increases faster than linear with respect to this quantity. For a known absorber thickness and a set of I- and δ-values, it is easy to calculate ΔE_p for any case. However, the average energy loss is the more fundamental quantity since (14) is dependent on the straggling theory as Nelms has pointed out [13].

8. *The upper half-point energy loss*

The energy loss measured from the primary peak to the upper half-point of the energy loss curve was introduced by Goldwasser, Mills and Hanson [7]. It is related to the most probable energy loss according to Landau's theory in the following way:

$$\Delta E_p = \Delta E_{\frac{1}{2}} + 1.58\, S_0. \tag{15}$$

Goldwasser, Mills and Hanson found $\Delta E_{\frac{1}{2}}$ more easy to localize than ΔE_p and the figures showed a better reproducibility. Again, the use of it is dependent on straggling theory, as is the case for ΔE_p.

9. *Multiple scattering corrections*

The theory given by Yang [34] has been used to correct for multiple scattering which gives the particle a longer path than the expected one. The measured absorber thickness should be multiplied by a factor f which is obtained from Yang's increase in path length Δ. Our case corresponds to Yang's case II because the detected particles leave the absorber nearly perpendicularly:

$$f = 1 + \frac{\Delta}{t}. \tag{16}$$

Yang states for this case

$$\langle \Delta \rangle_{\text{av}} = \frac{t^2}{3\, w^2}$$

Thus

$$f = 1 + \frac{t}{3\, w^2}. \tag{16 a}$$

The absorber thickness, t, is to be expressed in radiation lengths, X_0, and so:

$$f = 1 + \frac{m_s}{3\, X_0\, w^2}. \tag{16 b}$$

The property w is

$$w = \frac{2\, p\, \beta\, c}{E_s}. \tag{17}$$

E_s is an energy equal to 21 MeV [35]. Thus w is easily evaluated

$$w = \frac{m}{m_0}\beta \cdot \frac{m_0 c^2}{10.5}. \tag{17 b}$$

Numerically we get for 2.8 MeV

$$f = 1 + 3.43 \cdot \frac{m_s}{X_0}. \tag{16 c}$$

Table 3. Radiation lengths in some solid and liquid materials, calculated according to Bethe and Ashkin [10].

Material	Radiation length X_0 in g/cm²
Li	78.6
Be	63.6
Na	27.7
Mg	24.9
Si	21.7
K	17.2
LiH	75.1
C_8H_8 (*p*-styrene)	44.1
$(-CH-CH-)_p$ (*p*-ethene)	43.4
$C_6H_5CH_3$	43.5
C_7H_{16}	44.4
H_2O	35.9
CH_3OH	39.1
C_6H_6	43.4

The radiation length X_0 is given by

$$\frac{1}{X_0} = 4\,N\,\bar{\Phi}\,\ln 183\,Z^{-1/3}, \tag{18}$$

where

$$\bar{\Phi} = Z\,(Z+\zeta)\,5.80\cdot 10^{-28}\ \text{cm}^2. \tag{19}$$

(N is the number of atoms per cm³.)

X_0 is given by Bethe and Ashkin (correcting Rossi and Greisen's results) for some substances [10]. However, for many of our absorbers, it was necessary to calculate X_0 by means of (18) and (19). For chemical compounds, an additivity rule was applied. The resulting radiation lengths are listed in Table 3.

Equation (16*c*) together with the radiation lengths given by Bethe and Ashkin and those listed in Table 3 then give the corrections which were applied to all absorbers.

This proceudure has been used by Goldwasser, Millsand Hanson [7] and later by Hall, Hanson and Jamnik [36]. Hebbard and Wilson [37], using a Monte Carlo method for finding the path increase and using Molière's theory for the multiple scattering factor, got only half the correction reported by Yang. Apparently Hebbard and Wilson's case applies to the case I of Yang (particles leaving the absorber at all angles). But even if the two cases are not comparable, it should be noted that, if it turns out that Yang's factors have to be revised, a future revision of our data given below will have to be made.

10. *Radiation losses*

The energy loss due to the production of continuous electromagnetic radiation or bremsstrahlung has to be taken into account since it occurs simultaneously with the energy loss due to excitation and ionization. It can be calculated by the Bethe–

Heitler theory (see Bethe and Ashkin [10] who improved it to cover the radiation produced in the field of the electrons). Around 2.8 MeV, the energy loss is given by Bethe and Ashkin's formula (60a and 61) which after rearrangement gives:

$$-\left(\frac{d\bar{E}_0}{d\,m_s}\right)_{\text{rad}} = N_A \cdot \frac{Z\,(Z+1)}{A} \cdot \left(4\,\ln\frac{2\,E_0}{m_0 c^2} - \frac{4}{3}\right) 5.79 \cdot 10^{-28}\ \text{MeV} \cdot \text{cm}^2/\text{g}. \qquad (20)$$

Here E_0 is the total energy of the electron (kinetic energy plus rest mass energy).[1] Numerically (20) reduces for a kinetic electron energy of 2.8 MeV to:

$$-\left(\frac{d\bar{E}}{d\,m_s}\right)_{\text{rad}} = 10.29\,\frac{Z\,(Z+1)}{A}\ \text{keV cm}^2/\text{g}. \qquad (20\,a)$$

The energy loss due to radiation effects is then easily calculated for the elements studied. For chemical compounds it can be calculated by the additivity law.

Radiation losses do not alter the most probable energy loss appreciably [33] so their influence on this energy loss property can be neglected. They should, however, affect the average energy loss and should be taken into account when relative stopping powers are studied (see below). This has been done by Paul and Reich [38] and by Ziegler [39] in their evaluation of the average energy loss. However, it should be noted that electrons suffering radiation losses are deflected through larger angles than the average case because the losses are large. Thus some of them might escape detection when the instrument behind the absorber only accepts particles leaving the absorber within narrow angular limits (0.9° in the experiments to be described). This might cause some error, although small, which might be worth future theoretical elaboration. This applies to some extent also to ionizing collisions involving large energy transfers. The question will be further discussed below. Numerical results for some substances at 2.8 MeV are given in Table 4 below.

11. *Relative mass stopping power*

The comparison of the experimental average energy loss data was made by using the known concept of relative stopping power:

$$\bar{s}^{\text{sub}}_{\text{stand}} = \frac{-(d\bar{E}/d\,m_s)_{\text{sub}}}{-(d\bar{E}/d\,m_s)_{\text{stand}}}. \qquad (21)$$

The comparison of the energy loss of a substance with that of some standard seems to reduce some sources of error and does not presume an exact absolute calibration of the energy scale. (The bar for s and E refers the properties to average energy losses.) Disregarding the very slow variation of energy loss with particle energy, it is seen that (21) is independent of the absorber thickness. The energy loss due to radiation losses should be included before making actual comparisons with theory.

[1] Note that E_0 has another meaning than in (1).

Table 4. Relative stopping powers of various substances relative to beryllium at 2.80 MeV (for methods of calculation, see text).

I. Elements.

Z	Element	A	I (eV)	δ	$\frac{d\bar{E}}{dm_s}$	$\left(\frac{d\bar{E}}{dm_s}\right)_{\text{Nelms}}$	$\left(\frac{d\bar{E}}{dm_s}\right)_{\text{rad}}$	$\left(\frac{d\bar{E}}{dm_s}\right)_{\text{total}}$	$s_{\text{Be}}^{\text{sub}}$
3	Li	0.06640	39.0	1.29	1.517	1.51	0.018	1.535	1.029
4	Be	0.06817	64.1	1.56	1.469	1.47	0.023	1.492	1.000
6	C_{graph}	0.07673	78.1	1.35	1.640	1.64	0.036	1.676	1.123
11	Na	0.07349	143	0.38	1.552	—	0.059	1.611	1.080
12	Mg	0.07579	156	0.71	1.569	1.56	0.066	1.635	1.096
13	Al	0.07401	163	0.98	1.498	1.50	0.069	1.567	1.050
14	Si	0.07655	175	0.90	1.545	—	0.077	1.622	1.087
19	K	0.07464	228	0.31	1.511	—	0.100	1.611	1.079

II. Compounds.

Compound	A	I (eV)	δ	$\frac{d\bar{E}}{dm_s}$	$\left(\frac{d\bar{E}}{dm_s}\right)_{\text{Nelms}}$	$\left(\frac{d\bar{E}}{dm_s}\right)_{\text{rad}}$	$\left(\frac{d\bar{E}}{dm_s}\right)_{\text{total}}$
LiH	0.07730	39	1.58[a]	1.758	—	0.018	1.776
$C_6H_5CH_3$	0.08335	62.3	1.22	1.836	1.84	0.035	1.871
C_7H_{16}	0.08891	52.0	1.33[b]	1.972	—	0.033	2.005
H_2O	0.08526	74.0	1.08	1.855	1.86	0.044	1.899
CH_3OH	0.08629	64.8	1.09[b]	1.90	—	0.039	1.939
C_6H_6	0.08259	63.8	1.18[b]	1.813	—	0.035	1.848
C_5H_9Cl[c]	0.08147	86.2	1.2[b]	1.74	—		

[a] See Section VI.
[b] Calculated by Sternheimer's methods [14], other δ-figures according to Sternheimer's expressions [14].
[c] Used as cover for alkali and LiH absorbers.

This is done by changing the meaning of $\bar{s}$ so that

$$\bar{s}_{\text{stand}}^{\text{sub}} = \frac{(d\bar{E}/dm_s)_{\text{sub}} + (d\bar{E}/dm_s)_{\text{sub}}^{\text{rad}}}{(d\bar{E}/dm_s)_{\text{stand}} + (d\bar{E}/dm_s)_{\text{stand}}^{\text{rad}}}. \tag{21 a}$$

(The index sub indicates the substance under study.)

The radiation losses term is calculated by (20) and the ionization loss by (1). For a given energy we get

$$\bar{s}_{\text{stand}}^{\text{sub}} = \frac{(2\pi e^4 N_A/m_0 c^2 \beta^2)(Z/A)_{\text{sub}}[B - 2\ln I_{\text{sub}} - \delta_{\text{sub}}] + (d\bar{E}/dm_s)_{\text{sub}}^{\text{rad}}}{(2\pi e^4 N_A/m_0 c^2 \beta^2)(Z/A)_{\text{stand}}[B - 2\ln I_{\text{stand}} - \delta_{\text{stand}}] + (d\bar{E}/dm_s)_{\text{stand}}^{\text{rad}}}, \tag{21 b}$$

where B is a constant for a given energy. The standard has to be carefully selected among the best known cases. We have used aluminium and beryllium, the mean exitation potentials of which have been accurately determined with fast protons

[17, 18, 19] (and probably much better than what any electron energy loss study can afford). Since there seems to be agreement about the Caldwell data [17] (see above), we have adopted them (for numerical data cf. Table 4). Moreover, the δ-correction has been treated in some detail for these materials, especially by Sternheimer, and indications have been given of experimental confirmation [7]. Further arguments will be given below to support the use of beryllium as a standard.

By means of (21*b*), values of $\bar{s}$ have been computed for various substances for $E=2.8$ MeV (kinetic electron energy). The new set of I-data (Caldwell) has been used with slight modifications. The figures used by Nelms [13] in her extensive tabulation have been employed. In a few cases, however, no information exists. The choice of I-values is given in Table 4 and a further discussion is included in Sections V and VI. δ-data have been taken from the revised Sternheimer (1956) data [14*c*]. In some cases where no information apparently exists, we have calculated δ-data by Sternheimer's method. This will be further commented on when describing individual substances (cf. Appendix I).

For molecules, additivity was presumed in all cases except LiH where figures applying to the predictions by Brandt [4] by inferring the most probable alternative were employed. A further discussion will be given on LiH in Section VI.

The data in Table 4 have been given with three decimals despite the fact that the experiments cannot at present reach a corresponding precision. Wherever a comparison with Nelms' data was possible this has been indicated in the table. It is seen that no disagreement occurs.

It should be noted again that the theoretical predictions, as given by Table 4 for instance, involve an uncertainty due to the choice of the I and δ values. So a significant deviation of the experiment from the predictions may yield information, provided the general theory is assumed correct, concerning a more exact knowledge of I and δ, i.e. on the dispersive properties of matter. Such deviations are of great interest in this field of work.

12. *Comparisons between experiments and theory for the most probable energy loss properties*

The most probable energy loss ΔE_p and the related property $\Delta E_{\frac{1}{2}}$ (see Subsections 7 and 8 above) are not linear with respect to absorber thickness and so have to be considered for each absorber individually. For a pair of absorbers, the substance under investigation and the standard, one can form

$$s_{p\,\text{stand}}^{\text{sub}} = \left(\frac{\Delta E_p}{m_s}\right)_{\text{sub}} \Big/ \left(\frac{\Delta E_p}{m_s}\right)_{\text{stand}} \tag{22}$$

and the analogous property

$$s_{\frac{1}{2}\,\text{stand}}^{\text{sub}} = \left(\frac{\Delta E_{\frac{1}{2}}}{m_s}\right)_{\text{sub}} \Big/ \left(\frac{\Delta E_{\frac{1}{2}}}{m_s}\right)_{\text{stand}}. \tag{23}$$

Both properties are formed analogously to the relative mass stopping power (21) but do not of course have a definite physical meaning since they are influenced by the absorber thicknesses. We have found it useful to make comparisons in this form

since (22) and (23) give quantities which are of the order of one and which are in fact, for a narrow range of absorber thicknesses, not very variable and further not very different from $\bar{s}$.

As stated earlier, radiation losses need not be introduced into (22) and (23). All absorber thicknesses m_s are corrected for multiple scattering using (16*c*).

13. *Comparisons of experiments and theory for the straggling properties*

The theoretical predictions of the straggling parameter can be compared with experiment either by

$$\frac{\Gamma}{\Delta \bar{E}} = \frac{3.98 \cdot S_0}{(d\bar{E}/d\,m_s)_{\text{tot}} \cdot m_s} \tag{24}$$

or

$$\frac{\Gamma}{\Delta E_p} = \frac{3.98 \cdot S_0}{\Delta E_p}. \tag{25}$$

In (24), $(d\bar{E}/dm_s)_{\text{tot}}$ is the sum of the ionization and radiation losses.

In the case of (25), ΔE_p is calculated by means of (14*a*). The presentation according to (25) has been used by some workers [7, 40] but (24) might be more fundamental provided $\Delta \bar{E}$ is observed. Both ways of presentation avoid absolute calibrations. The formulas are, as is seen, based on Landau's treatment but 3.98 S_0 may of course be replaced by the somewhat larger result due to the Blunck–Leisegang theory.

The experiment gives the whole straggling distribution. This can, after appropriate scale unit conversions, be compared with the Landau distribution. The latter has not been given in a simple mathematical form but the function is available as a graph. We shall give a single comparison of this kind in Section V.

14. *Other properties*

Experiments yield quotients for each absorber such as $\Delta E_p/\Delta \bar{E}$, $\Delta E_{\frac{1}{2}}/\Delta \bar{E}$ and $\Delta E_{\frac{1}{2}}/\Delta E_p$ which can be compared with theoretically computed figures. These quotients are obtained as by-products and are properties related to the straggling curve and other theoretical predictions. As they are less tedious to evaluate than the distribution curve, some use will be made of them.

III. Earlier experiments on electron energy loss (mainly above 1 MeV)

Energy loss studies on electrons in the range above 1 MeV have been performed by Paul and Reich [38] (2.8 and 4.5 MeV), Goldwasser, Mills and Hanson [7] (9.6 and 15 MeV), Hall, Hanson and Jamnik [36], Goldwasser, Mills and Robillard [41], Ziegler [39] (32 MeV) and Hudson [40] (150 MeV). In addition, there are studies with emphasis on straggling by Birkhoff *et al.* [8], Kageyama [44] and some others quoted in Birkhoff's review [8]. At 1 MeV, there is an investigation by McDonell *et al.* [42] which also emphasizes straggling phenomena. At 0.6 MeV, there are the studies of Chen and Warshaw [43].

Most of these studies are devoted to the most probable energy loss and the straggling distribution or the dependence of energy loss on energy. The experimental difficulties involved in measuring the average energy loss at high energies or using radioactive sources cause a long tailing-off of the low-energy end of the Landau curve and also intensity difficulties. It is only in the works by Paul and Reich [38] and Ziegler [39] that average energy loss data are given. Only the former were available to Nelms for comparisons with theory [13]. At 32 MeV, radiation accounts for about one-fifth of the total energy loss and accordingly Ziegler was able only to present average energy loss data for Be and C. The precision of Paul and Reich and of Ziegler is limited. The former authors did not have the energy stability and narrow energy distribution that are available now and Ziegler's studies apparently were difficult due to the radiation effects and also to some special ghost lines in the instrument. The best of the precisions quoted is about 5 % (cf. [5, 6]).

The work of the Illinois group is admirable [7, 36, 41]. They report the probable energy losses for Be, Al, Cu and Au and polystyrene for energies of 3–15 MeV and the straggling distributions. On the whole, a good agreement with theory was found after introducing multiple scattering corrections, density effect and straggling. From our point of view with its emphasis on material properties, the direct proof of the density effect by using gases and solid polymers of the same composition is of great interest [41].

To sum up, many aspects of the electron energy loss theory have been studied and verified but very few data are available on average energy loss properties, particularly in the range 1–5 MeV which is the domain of beta-radioactivity and in which radiation losses are still small. The existing data are of poor precision and generally less exact than the data from heavy particle stopping. On the whole, the experiments confirm within their accuracy the theoretical predictions including the density effect. Many indications exist, however, that the straggling distributions are much broader than Landau and even Blunck and Leisegang predict. The present study was therefore planned to fill some of the existing gaps.

IV. Planning of the experiments and methods of evaluation

1. *General*

The choice of the most suitable energy region for energy loss studies on electrons in order to achieve optimum precision has been described in another paper by the author [1]. A too low energy gives too large multiple scattering corrections and a too high energy too large radiation losses. Even if both can be corrected for by theory, they increase the total uncertainty and so a good compromise has to be made. The choice of 2.8 MeV and the limitation to low atomic number materials might be such a compromise. The absorber thicknesses have to be large enough to render the energy loss measurable with sufficient precision. In particular, the width of the energy loss spectrum should be large in comparison with the width of the primary line. A factor of at least 5–10 in the half-widths is needed in order to avoid corrections. The choice of absorber thickness is further governed by the large intensity losses due to scattering. This effect increases rapidly with the atomic number of the absorber.

As will be described later, it turns out that the accuracy of the average energy loss studies is profoundly influenced by the parameters mentioned. A limitation to $Z < 20$ has been found necessary for the conditions selected. Generally, absorbers of 100–200 mg/cm^2 thickness have been used at 2.8 MeV. A total accuracy of 2 % in relative stopping power has been aimed at.

All experiments have been designed to give the relative stopping power and straggling parameters expressed relative to some energy loss property. Beryllium has been selected as the best standard absorber. In addition to the reasons given above, it has a low atomic number, and hence small corrections for multiple scattering and radiation, and further the low-energy tail can be covered better than in the case of, say, aluminium which is often used as a standard in this field. Moreover, pure and uniform specimens are available which can be machined to good geometrical properties and the material is not attacked by moist air at ordinary temperatures. On the other hand, metallic beryllium is an exceptional material with two valence electrons (of the four) and hence has an abnormal stopping power as predicted by A. Bohr [45]. Its I- and δ-values seem to be very well known, however. In a few cases, aluminium has been used as a standard, particularly for the liquids.

By relying on theory for the beryllium standard, the energy scale factor was obtained. It has been shown [6] that the relation between momentum change and the corresponding energy change deviates from linearity by a very small amount in the region used (2.2–2.9 MeV).

2. *Experimental method*

The method for recording energy loss spectra is the subject of a special paper by the author [6]. It will only be recalled here that the energy loss spectrum of an absorber and the primary line are obtained on an XY-recorder of good performance. It was found possible to record the spectra of two or even three absorbers on the same paper. Thus the results for each substance relative to the standard are given by the same document. Each substance has often been studied several times and with different absorber thicknesses. Due to intensity variations and accelerator failure, severe restrictions have been placed on records which might be suspected to be less good. Generally, all records taken when any part of the equipment was known to be defective have been discarded. The approved records correspond to intensity fluctuations by better than ± 5 % (of a symmetrical kind). The data presented were taken when the magnet scanning was on an established hysteresis cycle. However, there are some records (called the A series) which were taken without this precaution at a time when it was not clear that the precision could be brought to a level where it is affected by the hysteresis phenomenon. In these cases, the first sweep starts from a low current and, by recording between about 2.4–2.9 MeV, the first energy loss curve is thereby obtained. It then moves back to 2.4 and thereafter records the second absorber on the upward direction etc. It is clear that the first record will yield too low energy losses. Empirically it has been found that the difference is 1.0 % by taking an average of the two types of records. The inclusion of records obtained without these precautions would increase the number of data but, of course, they would have to be considered less reliable even if the correction was a small one.

3. *Treatment of records*

The approved records have been evaluated to give the ΔE_p and $\Delta E_{\frac{1}{2}}$ losses in relative units by methods described elsewhere [6].

The average energy loss is obtained by taking the center of gravity of the energy loss curve after it has been corrected for momentum transmission change band (practically, this means that each ordinate of the different strips has been divided by the abscissa in the numerical evaluation). It was found that the tail can be approximated by an exponential and hence, by assuming this to be correct even outside the experimentally available region, the average energy loss could be corrected for the most distant part of the tail. As will be seen from the detailed data, this procedure, which is believed to be an improvement, yields a rather small correction for low Z (up to Be for instance) but gets more and more pronounced for higher Z as can be expected physically. Since this procedure does not seem to have been used before, it will be further illustrated and discussed below.

The center of gravity of the primary line has been evaluated and all average energy loss data measured from this point. It is shifted to the low energy side by about 0.43‰ or 15 % of the half-width measured from the peak.

The half-width of the energy loss curve or straggling parameter is determined from the acutal records. It has to be somewhat increased due to the above-mentioned correction for momentum width at different moments. This was made by means of a correction factor obtained from a few treated curves. Because the emphasis of this work is not on straggling phenomena, we have not corrected the energy loss curve for the finite primary line width by the folding techniques [8, 37, 42]. In most cases, the half-width of the energy loss curve (S) is 5–10 times the same property of the primary line (ε). The latter is usually 2.8–3.2‰ of the primary momentum. We have therefore corrected the energy loss curve found by simply assuming a Gaussian distribution:

$$\Gamma^2 = S^2 - \varepsilon^2. \tag{26}$$

By means of the procedures described, several properties describing the energy loss process are available for the substance under study and the standard. and comparisons with theory are available according to Section II of this paper. In the following two sections, results from the first sets of experiments will be reported.

V. Electron energy loss studies on some light elements

1. *Materials and techniques*

Care has been taken to procure materials not only suitable for forming or machining plane-parallel bodies but also of the highest available purity. As can be shown by elementary calculations, the energy loss is not very sensitive to the purity. So impurities of the order of one or two per cent can be corrected for without appreciable errors. Metals (except the alkali ones) have often been procured as rolled metal sheets of even quality. An area of the order 1 cm² has been cut out or stamped out and the area and weight measured by standard methods.

In some cases, the absorbers have been machined to the thickness required (e.g. Be, Mg).

For the alkali metals (Li, Na and K), a special technique was developed after testing some possible methods. The metal was procured in lumps large enough to

permit areas of about one cm^2 to be obtained without using any superficial part that may have been attacked chemically. A dry-box (from Townson & Mercer Ltd, Croydon, England) flushed with nitrogen (low dew-point, $-75°$) and further dried with desiccants was used as the working area. A sheet of appropriate dimensions was cut out and pressed between two steel plates in a special framework to form a plane-parallel layer. Then, by a special device, edges were cut using two razor blades at a fixed and known distance (1 cm). This process was repeated for the perpendicular direction and the piece weighed within the box with a torsion balance (Sartorius design). (The balance has been tested at intervals by comparing with a more accurate balance.) The resulting alkali metal absorber was then enveloped in a tight bag of 0.6 mg/cm^2 pliofilm and weighed again. The absorber was then taken out into the laboratory air, mounted in the absorber position of the betatron, measured in the apparatus and restored to the dry-box where it was weighed again. The largest weight increase was about 0.1 % per hour and was taken into account although small. (A single run takes about one hour.)

The area of the alkali metal absorbers may not be exactly the assumed one because the edge cannot be considered to be exactly sharp due to the properties of the metals. We must admit a maximum error of 1 % in these cases. The following list gives a more detailed acount concerning the materials used:

Lithium was procured from Johnson, Matthey & Co. Ltd., London, in the form of a lump $140 \times 60 \times 20$ mm in kerosene. Typical analysis: Na 0.12 %, K 0.003 %, Fe 0.006 %, Ca 0.019 % and N 2.24 %.

Beryllium was obtained from Brush Beryllium Corp., U.S.A., and from New Metals Inc., London. It was stated that the purity was higher than 99.5 %.

Carbon was studied in the form of reactor grade graphite (Type AUC, kindly furnished by Skandinaviska Grafitindustri AB, Trollhättan, Sweden). It was guaranteed to have a carbon content of at least 99.92 %, the rest being approximately 0.04 % Fe and 0.01 % Al. No hydrogen was present. The density was at least 1.63 g/cm^3. The pores may, according to the manufacturer, have been oriented in the length direction. The plate used was cut perpendicular to this direction. We shall discuss this matter further below.

Sodium was of pure quality, from Merck, Germany.

Magnesium was machined from a large piece of high purity.

Aluminium consisted of rolled sheets from AB Svenska Metallverken, Finspång, Sweden. The purity was very high, at least 99.9 %.

Silicon. A piece of silicon was kindly furnished by Hafo (a Swedish semi-conductor research station in Stockholm). It possessed a very high purity from our point of view (>99.9 %). The piece was monocrystalline and hence the results can be assigned to a single-crystal material.

Potassium was procured from Merck, Germany.

The plastic material (for alkali metals), pliofilm, was selected because of its low water permeability and because it is one of the thinnest materials of this kind. It was obtained from the Goodyear Co, U.S.A., and is chemically a "rubber hydrochloride" and can be regarded as C_5H_8HCl with sufficient accuracy for our purpose.

The uniformity of nuclear absorbers is always a problem. The materials listed above do not present any difficulties except for graphite, the porosity of which will be discussed below. (The magnesium absorber might also be non-uniform, cf. below.) An inspection of the specimens by beta-ray transmission methods has been arranged but this was not judged necessary for the present investigation.

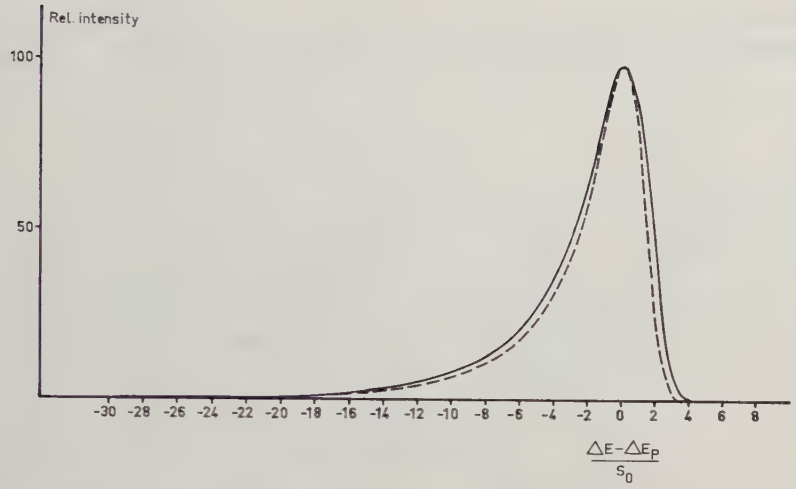

Fig. 3. Experimental Landau curve obtained from treating energy loss run for 187.1 mg/cm² Be absorber. Dashed curve: Landau theory. It is seen that the experimental distribution is broader than the theoretical one.

2. *Results*

(*a*) *General*

The results of the energy loss measurements for the elements studied here will be given in the following sections. Some cases of special interest will first be described in some detail. The remaining cases will then be more briefly presented as tables.

The *form* of the energy loss curve has been studied for one case, namely beryllium, using an absorber 187.1 mg/cm². The intensity data were corrected as described above for momentum band transmission. The energy loss axis was then transformed, using a spectrometer constant (keV/amp) obtained from average loss measurements (see below), to Landau units: $\Delta E - \Delta E_p/S_0$. The maximum point of the energy loss curve was taken as zero for the X-axis. The resulting curve is shown in Fig. 3. It is seen that the shape of Landau's distribution is broader than the theoretical one. This point will be examined more closely below in connection with the comparison of the experimental figures for the half-width of the energy loss distribution.

Corrections for covers and liquid cell windows were made by considering

$$q' = \frac{\Delta \bar{E}_{\text{sub}} + \Delta \bar{E}_{\text{cover}}}{\Delta \bar{E}_{\text{stand}}}, \tag{27}$$

which is the quantity obtained from the energy loss records. It is written in the form

$$q' = \frac{\Delta \bar{E}_{\text{sub}}}{\Delta \bar{E}_{\text{stand}}} + \frac{\Delta \bar{E}_{\text{cover}}}{\Delta \bar{E}_{\text{stand}}}. \tag{27 a}$$

The last term (denoted δ_{cover} below) was taken from theoretical estimates (cf.

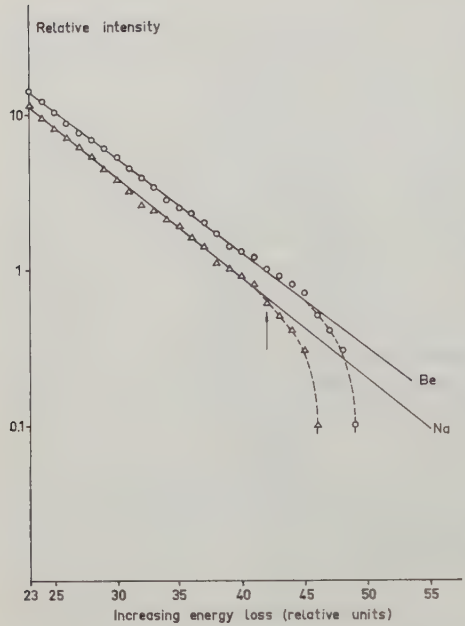

Fig. 4.

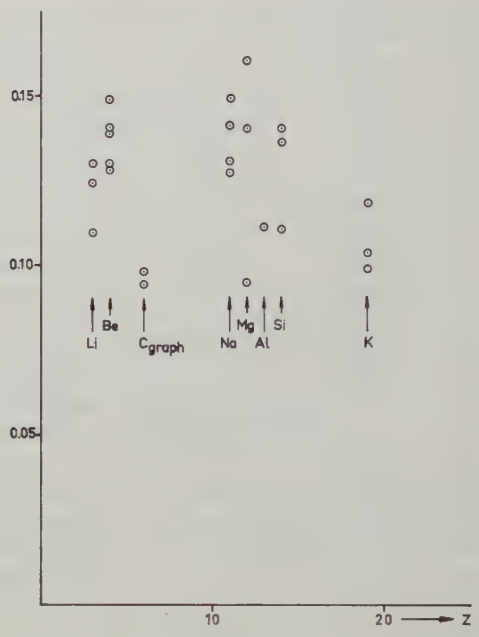

Fig. 5.

Fig. 4. Examples of logarithmic curves for approximating tails of energy loss curves of sodium and beryllium (run no. 62:60). The curves start at an abscissa of 23 which corresponds to about 10 % of the peak intensity. It is seen that the tails can be approximately described by exponentials. Integration from the arrow to infinity replaces the inaccurate experimental data at large energy losses.

Fig. 5. Tail coefficient c (in e^{-cx} according to Fig. 4) as a function of Z. The trend downwards with Z is indefinite but is clearly seen in Fig. 4. (c is expressed in relative units.)

Table 4). $\bar{s}^{\text{sub}}_{\text{stand}}$ is then, of course, got by means of

$$\bar{s}^{\text{sub}}_{\text{stand}} = (q' - \delta_{\text{cover}}) \frac{m_{\text{stand}}}{m_{\text{sub}}}. \qquad (27\,b)$$

For the covers employed for the alkali metals and LiH (using 187.1 mg/cm² Be as standard), $\delta_{\text{cover}} = 0.0074$ which is very small in relation to q' (about unity). The stopping power of mica (cell, liquid windows) has been approximated by that of aluminium. An analogous procedure was used for ΔE_p and $\Delta E_{\frac{1}{2}}$.

For the sake of clarity we shall describe some runs with a silicon absorber in some detail. Three successful runs were made with a single monocrystalline silicon absorber 133.7 mg/cm². As for all other cases, the tail of the low-energy part of the energy loss spectrum was found to be approximately exponential (cf. Fig. 4) and the average loss was corrected by integrating both intensity and intensity times energy loss from a point (x_1 on energy loss axis) where deviations between the exponential and the experimental data start to occur (this is shown in Fig. 4). The integration is extended

Table 5. Average energy loss evaluation for silicon compared with a beryllium absorber 187.1 mg/cm² (after correction 188.9). Absorber thickness 133.7 (after correction for multible scattering and air 136.0 mg/cm²).

Run	$\bar{x}_{Be}$ Primary value	$\bar{x}_{Be}$ Corr. for tail	$\bar{x}_{Be}$ Corr. for prim. line	$\bar{x}_{Si}$ Primary figure	$\bar{x}_{Si}$ Corr. for tail	$\bar{x}_{Si}$ Corr. for prim. line	$\bar{s}^{Si}_{Be}$		$\bar{s}^{Si}_{Be}$ Corr. for hysteresis		Theor. figure $\bar{s}^{Si}_{Be}$
45 : 60 *A*	7.07	7.10	7.06	5.42	5.48	5.44	1.060	av. 1.051	1.067	av.[a] 1.060	1.087 (2.5% larger than exp.)
46 : 60	7.22	7.25	7.22	5.51	5.56	5.52	1.048		1.059		
47 : 60 *A*	6.95	6.97	6.93	5.29	5.32	5.28	1.047		1.054		

[a] 46 : 60 is given three times the weights of 45 and 47 : 60.

to infinity by means of (y is intensity):

$$\Sigma y = \int_{x_1}^{\infty} e^{-cx}\, dx = \frac{e^{-cx_1}}{c}, \tag{28 a}$$

$$\Sigma y \cdot x = \int_{x_1}^{\infty} x e^{-cx}\, dx = \frac{e^{-c\ 1}}{c^2}(1 + cx_1). \tag{28 b}$$

c was evaluated for each curve by the method shown in Fig. 4 (for Na and Be absorbers) and (28a) and (28b) were introduced in the numerical evaluation of the energy loss [6] (center of gravity). It was found that c decreases with the atomic number of the absorber (cf. Fig. 4, the collection of all c-data in Fig. 5 does not show this trend clearly) as might be expected. The quantity c is also related to the absorber thickness but the relation has not been studied.

Table 5 summarizes the data for an average energy loss evaluation. The primary value for the average loss was measured from the peak of the line. A small correction has been introduced, as is seen, to shift it to the center of gravity of the primary line.

The theoretical $\bar{s}$-value in Table 5 is based on an I-value of 175 eV and a δ-value of 0.90 found by using the dispersion oscillator scheme given in Appendix I. It is seen that the experimental figure is 2.5 % smaller than the theoretical one. This is judged to be somewhat outside the accuracy and so it might be taken as an indication of a small discrepancy. This point will be discussed further (see below).

The results from the studies on ΔE_p and $\Delta E_{\frac{1}{2}}$ using the I- and δ-values given above are shown in Table 6.

It is seen that also this result indicates a discrepancy of 2.2 % but it cannot, however, be stated to be significant. The straggling parameter is given in Table 7.

Further data on the silicon absorber are given in Tables 8–10, viz. $s_{\frac{1}{2}}$, $\Delta E_p/\Delta\bar{E}$ and $\Delta E_{\frac{1}{2}}/\Delta\bar{E}$.

Table 6. Most probable energy loss of the silicon absorber as compared with beryllium (for absorber data see Table 5).

Run	Experimental ΔE_p-ratio	$s^{Si}_{p_{Be}}$		Theory $\Delta E_{p_{Be}}$ keV	Theory $\Delta E_{p_{Si}}$ keV	$s^{Si}_{p_{Be}}$ theoretical	Difference exp.-theor. δ'
45 : 60 A	0.729	1.009	av.				
46 : 60 A	0.729	1.009	1.004	234.9	174.2	1.027	−2.2 %
47 : 60 A	0.719	0.995					

Table 7. Straggling parameter for silicon absorber.

Run	$\frac{\Gamma}{\Delta \bar{E}}$	$\frac{\Gamma}{\Delta \bar{E}\ \text{corr.}}$[a]		Theory $\Gamma = 3.98 s_0$ keV	$\Delta \bar{E}_{\text{theor.}}$ keV	$(\Gamma/\Delta \bar{E})_{\text{th}}$	Deviation factor f
45 : 60	0.271	0.282	av.				
46 : 60	0.258	0.269	0.28	42.6	221.3	0.192	1.47
47 : 60	0.283	0.295					

[a] This correction accounts for the instrumental transmission change with momentum (correction factor is 1.042 in our runs at 2.8 MeV).

(b) Results of average energy loss studies

Energy loss records were taken for absorbers consisting of the elements Li, Be, C (graphite), Na, Mg, Al, Si and K. Beryllium (or aluminium) was always used as standard and all data were expressed relative to it. An example of an energy loss run is shown in Fig. 6. Table 8 lists the absorbers used and shows the application of Yang multiple scattering corrections for 2.8 MeV.

The results of 21 successful energy loss runs are given in Table 9 and Fig. 7. The figure shows the deviation, δ', of the experimental relative stopping power from the theoretical calculations (cf. Table 4 above and text). The accuracy assigned to each point in the figure is an estimate taking into account the intensity variations, accuracy of instruments used, methods of evaluation, hysteresis effects and evaluation of the mass per unit area. Mostly ± 1.5 % is believed to be the accuracy obtained except for the alkali metals where ± 2 % is thought more likely (because of the difficulties in shaping the absorbers). In a few cases (e.g. magnesium), the reproducibility is outside the accuracy stated. This might have been due to structural irregularities.

The upper part of Fig. 7 (7*a*) shows that, on the whole, a very satisfactory agreement with theory has been obtained. However, there are more deviations in a negative direction than in a positive one and this might indicate some systematic trend. The most probable cause of the deviations seems to be the radiation loss correction in the theoretical expression for the experimental relative stopping power. It has been customary in this field to include it as has been done here [38, 39]. The electrons suffering radiation losses are likely to be angularly deflected from the geometrical path since large individual energy losses occur (Heitler [47]) as compared with the

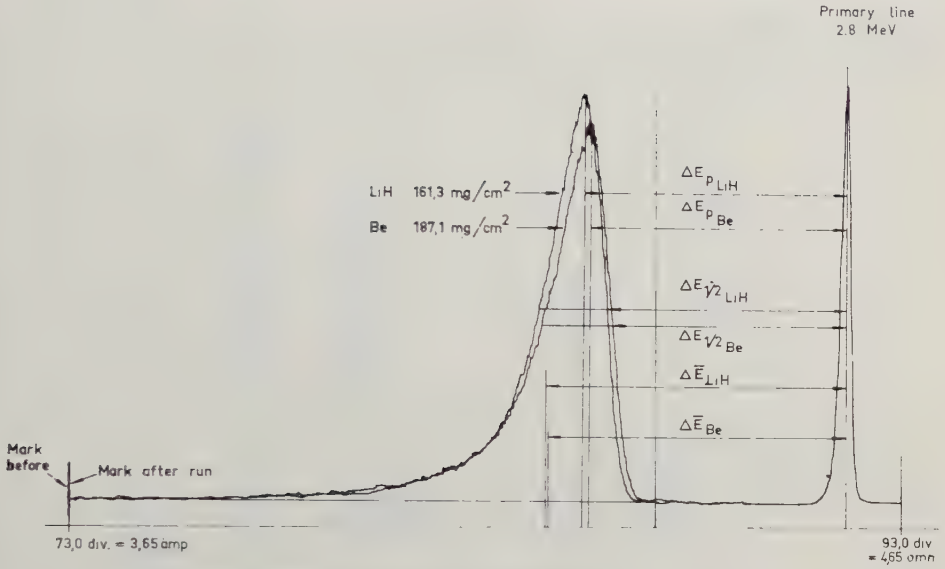

Fig. 6. Energy loss record for LiH and Be (run no. 51:60).

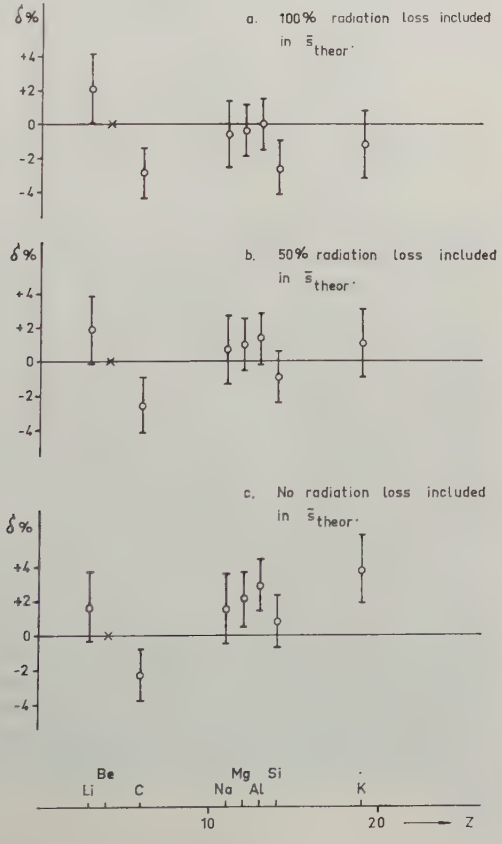

Fig. 7. Average energy loss of 2.8 MeV electrons. Deviation δ', defined as $(s_{exp.} - s_{th})/s_{th}$, as a function of Z for seven elements using beryllium as a standard (Be: ×). Three cases of different theoretical interpretations as to the inclusion of radiation losses are given. It might be pointed out that case (*b*) gives the best results of these three interpretations.

Table 8. Absorbers used for energy loss studies of elements in the solid state.

Element	Run	m_s mg/cm²	m_s[a] corr.
Li	32, 33, 66	137.4	137.9
Be	(most)	187.1	188.9
C	48, 49	157.2	159.1
Na	58, 62	147.5	150.1
		159.4	162.4
Mg	35, 42, 44, 66	134.5	136.9
Al	36, 37, 32, 33	137.2	139.9
Si	45, 46, 47	133.7	136.5
K	30	128.7	131.8
	31	135.7	139.3
	64	166.9	172.2

[a] Corrected for multiple scattering (cf. Section II) and air displacement.

Table 9. Results of average energy loss measurements.

Z	Element	Run	δ_{Be}^{sub}	Rel. weight	$\bar{\delta}_{exp.}$ average	Exp. accuracy, %	Theoretical estimates: 100 % rad. $\bar{S}_{Be}^{sub}$	100 % rad. δ' %	50 % rad. $\bar{S}_{Be}^{sub}$	50 % rad. δ' %	No rad. $\bar{S}_{Be}^{sub}$	No rad. δ' %
3	Li	32 : 60 *A*[a]	1.048	1	1.051	±2	1.029	+2.1	1.031	+1.9	1.033	+1.7
		33 : 60[a]	1.063	1								
		66 : 60[a]	1.041	1								
6	$C_{graph.}$	48 : 60	1.080	1	1.09	±1.5	1.123	−2.9	1.119	−2.6	1.116	−2.3
		49 : 60	1.10	1								
11	Na	58 : 60	1.081	1	1.073	±2	1.080	−0.6	1.065	+0.7	1.056	+1.6
		62 : 60	1.066	1								
12	Mg	42 : 60	1.086	3	1.092	±1.5	1.096	−0.4	1.081	+1.0	1.068	+2.2
		44 : 60	1.040	1								
		66 : 60[a]	1.131	1								
		35 : 60[a]	1.122	1								
13	Al	36 : 60 *A*	1.038	1	1.050	±1.5	1.05	0.0	1.035	+1.4	1.020	+2.9
		37 : 60	1.057	3								
14	Si	45 : 60 *A*	1.067	1	1.059	±1.5	1.087	−2.6	1.069	−0.9	1.051	+0.8
		46 : 60	1.059	6								
		47 : 60 *A*	1.054	1								
19	K	64 : 60	1.055	3	1.066	±2	1.079	−1.2	1.054	+1.1	1.028	+3.2
		30 : 60[a]	1.046	1								
		31 : 60[a]	1.105	1								

[a] Compared with Al 137.2 mg/cm² absorber, all others compared with Be 187.1 mg/cm².

ionization losses. (This might be the case even for K-electron excitations.) In a narrow geometry accepting only electrons within 0.9° from the normal, those electrons which suffer large losses are likely to be undetected. It appears therefore that a theoretical calculation should be made of the fraction of the average energy loss due to radiation which occurs at different angular limitations of the emerging beam.

Table 10. Data concerning most probable energy loss for 2.8 MeV electrons in some elements in solid form expressed as s_p and $s_{\frac{1}{2}}$ (cf. text).

Z	Element	Run	m_{sub} [b] mg/cm²	s_p exp.	s_p theor.	δ'%	$s_{\frac{1}{2}}$ exp.	$s_{\frac{1}{2}}$ theor.	δ'%
3	Li	32 : 60 *A* [a]	137.9	1.072	1.030	+4.7	1.095	1.045	+1.2
		33 : 60 [a]	137.9	1.087	1.030		1.105	1.045	
		36 : 60 [a]	157.7	1.052	1.038	1.3	1.084	1.053	+3.0
6	$C_{graph.}$	48 : 60	159.1	1.071	1.112	−2.9	1.055	1.111	−5.3
		49 : 60	159.1	1.088			1.049	1.111	
11	Na	58 : 60	150.1	1.055	1.046	+0.9	1.026	1.042	−1.5
		62 : 60	162.4	1.055	1.050	+0.5	1.026	1.047	−2.0
12	Mg	35 : 60 [a]	136.9	1.071	1.047	+2.3	1.074	1.049	
		42 : 60	136.9	1.037	1.042	+0.9	1.031	1.036	−0.5%
		44 : 60	136.9	1.063	1.042		1.031	1.036	(Be)
		66 : 60 [a]	136.9	1.046	1.047	−0.1	1.057	1.049	+1.6% (Al incl. 35 : 60)
13	Al	36 : 60 *A*	139.9	0.992	0.996	−0.4	0.953	0.987	−2.9
		37 : 60	139.9	0.992	0.996		0.962	0.987	
14	Si	45 : 60 *A*	136.5	1.009	1.027	−2.2	0.965	1.017	−4.5
		46 : 60	136.5	1.009			0.983		
		47 : 60	136.5	0.995			0.969		
19	K	30 : 60 [a]	131.8	1.014	0.999	+1.5	1.005	0.999	+0.6
		31 : 60 [a]	139.3	1.032	1.003	+2.9	1.011	1.003	+0.8
		64 : 60	172.2	1.007	1.011	−0.4	0.979	1.003	−2.4

[a] Compared with Al 137.2 mg/cm² absorber, all others compared with Be 187.1 mg/cm².
[b] Corrected.

In Fig. 7 we have accordingly presented comparisons of experiments with theory for the case where none or half of the radiation loss contribution is included. It is seen that the former case (no bremsstrahlung included) leads to over-compensation but that an intermediate case yields a symmetrical distribution of the deviations. Of course, the accuracy does not permit any statement concerning the fraction of the energy loss to be included. There is some doubt about the Yang multiple scattering correction because Hebbard and Wilson had to halve it to obtain agreement with a more accurate theory [37]. It seems that the experimental evidence has not yet been solidly established [42] and, moreover, Hebbard and Wilson have only considered the case of particles emerging in all directions (where the theory might be less good than for the case of normally emerging particles). In the present case, the uncertainty in the multiple scattering is not as large as that in the radiation losses and so the latter should be considered first.

It might be added in connection with the results in Table 9 that the treatment of twenty runs with the beryllium absorber gave a spectrometer constant of 778.6 keV/amp or 2630 gauss · cm/amp in this region provided the radiation losses were included. This is larger (about 9 %) than the value found by beta-spectroscopy methods in lower energy regions (0.2–2 MeV). The reason is likely to be a curvature in the dependence of magnetic flux density of coil current above 2 MeV.

Table 11. Straggling parameter Γ as $\Gamma/\Delta\bar{E}$, $\Delta E_p/\Delta\bar{E}$ and $\Delta E_{\frac{1}{2}}/\Delta\bar{E}$ and comparisons with theory for light elements.

Z	Element	Run	Absorber mg/cm²	$\left(\frac{\Gamma}{\Delta\bar{E}}\right)_{exp.}$	$\left(\frac{\Gamma}{\Delta\bar{E}}\right)_{theor.}$	$\left(\frac{\Gamma}{\Delta\bar{E}}\right)_{exp.} \Big/ \left(\frac{\Gamma}{\Delta\bar{E}}\right)_{theor.} = f$		$\left(\frac{\Delta E_p}{\Delta\bar{E}}\right)_{exp.}$	$\left(\frac{\Delta E_p}{\Delta\bar{E}}\right)_{theor.}$	$\delta\left(\frac{\Delta E_p}{\Delta\bar{E}}\right)$ %	$\left(\frac{\Delta E_{\frac{1}{2}}}{\Delta\bar{E}}\right)_{exp.}$	$\left(\frac{\Delta E_{\frac{1}{2}}}{\Delta\bar{E}}\right)_{theor.}$	$\delta\left(\frac{\Delta E_{\frac{1}{2}}}{\Delta\bar{E}}\right)$ %
3	Li	32 : 60	137.9	0.214	0.176	1.22	av. 1.24	0.859	0.831	+2.7	0.796	0.761	+3.2
		33 : 60	137.9	0.223	0.176	1.27		0.849	0.831		0.775	0.761	
		36 : 60	157.7	0.217	0.176	1.23		0.864	0.837	+3.2	0.784	0.767	+2.2
4	Be	36 : 60	188.9	0.225	0.186	1.22		0.823	0.836	+1.0	0.765	0.759	+2.9
		37 : 60	188.9	0.227				0.865			0.797		
6	$C_{graph.}$	48 : 60	159.1	0.272	0.187	1.46		0.852	0.826	+3.0	0.755	0.751	+0.3
		49 : 60	159.1	0.278		1.44		0.851			0.750		
11	Na	58 : 60	150.1	0.252	0.186	1.35		0.845	0.807	+4.7	0.756	0.733	+3.1
		62 : 60	162.4	0.273	0.186	1.47		0.869	0.810	+7.3	0.775	0.736	+5.3
12	Mg	35 : 60	136.9	0.257	0.189	1.31		0.808	0.793	+3.5	0.730	0.718	+2.6
		42 : 60	136.9	0.252				0.826			0.744		
		44 : 60	136.9	0.240				0.876			0.779		
		66 : 60	136.9	0.242				0.775			0.693		
13	Al	36 : 60	139.9	0.272	0.193	1.37		0.809	0.790	+3.1	0.722	0.713	+2.8
		37 : 60	139.9	0.259				0.820			0.743		
14	Si	45 : 60	136.5	0.282	0.192	1.47		0.820	0.787	+4.7	0.706	0.711	+2.1
		46 : 60	136.5	0.269				0.837			0.747		
		47 : 60	136.5	0.295				0.814			0.726		
19	K	30 : 60	131.8	0.262	0.189	1.45		0.821	0.768	+7.0	0.726	0.693	+3.6 (av.)
		31 : 60	139.3	0.275				0.800	0.771	+3.8	0.703	6.696	
		64 : 60	172.3	0.283				0.832	0.781	+6.5	0.739	0.706	

Fig 8.

Fig. 9.

Fig. 8. Most probable energy loss data for 2.8 MeV electrons. Representation analogous to that of Fig. 7. Circles: comparisons with beryllium. Triangles: comparisons with aluminium.

Fig. 9. Energy loss $\Delta E_{\frac{1}{2}}$. Deviations between experiments and theory shown analogously to Figs. 7–8.

(*c*) *Most probable energy loss and* $\Delta E_{\frac{1}{2}}$.

Table 10 summarizes the data concerning most probable energy loss and $\Delta E_{\frac{1}{2}}$ (for definitions and theoretical calculations, see Section II). These data are compared with theory and the results are given in Table 10 and in Figs. 8 and 9 as percentage deviations from theory. These properties are not appreciably affected by radiation losses but, on the other hand, the comparison is greatly dependent on the correctness of Landau's straggling theory. The latter is known to give too narrow distributions for electrons (cf. Section II and Fig. 3 and (*d*) below) and so the deviations might probably be much smaller if an exact theory existed. Nelms [13], by using similar arguments, holds the average energy loss property to be more fundamental than the others.

Nevertheless the results as given in Table 10 and Figs. 8 and 9 show that no very large deviations have been encountered in the cases studied.

(*d*) *Straggling parameter*

Table 11 gives the straggling parameter Γ (corrected for the half-width of energy loss curve) divided by the average energy loss. It seems that this presentation, despite the errors involved in $\Delta\bar{E}$ (cf. above), is to be preferred to $\Gamma/\Delta E_p$. Fig. 10 shows the experimental quotient divided by the expected theoretical one. The result is beyond any doubt a deviation which increases with the atomic number. Some improvement is got by using Blunck and Leisegang's theory [37] (see Section II) but not very much. It would seem that the view of Hines [32], that both theories should be revised to include the nature of the charged particle, is justified.

An interesting point concerning Fig. 10 is the case of reactor graphite. It seems indicated here that the straggling curve is more than 10 % larger than what would be expected from the other elements. This observation is probably linked with the fact that this piece of graphite had a large pore volume (30–40 %). Moreover, the piece was cut in a direction expected to have emphasized the effect (cf. above). The presence of pores may be expected to broaden the straggling curve since some paths

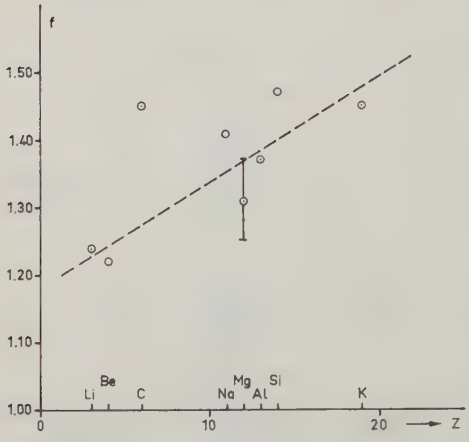

Fig. 10. Straggling parameter $\Gamma/\Delta\bar{E}$ as found experimentally and divided by the same property as predicted from Landau's theory. Deviation factor, f, increases with Z. Estimated accuracy is noted in one case but is thought to be the same for all. Note the large f figure for reactor graphite, assumed to be caused by porosity effects.

taken by the electrons will be within the gas enclosed within the pores. Further studies will be made on this interesting effect. (A small diamond plate will be examined in the near future.)[1] This observation might possibly lead to a method for studying pore distributions.

(*e*) $\Delta E_p/\Delta\bar{E}$ and $\Delta E_{\frac{1}{2}}/\Delta\bar{E}$

These properties, like Γ, reflect the form of the energy loss curve. They are given in Table 11 together with the percentage deviations from theory. Since they are by-products of our studies, they will not be discussed in detail. The positive deviations for $\Delta E_{\frac{1}{2}}/\Delta\bar{E}$ are most probably due to an underestimation of the straggling. A similar cause may be responsible for the positive deviations for $\Delta E_p/\Delta\bar{E}$.

VI. Electron energy loss studies of some chemical compounds

1. *General*

Certain chemical compounds were selected for electron energy loss studies, namely four organic liquids (heptane, methanol, toluene and benzene) water and heavy water, and lithium hydride. All these compounds have low mean atomic numbers and thus the corrections for multiple scattering and radiation are small. For the aluminium standard in the case of water and the organic compounds, there are—as was shown in Section V—corrections introducing some uncertainty. Our scope here was mainly to make comparisons with theoretical calculations based on the additivity rule and the

[1] *Note added in proof:* A diamond plate 301 mg/cm² thickness was kindly placed at our disposal by Mr. J. F. H. Custers and Mr. R. G. Mason, Industrial Distributors (1946) Ltd., Johannesburg, South Africa. By comparing it with a graphite plate, it was found that the straggling parameter was 17 % less for diamond. The f-value (cf. Table 11, p. 128) thus is found to be 1.24, which fits well into Fig. 10 for low 2-elements. Thus the idea that porosity plays a rôle in the straggling, as assumed, is well justified.

Table 12. Average energy loss studies on four organic liquids placed in a 1.5 mm liquid cell and compared with 137.2 mg/cm² Al absorber.

Corrections have been made for cell window thicknesses. δ' is the percentage deviation from theory, $\delta' = (s_{exp.} - s_{theor.})/s_{theor.}$, when the radiation losses are fully included. δ'' is the same property but with only half the radiation loss contribution included. It is seen that this does not improve the agreement.

Compound	Run	$\bar{s}^{sub}_{Al}$	$\bar{s}_{exp.}$ av.	$\bar{s}_{theor.}$	δ' %	δ'' %
n-Heptane C_7H_{16}	20 : 60 *A*	1.293	1.263	1.280	−1.3	−2.6
	21 : 60	1.234				
Methanol CH_3OH	16 : 60	1.216	1.216	1.237	−1.7	−2.8
Benzene C_6H_6	22 : 60	1.178	1.178	1.179	−0.1	−1.3
Toluene $C_6H_5CH_3$	20 : 60 *A*	1.192				
	21 : 60	1.192	1.187	1.194	−0.6	−1.7
	22 : 60	1.177				

appropriate density corrections (Table 4 in Section II). We concentrated our attention on average energy loss studies since they are at present the only ones comparable with theory. The methods used were the same as those employed for the elements. In all cases, the low-energy tail was approximately exponential and permitted corrections to be made as described above.

2. *Organic liquids*

Table 12 summarizes the results for the four organic liquids *n*-heptane, methanol, benzene and toluene. They were placed in liquid cells of the type described previously [6]. Samples of reagent grade were procured and, since the cells used possessed no soluble material in contact with the liquids, they were not likely to become contaminated. The mica windows were each 3–4 mg/cm² and so a correction was made for them by the method described in Section V.

It is seen from Table 12 that the largest deviation (δ') from the theoretical calculations is 1.7 %—in most cases, the deviations are within 1 %. A reduction in the contribution from radiation loss, as described above for the elements, did not improve the agreement.

Within the precision obtained (about 1–1.5 %), we did not observe any effect due to chemical structure even if the figures are in the expected direction of a higher stopping power for the two aromatic compounds as compared with the aliphatic ones.

3. *Light and heavy water*

Distilled water and heavy water, 99.75 % in D, were examined in the cells described. Some runs were made with both H_2O and D_2O on the same record. They were put in cells of identical thickness, 1.5 mm, but with slightly different window thicknesses. The two energy loss curves were identical in shape and position within the experimental accuracy and after having taken the difference in window thickness into account. A numerical evaluation (run 24:60) showed that the energy loss in

Table 13. Average energy loss studies on water in a 1.5 mm liquid cell as compared with a 137.2 mg/cm² aluminium absorber. Corrections for cell window thickness have been introduced. Theoretical figure (including radiation losses): 1.211, i.e. 1.1 % difference from average value.

Run	$\bar{\delta}_{Al}^{H_2O}$
6 : 60 *A*	1.242
7 : 60 *A*	1.209
9 : 60	1.233
10 : 60	1.214
24 : 60	1.223
Average	1.224 ± 1.1 % (S.D.)

1.5 mm liquid layers agreed exactly. The deviation figure obtained was 0.0 % but this was fortuitous and ±0.5 % is to be expected as the accuracy even when such a direct comparison is made.

This result is nearly self-evident from the theoretical point of view. Upon employing the energy loss per unit length (by rearranging (1)), we see that the number of electrons/cm³ is the deciding factor and this is equal for isotopic compounds. The mean ionization potential should also be nearly identical since it reflects the electronic excitation properties. The density correction, δ, should also be nearly identical according to similar arguments. Also the multiple scattering and radiation corrections should be nearly identical.

Some runs with water in comparison with aluminium are presented in Table 13. It is seen that the different runs agree rather well, the standard deviation being ±1.1 %. The agreement with theory is very satisfying. Taking merely half of the radiation losses, a deviation of only 0.3 % is obtained between experiment and calculated figure.

4. *Lithium hydride*

(*a*) *Experiments*

Lithium hydride was procured from Degussa, Germany, as a fine powder of 96 % purity. The material was pressed mechanically in a special hydraulic device shown in Fig. 11. This device was placed in the dry-box described above (section V) and all manipulation and weighing were performed inside it since the substance reacts rapidly with air and moisture. The pressure used was about 6000 kg/cm². This pressure yields, according to Gibb and Messer [48], almost the theoretical density. Apparently very uniform absorbers are obtained. Envelopes of 0.6 mg/cm² pliofilm were employed as with the alkali metal absorbers. The weight increase between runs was about 0.15 %.

The results obtained for LiH are presented in Table 14. Part (*a*) contains runs taken after scanning had been made twice or more. Part (*b*) gives the results obtained when the runs started from zero current. These latter runs (called A runs) have to be corrected for hysteresis and are therefore given less weight. The weighted average found is, as seen from Table 14, $\bar{\delta}_{Be}^{LiH} = 1.169$.

This figure has to be corrected for impurities in the material. The LiH content is stated by the manufacturer to be about 96 %, the rest being unreacted lithium and

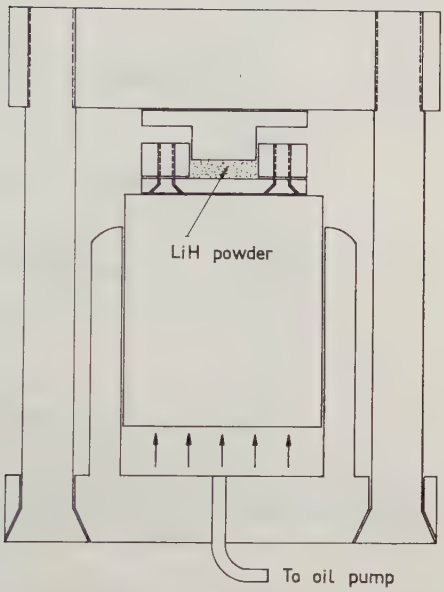

Fig. 11. Hydraulic press for the pressing of the LiH absorbers. All clearances are exaggerated in the sketch. Steel is used as material for the construction.

Table 14. Average energy loss measurements on lithium hydride as compared with a 187.1 mg/cm² beryllium absorber.

A correction for the 1.2 mg/cm² pliofilm envelope has been made. Average for (*b*) after correction for hysteresis (+1.0 %): 1.176. Weighted average ((*a*) 3 times the weight of (*b*)): 1.169.

(*a*) *Normal runs* (on an established hysteresis cycle).

Run	LiH absorber thickness mg/cm²	Thickness (corr. for multiple scattering)	δ_{Be}^{LiH}
51 : 60	161.3	162.3	1.164
53 : 60	147.2	148.0	1.181
54 : 60	147.4	148.2	1.157
Average			1.167

(*b*) *Runs started from zero spectrometer current* (A-series).

Run	LiH absorber mg/cm²	LiH absorber corrected mg/cm²	δ_{Be}^{LiH}
50 : 60	161.1		1.171
52 : 60	147.0		1.157
55 : 60	165.6	166.6	1.166
Average			1.165

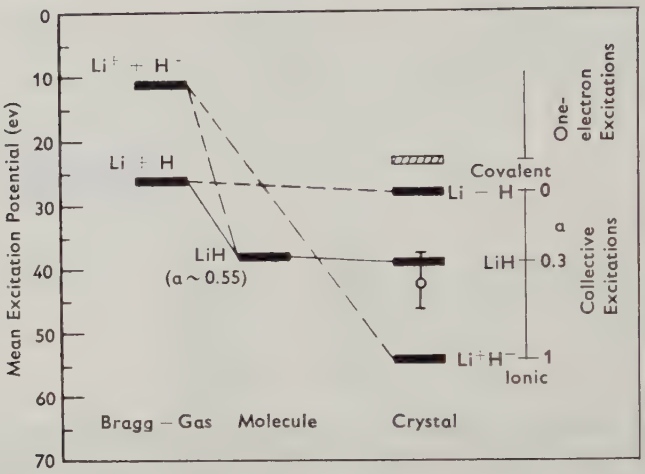

Fig. 12. Mean excitation value for LiH in different valence states as compiled from Brandt [4]. Experimental figure 42.5 ± 4.5 eV is introduced in the figure and indicates a collective excitation mechanism with an a value near the expected one.

sodium. Assuming the composition to be 96 % LiH, 3.25 % Li and 0.75 % Na and the additive law to be true, we get a corrected figure of $\bar{s}_{Be}^{LiH} = 1.175$ (i.e. only about a 0.5 % correction). Thus it is seen that the correction is not very sensitive to the impurities and their exact composition.

(b) Comparison with theory

As was stated in the introduction, LiH is perhaps the best case for testing the effect of "chemical" factors on stopping power because half of the electrons are valence electrons. Brandt [4] has given a detailed theoretical picture and has made estimates of the mean excitation potential (I).

Brandt considers the possible existence of collective excitations in the solid LiH. Such excitations seem to be indicated in metals and also in insulators. No proof has been given for the latter case however. Discussing one-electron excitations and collective exitations in terms of the "optical" model and the statistical model, Brandt provides a very illuminating diagram (reproduced here in Fig. 12) giving the mean excitation potential for the "Bragg gas" (exact additivity) of $Li^+ + H^-$ or Li + H atoms, the molecule LiH in the gaseous state ($a \sim 0.55$, where a is the formal charge $Li^{+a}\ H^{\ a}$) and finally the molecule in the crystalline state. The latter case is divided into two main sections, the one-electron excitation case and the collective excitation case. The latter is characterized by higher values for the mean excitation potentials. The actual figure, as is seen from Fig. 12, is dependent on the charge distribution of the constituent atoms.

Quantum mechanical calculations (Ewing and Seitz [49] and Lundquist [50]) give $a = 0.3$ whereas X-ray scattering experiments give $a = 0.46$ [51].

It is seen from these data and Brandt's figure that an I-value close to 39 eV is the most probable one. Accordingly we have introduced this figure and the corresponding δ-value calculated according to Sternheimer [14] into the theoretical expression for $\bar{S}$ (see Section II).

Table 15. Basis of the assumed density correction for solid LiH.

$I = 39$ eV. δ for 2.8 MeV from the figures given here was 1.575.

Oscillator	Oscillator strength	Energy eV	l_i [b]
f_1	2/4	14.5[a]	0.779
f_2	2/4	104.9	5.676
$\hbar\nu_p = 1.369$ Ry			

[a] Plasma energy.
[b] In units of plasma energy for all electrons.

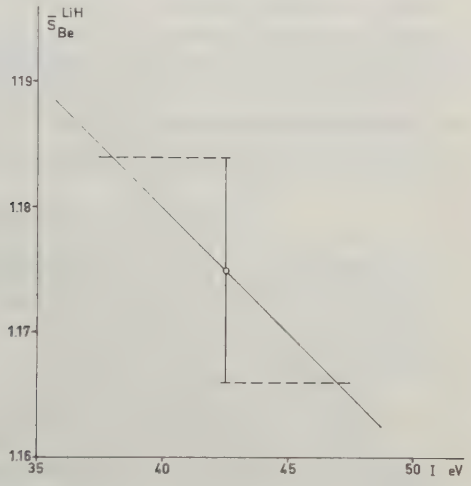

Fig. 13. $\bar{\delta}^{LiH}_{Be}$ as a function of the mean excitation potential I. δ-corrections according to Sternheimer's theory [14].

The δ-correction is made using the figures in Table 15. Inserting this value, we get for $I = 39$ eV (upon including the whole radiation loss):

$$\bar{\delta}^{LiH}_{Be} = 1.181.$$

(If half of the radiation loss is included, we get $\bar{\delta}^{LiH}_{Be} = 1.184$.)

The experimental figure was 1.175 and thus experiment and theory differ by only 0.5 %.

The assessing of an actual I-value and the error in it has to be made provisionally because the manner of calculation of the density effect is itself closely linked with the excitation model and the figures employed. Using Sternheimer's method of 1952 [14*a*] to raise all transition frequencies by a common factor to suit a particular I-value, we arrived at a connection between $\bar{\delta}^{LiH}_{Be}$ and I, as is shown in Fig. 13. This gives $I = 42.5 \pm 4.5$ eV for LiH or close to the region predicted by Brandt for the collective excitation model and a charge value near that calculated quantum mechanically and that found from X-ray scattering data [51].

Even if the manner of δ calculation needs further theoretical study, we have evidence favouring the collective excitation case against the one-electron case as is seen in Fig. 12 where our experimental value and its estimated uncertainty limits are introduced. It is quite clear that electron stopping power measurements in the

MeV region cannot provide any exact a-value. This is due to a counteracting effect of δ on I thus rendering the stopping power less sensitive to the I-value. This effect lies partly in the zero-energy polarization effect and so the precision of experiments with fast protons, for instance, will also be influenced to some extent.

ACKNOWLEDGEMENTS

The author is greatly indebted to Mr. Bernt Sjöstrand, who has operated the apparatus and taken the experimental records with the greatest skill and patience. He has also assisted in the very tedious numerical evaluation work. Many practical suggestions concerning the accurate cutting of the alkali metals and the difficult forming of the lithium hydride absorbers stem from him.

The author wishes to thank Dr. W. Brandt, Du Pont & Nemours Company, Wilmington, U.S.A., for many theoretical discussions and general encouragement, especially on the LiH problem, Prof. J. Lindhard, Aarhus, for some theoretical discussions during the earlier phase of this work, and Prof. O. Lamm, Head of this Institute, who not only introduced the author to the field of the interaction of charged particles with matter but also provided excellent working conditions.

Division of Physical Chemistry, Royal Institute of Technology, Stockholm 70, Sweden

REFERENCES

1. WESTERMARK, T., A double-focusing magnetic spectrometer for studies of energy losses in matter of electrons from a 5 MeV betatron. *Nucl. Instr. 1960/61* (in print).
2. FOURNIER, G., *Compt. rend. 196*, 412 (1933). *Actualités sci. et ind. 57*, 1933.
3. WESTERMARK, T., *Phys. Rev. 93*, 835 (1954).
4. BRANDT, W., *Phys. Rev. 111*, 1042 (1958).
5. WESTERMARK, T., Energy distribution and energy stability of the electron beam from a 5 MeV betatron. *Nucl. Instr. 1960/61* (in print).
6. WESTERMARK, T., Measuring techniques for energy loss studies of 2.8 MeV betatron electrons in matter. *Nucl. Instr. 1960/61* (in print).
7. GOLDWASSER, A. E., MILLS, F. E., and HANSON, A. O., *Phys. Rev. 88*, 1137 (1952).
8. BIRKHOFF, R. D., The passage of fast electrons through matter, Handbuch der Physik XXXIV, p. 53. Springer Verlag, Berlin, 1958.
9. PAUL, W., and STEINWEDEL, H., Interactions of electrons with matter. Ch. I in Beta- and Gamma-ray Spectroscopy, ed. K. SIEGBAHN, North Holland Publishing Company, Amsterdam, 1955.
10. BETHE, H. A., and ASHKIN, J., Passage of radiations through matter. *In* Experimental Nuclear Physics, Vol. I, ed. E. SEGRÉ, John Wiley, New York, 1953.
11. UEHLING, E. A., Penetration of heavy charged particles in matter. *Ann. Rev. Nucl. Science 4*, 315–350 (1954).
12. BRANDT, W., *Health Physics, 1*, 11–20 (1958).
13. NELMS, A. T., Energy loss and range of electrons and positrons. *Nat. Bur. Standards U.S.* (*a*) *Circ.* 577 (1956), (*b*) Supplement to the same (1958).
14. STERNHEIMER, R. M., (*a*) *Phys. Rev. 88*, 851 (1952); (*b*) *ibid. 91*, 256 (1953); (*c*) *ibid. 103*, 511 (1956); (*d*) *ibid. 115*, 137 (1959).
15. BRANDT, W., *Phys. Rev. 104*, 691 (1956); erratum, see *Phys. Rev. 105*, 1933 (1957).
16. BAKKER, C. J., and SEGRÉ E., *Phys. Rev. 81*, 489 (1951).
17. CALDWELL, D. O., *Phys. Rev. 100*, 291 (1955).
18. BICHSEL, H., MOZLEY, R. F., and ARON, W. A., *Phys. Rev. 105*, 1788 (1957).
19. BURKING, V. C., and MACKENZIE, K. R., *Phys. Rev. 106*, 848 (1957).
20. BLOCH, F., *Z. Physik 81*, 363 (1933).
21. WILSON, R. R., *Phys. Rev. 60*, 749 (1941).
22. WESTERMARK, T. *Phys. Rev. 93*, 400 (1954).
23. PHILIPP, K., *Z. Physik 17*, 23 (1923).
24. ANIANSSON, G., *Phys. Rev. 98*, 300 (1955).
25. PALMER, R. B. J., and SIMONS, H. A. B., *Proc. Phys. Soc. London 74*, 585 (1959).

26. Westermark, T. (unpublished).
27. Smith, V. N., and Otvos, J. W., *Anal. Chem. 26*, 359 (1954), Gray, P. R., Clarey, D. H., and Beamer, W. H., *Anal. Chem. 6*, 582 (1960) and further references quoted by them.
28. Thompson, T. J., Effect of chemical structure on stopping powers for high-energy protons. *University of California Radiation Laboratory Report* UCRL-1901 (1952) (unpublished).
29. Williams, E. J., *Proc. Roy. Soc. London, 125*, 420 (1929).
30. Landau, L., *J. Phys. U.S.S.R., 8*, 201 (1944).
31. Blunck, O., and Leisegang, S., *Z. Phys. 128*, 500 (1950).
32. Hines, K. C., *Phys. Rev. 97*, 1725 (1955).
33. Blunck, O., and Westphal, K., *Z. Physik. 130*, 641 (1951).
34. Yang, C. N., *Phys. Rev. 84*, 529 (1951).
35. Rossi, B., and Greisen, K., *Rev. Mod. Phys. 13*, 262 (1941).
36. Hall, H. E., Hanson, A. O., and Jamnik, D., *Phys. Rev. 115*, 633 (1959).
37. Hebbard, D. F., and Wilson, P. R., *Australian J. Phys. 8*, 90 (1955).
38. Paul, W., and Reich, H., *Z. Physik 127*, 429 (1950).
39. Ziegler, B., *Z. Physik 151*, 556 (1958).
40. Hudson, A. M., *Phys. Rev. 105*, 1 (1957).
41. Goldwasser, E. L., Mills, F. H., and Robillard, T. R., *Phys. Rev. 98*, 1763 (1955).
42. McDonell, J. A., Hanson, M. A., and Wilson, P. R., *Australian J. Phys. 8*, 98 (1955).
43. Chen, J. J. L., and Warshaw, S. D., *Phys. Rev. 84*, 355 (1957).
44. Kageyama, S., and Nishimura, K., *J. Phys. Soc. Japan 7*, 292 (1952); *8*, 682 (1953).
45. Bohr, A., *Kgl. Danske Videnskab. Selskab. Mat.-fys. Medd. 25*, 19, 1–52 (1948).
46. Hill, R. D., Appendix VI in Beta- and Gamma-ray Spectroscopy, see ref. 9 for place of publication etc.
47. Heitler, W., Quantum Theory of Radiation. Oxford Univ. Press, 1950.
48. Gibb, T. R. P., and Messer, C. E., A survey report on lithium hydride, *At. Energy Commission U.S.A., Document* NYO, May 2, 1954 (p. 27).
49. Ewing, D. W., and Seitz, F., *Phys. Rev. 50*, 760 (1936).
50. Lundquist, S. O., *Arkiv Fysik 8*, 177 (1954).
51. Cochran, W., *Rev. Mod. Phys. 30*, 47 (1958).

APPENDIX I

Calculation of density effect for Si, K and Na

The method due to Sternheimer described in Section II (*d*) has been used for Si, K and Na. δ-figures are needed for comparisons with experiments. No calculations for these elements have been found in the literature.

Table 16. Calculation of density effect. I is in eV. The l_i are in units of $h\nu_p$. $h\nu_p$ is in Rydberg units.

Element	Na	Si	K
l_1	97.6	135.6	380
l_2	5.64	7.9	26.3
l_3	0.30	0.54	3.82
l_4			0.23
f_1	2/11	2/14	2/19
f_2	8/11	8/14	8/19
f_3	1/11	4/14	8/19
f_4			1/19
I	143	175	228
ϱ	1.79	2.35	1.96
$h\nu_p$	1.45	2.34	1.385
δ at 2.8 MeV	0.38	0.90	0.31

The calculations follow, even in details, those of Sternheimer [14*c*] and some frequencies have been interpolated from his data. Ionization potential data were taken from Hill's tables [46]. Table 16 summarizes the calculations. The I-values inferred have been discussed above (cf. Table 5).

For Na and K, the outermost electron has been treated as a conduction electron ($\bar{\nu}_i=0$, $l_i=\sqrt{f_i}$).

The four outer electrons of Si have also been treated as conduction electrons, a matter that may be debatable since the material is a semi-conductor. The plasma energy obtained is 1.25 Ry or 17.0 eV. Birkhoff (p. 82, Table 9, ref. [8]) quotes data of Martin and Leder for discrete energy losses in thin layers. The figure for Si is 16.9 eV which might justify our assumption.

Tryckt den 14 mars 1961

Uppsala 1961. Almqvist & Wiksells Boktryckeri AB

ARKIV FÖR KEMI Band 17 nr 11

Communicated 26 October 1960 by Arne Ölander and Ole Lamm

Observations of light emitted upon dissolution in luminescent liquids of irradiated NaCl, LiF, KI and some organic solids

By T. Westermark and B. Grapengiesser

With 10 figures in the text

SUMMARY

By means of a photomultiplier arrangement, light flashes can be detected when irradiated solids are dissolved in liquids. For instance, solutes which are at the same time fluorescent and surface active become electronically excited and give strong fluorescence (e.g. PPO in water–dioxane, Belloid TD in water) upon addition of irradiated NaCl. Moreover, aqueous Tl–salt solutions also give strong fluorescence with irradiated NaCl. The light emission of these three systems can be easily seen by the naked eye. After calibration with tritium beta rays, the results for NaCl are tentatively interpreted in terms of stored energy. Hygroscopic substances like KI and some organic solids lose this irradiation effect after storage in air of high humidity. Treatments of polystyrene sheets with radiation and with electrical discharges give qualitatively the same effects.

I. Introduction

It has been found in this laboratory [1] that irradiated solids give rise to chemical reactions upon dissolution in some of the measuring systems employed in chemical radiation dosimetry. The idea was put forward that these changes were caused by structural defects in the irradiated solids. It was logical then to see whether dissolution of the solids in liquid scintillators could excite the fluorescent solutes electronically and thus cause a light emission. If this is the case, a new method for measuring stored energy could be developed and the results compared with those of the radiation chemical method. It turned out that certain liquid systems exhibited luminescence which could even be seen by the naked eye [1, 3]. A brief report has been published [3]. The present report will describe the results more fully and deal with more extensive studies.

II. Materials, irradiation and storage

The experiments were made using the alkali halides LiF, NaCl and KI and some organic solids. Table 1 of the following paper summarises the details of the irradiation procedures and doses [2]. We recall here only that the materials had been irradiated by Co^{60} gamma rays and 2 MeV electrons in doses ranging from a few Mrad up to 200 Mrad. Fine powders were used in all cases except for polystyrene which was in

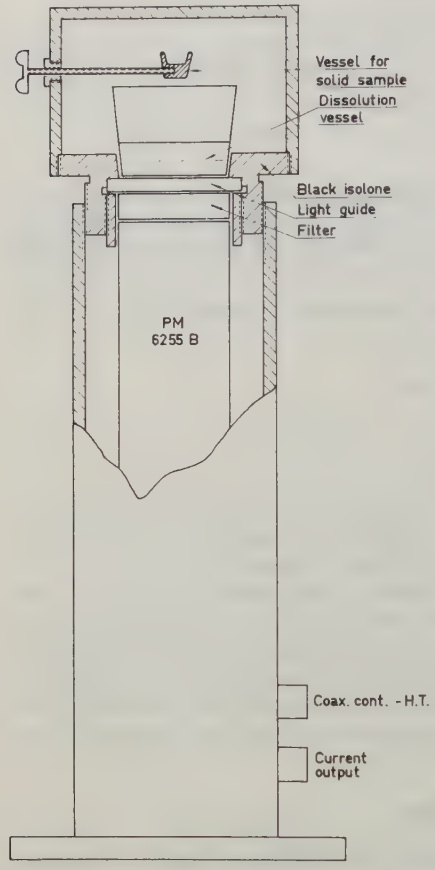

Fig. 1. Photometer unit. (Design: T. Westermark, H. Lindroth and B. Grapengiesser.) Dissolution vessel of quartz glass (Ekco's design for liquid scintillation counting).

sheet form. The latter was also treated by means of electrical discharges (see Section VI).

The materials were stored under dry conditions in a refrigerator at +4°C. Some samples were placed in contact with air of known humidity.

III. Methods

1. *Apparatus*

Fig. 1 shows the apparatus used. A vertical photomultiplier (shortened to PM) tube is mounted inside a light-tight cylindrical brass case. A quartz glass vessel (of Ekco design), 4.5 cm in diameter and about 4.0 cm high, is placed above the tube. The vessel contains the liquid of interest (see below). Using a mechanical manipulator, the solid (usually 10 or 100 mg) can be poured into the liquid at a certain moment after closing the apparatus and applying a high voltage to the PM tube. (In a few cases, the solid was placed in the lower vessel and liquid poured into it.) The gas

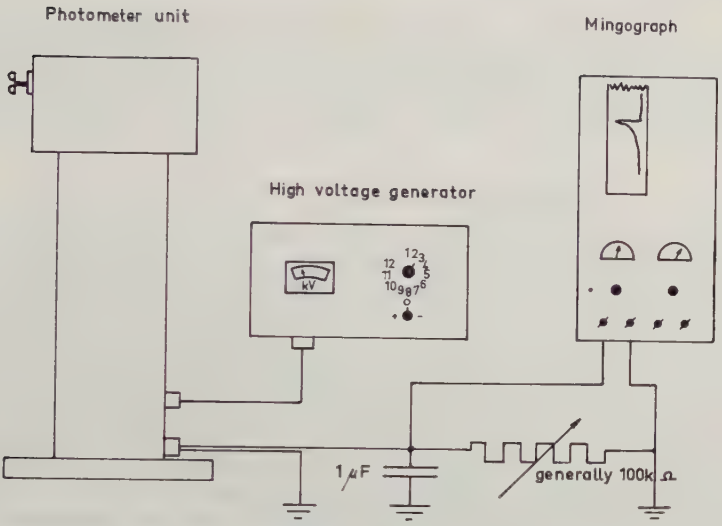

Fig. 2. Recording apparatus used. High voltage generator of Ljunggren–Kuhlemann design. Mingograph 230B from Elema–Schönander Company.

atmosphere in the space above the PM tube can be varied at will since tubes with stopcocks are provided. The experiments reported in this paper have, however, all been made in air.

Circular filters of known transmission properties can be placed between the glass vessel and the PM tube. This enables us to get an idea of the spectral distribution of the light emitted. The response of the tube used, EMI 6255B, extends far into the ultraviolet region (ref. [1], Fig. 7).

The high-tension unit is variable in many steps from 620 to 1300 V and is very stable, viz. ± 0.3 ‰ (constructed by B. Kuhlemanns Ingenjörsbyrå, Stockholm). The response of the photomultiplier to light, of course, increases rapidly with the voltage in this region. This fact enabled us to choose a sensitivity appropriate to each experiment. The response is linear up to 40 μA at any voltage in the range. The dark current is about 0.24 μA at 1300 V. No appreciable fatigue effects have been encountered with the tube.

The light emission is often initially very fast and so a fast recording unit has been selected, namely a Mingograph, type 230B from the Elema–Schönander Company, Stockholm. Usually a recording speed of 0.5 cm/sec has been used. A condenser has been introduced to smooth out the light output curve. Fig. 2 summarizes the recording system.

The optical efficiency of the light collection when a solid powder is poured into a liquid is, of course, by no means an optimum one. Some light might be lost by self-absorption or by its being directed upwards. The measurements do not, however, require a high accuracy at the present stage. It may be seen from Figs. 3 and 6 that a reproducibility within 20 % is obtained despite these difficulties.

2. *Liquids used*

Any liquid may be placed in the vessel, e.g. water, aqueous solutions, organic solvents or organic scintillator systems. The water used was distilled but not air-free.

The solutes used in the aqueous solutions were Tl-ions, lanthanide ions, diphenyloxazole (PPO), dioxane, dioxane plus naphthalene, etc. The organic system preferred was the commercial one, NE213, from Nuclear Enterprises, Canada, which is composed of xylene and POPOP. Further details concerning the liquids are given in Section IV.

3. *Calibrations with ionizing radiation*

Calibration experiments using liquids of the same kind and in exactly the same geometry as that used for the dissolution experiments have been carried out. Tritium has been used in the form of water (12.26 *y* half-life, 18 keV maximum beta energy). Cs^{137} sources of known strength have also been used (0.5–1.7 mC). They have been simply placed on top of the photometer unit in a special position. In both cases. the dose-rate given to the liquid was calculated straightforwardly. An absolute calibration of the tritium water was obtained by counting in a liquid scintillation unit (Model Ekco N-612) and comparing in the same geometry with a standard solution of known absolute strength (from New England, Nuclear Corporation). This was kindly done for us by the Isotopes Techniques Laboratory, Stockholm.

The constant output due to the tritium samples or the Cs^{137} radiation, together with the known recording speed, permits the tentative translation of the light pulses recorded into equivalent doses.[1]

It was found that some of the aqueous solutions, for instance the thallium and lanthanide ones, as well as the PPO system did not respond sensitively to external gamma radiation. The background response, which was seen in pure water for instance, was assigned to fluorescence in the tube material and a small direct gamma sensitivity of the electrodes [4]. It may also have been due to Čerenkov radiation. Often this response was much higher than that of the liquid. This was the reason for turning to tritium since its beta rays cannot produce any Čerenkov radiation and cannot reach the electrodes. Some small fraction of the beta particles might, however, reach the surface layer of the glass. The internal beta dose rate was very high for the concentration used ($\sim$100 mC/ml).

IV. Observations

1. *Sodium chloride*

With *pure water*, a light pulse is readily observed, but the integrated light is small. The form of the pulse is characterized by a sharp rise ($\sim$0.5 sec) and a gradual decrease apparently related to the dissolution process. The long "tail" gives rise to some difficulty in the integration (cf. Fig. 8 of ref. [1]). There is no possibility of a reliable calibration in this case, but rough comparisons with other data yielded a very low order of radiomimetic efficiency η_r (defined in [1–2]). The magnitude was 10^{-8}. The integrated output increases with the dose received by the NaCl according to Fig. 3 of this paper. Note that the stored energy figure found by this method is much lower than that found by methods described below (cf. sec. V).

The dioxane-water–PPO system due to Kallman and Furst [6] yielded an efficiency which was lower than that for pure water. Fig. 4 gives the dependence, in relative units, of the light output on water content (no naphthalene was added). It is seen from this figure that low dioxane contents are much more favourable (see below).

[1] We disregard at this stage possible differences due to the different radiations.

Fig. 3.

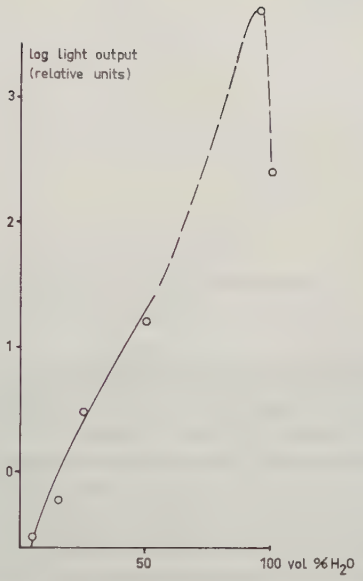

Fig. 4.

Fig. 3. Apparent stored energy plotted against radiation dose for sodium chloride irradiated with 2 MeV electrons from a van de Graaff machine in Köln by the Leybold Company (July 20, 1959) and dissolved in 20 ml water. 1, without filter; 2, Barr and Stroud filter 0 × 7; 3, Barr and Stroud filter 0 × 9 A. (0 × 7 has a transmission between about 2000 and 3800 A and 0 × 9 A between about 3200 and 3800 A.) Experiments were made in the spring of 1960.

Fig. 4. Light output on a logarithmic scale (relative units) for sodium chloride plotted against water content of luminescence liquid: water and PPO (1 g/l) mixed with dioxane (point at 100 % H_2O is with no PPO).

As was described in [1], several systems were investigated which were likely to be more efficient, namely fulfilling the condition of being both surface active (or not surface active at all) and fluorescent at the same time. The idea is to have a high concentration of the fluorescent solute in the contact zone where dissolution takes place. The fluorescence has then a greater chance of competing with the excitation of water which latter is likely to lead to free radicals or, by the new Weiss mechanism [7], to polarons. Two organic substances fulfilling these conditions were found. *PPO* has apparently a slight solubility in water and this dilute solution was used. It was shown by surface tension measurements that the solution is surface active. The emission spectrum has a peak at 3800 Å [9]. It was found that the addition of dioxane increased the light output. Good results have been obtained with 5 % dioxane. (This fact is reflected also by Fig. 4.) A commercial naphthalene sulphonic acid reacted with formaldehyde, called *Belloid TD* (from the Geigy Company), was also used in aqueous solution.

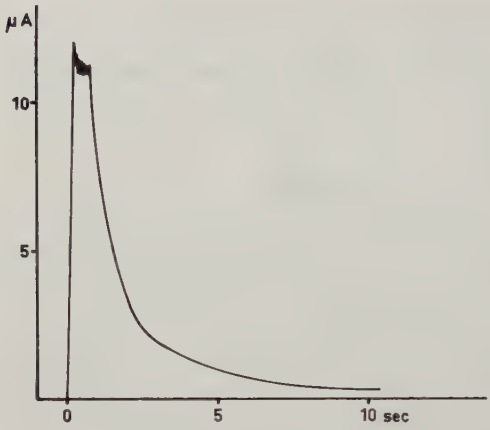

Fig. 5. Typical luminescence pulse obtained by placing 10 mg fine-grained sodium chloride, previously irradiated with 2 MeV electrons from a van de Graaff machine in Köln by the Leybold Company (July 20, 1959) to a dose of 20 Mrad, in a solution of 2 g/l Belloid TD in water.

Both of these solutions yielded strong luminescence pulses of the same characteristic form as those for water. The output was roughly a thousand times that for water. Fig. 5 shows a typical example. The light flashes could be easily seen in the dark-room. They were of about the same magnitude as the light from a luminescent watch. Upon taking a larger amount of NaCl, say some hundred mg, which is not dissolved immediately, new light flashes were obtained on shaking gently. The colour was bluish in both cases. No accurate quantitative calibrations were made but η_r was estimated from the data to be of the order of 10^{-3}.

Further experiments were performed using aqueous *thallium salt solutions* (chloride and nitrate) without any pH adjustment. The emission spectrum has a poorly defined maximum at 3700 Å [8]. The use of Tl ions in small amounts in alkali-halide crystals is well-known in modern scintillation detection. According to Pringsheim's mono-

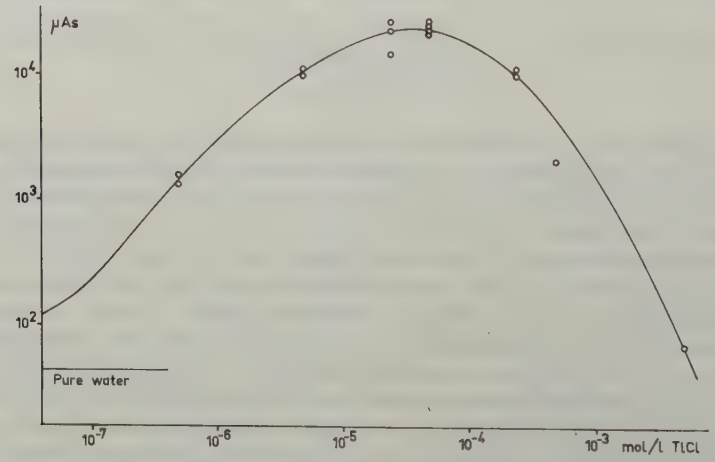

Fig. 6. Integrated light output for dissolution of irradiated NaCl in aqueous solutions of TlCl. The output is shown as a function of the TlCl concentration. The light output in pure water is also shown.

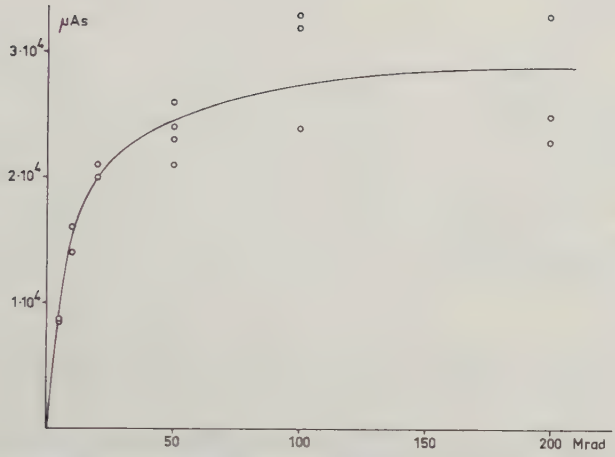

Fig. 7. Integrated light output for TlCl (0.01 g/l) as a function of the dose given to the solid NaCl. The scattering of the points at each dose level seems natural with regard to the dissolution methods employed.

graph ([8], p. 499), the anion is of less influence (unless it is a quencher) and it seems as though the hydrated Tl^+ ion is the species excited. A weaker fluorescence is ascribed to complex species such as $(TlCl_3)^{2-}$ and $(Tl\ Br_3)^{2-}$.

The light flashes obtained using thallium solutions were also easily seen in the darkroom with the naked eye. The pulses recorded in our photometer were of the same form as for the other systems (see, for example, Fig. 1 in ref. [3]). The total light output varied with thallium concentration (other parameters being kept constant) and showed an optimum at about 0.01 g/l (cf. Fig. 6). For comparison, the low level of the pulses obtained in pure water is shown in the same diagram. The integrated light output as a function of the dose given to the solid sodium chloride is shown in Fig. 7. It shows again the same general saturation behaviour as that found for pure water (Fig. 3) and by the chemical methods [2].

Fig. 8 shows the response of Tl solutions to tritium water. Even here an optimum was obtained but it was shifted to a higher Tl concentration. This was shown to be caused in part by an effect due to the sodium chloride. This effect is known from U.V. excitation [8] but the matter was not investigated in detail. A suggestion that the response is wholly due to bremsstrahlung and not to an excitation of Tl^+ was disproved by experiments using $Pb(NO_3)_2$ (cf. Fig. 9).

Ions of the lanthanide series are known to give good quantum efficiencies for U.V. light [8]. Both absorption and emission are confined to narrow bands of characteristic wave-lengths. We have studied solutions of spectroscopically pure Gd^{3+}, Nd^{3+}, Sm^{3+}, Tb^+ and Eu^{3+} salts (procured from Johnson & Matthey & Co. Ltd, London). In no case were light pulses found which were larger than those obtained in pure water.

2. *Lithium fluoride*

Lithium fluoride was subjected to a few preliminary experiments. This substance has been fairly thoroughly investigated with regard to thermoluminescence and F-center formation by irradiation [10]. According to Daniels *et al.*, it is a good object of

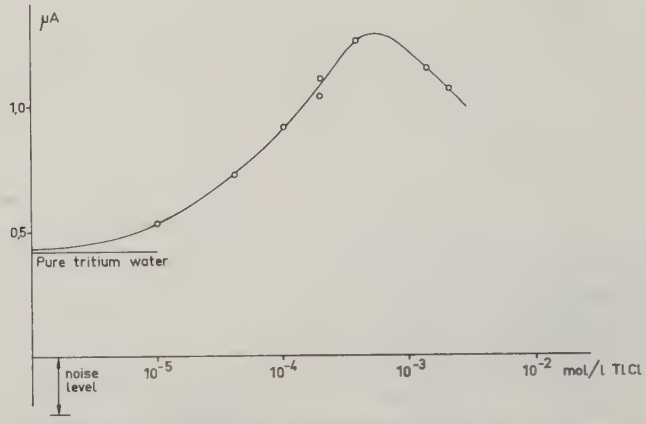

Fig. 8. Calibration of the thallium solutions with tritium water. Output current of PM tube is given as a function of concentration. Addition of more NaCl raises the high concentration side and so the optimum might be shifted closer to that shown in Fig. 6. A weak light emission for tritium water itself (without Tl^+) has been detected (cf. figure). The cause of this might be a fluorescence in the glass surface, impurities in the water used or a weak fluorescence of the water itself. A decision between these alternatives cannot be made without further experiments.

study among the alkali halides because, among other things, it is not hygroscopic. The low solubility, however, made it less easy to study in these dissolution experiments. Light pulses were nevertheless obtained. If the whole photometer unit was shaken gently, the light output increased again. This phenomenon could be repeated, as is seen in Fig. 10. These observations show, no doubt, that the light emission is connected with the dissolution process.—Such repeated light flashes have also been observed visually.

3. *Potassium iodide*

Irradiated potassium iodide gave light pulses in pure water of the same magnitude as in the case of sodium chloride. Some samples were stored in contact with the air in the laboratory. With these samples, it was observed that the light output gradually decreases. After 24 hours, no light pulses could be detected at all. This was most probably due to sorption of moisture from the air.

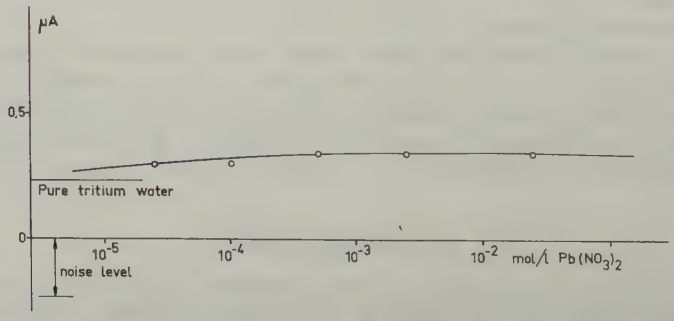

Fig. 9. Investigation of possible luminescence of lead solutions using tritium water. Output current of PM tube is given as a function of concentration.

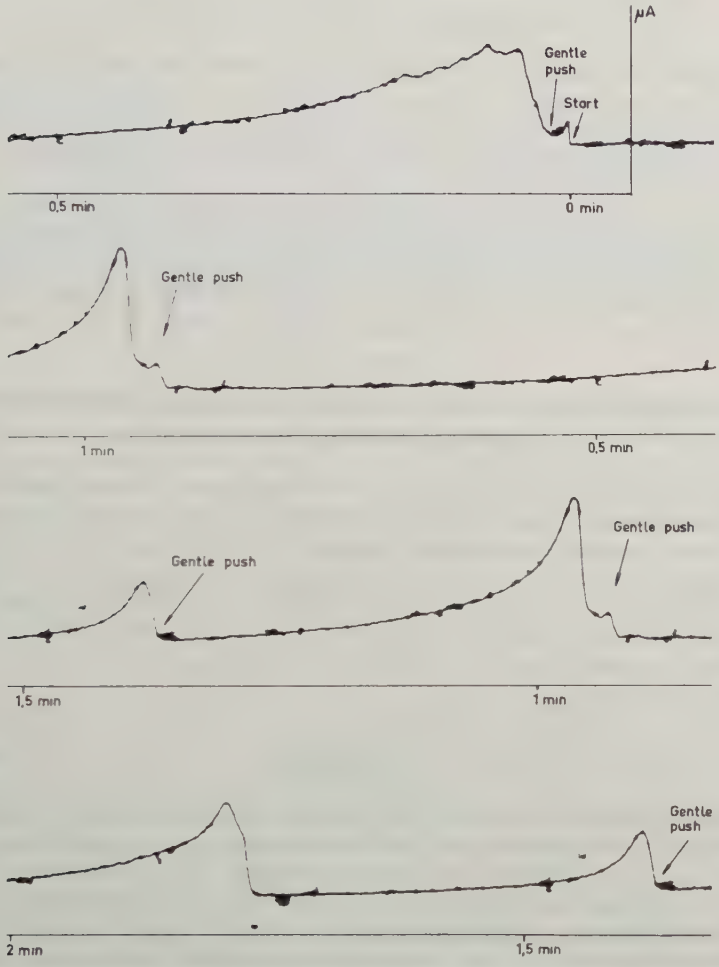

Fig. 10. Light output for irradiated LiF in TlCl solution. By gently shaking the photometer, the dissolution process is enhanced and new light peaks are obtained.

4. *Organic solids*

We shall briefly state here the results of a few observations on irradiated organic solids.

Irradiated glucose and sucrose both gave small light pulses in water. It is probable that this is the same effect as that found by Ahnström and von Ehrenstein [11]. Neither PPO, Belloid TD nor Tl^+ ions increased the light output appreciably.

Alginic acid was selected to represent a case where treatment with water vapour is possible due to the hydrophilic nature of the substance. The material was irradiated in a dry form and gave upon dissolution in water the normal light output but with long tails due to the low solubility which were difficult to integrate. Storage at 20°C and 98 % relative humidity for 30 h eliminated the irradiation effect completely. Similar results were obtained for glucose and sucrose (storage 120 h).

V. Calculation of stored energy for NaCl

By assuming that part of the stored energy behaves like radiation upon dissolution [2], we can use the light output data for NaCl in Tl^+ solution (cf. Fig. 6) and the tritium calibration (cf. Fig. 8) to calculate the energy stored and the radiomimetic efficiency. Such a procedure for a concentration of 0.01 g TlCl/l gives $1.5 \cdot 10^8$ erg/g or $\eta_r = 3\,\%$.

This means that the Tl experiments yield the same order of magnitude as the chloroform–water experiments [2], but it must be borne in mind that it has to be assumed that the beta doses from tritium can be used directly for this calculation, i.e. that the excitation efficiency is the same. It might be pointed out that the quantum energy of the Tl emission (~ 3700 Å) is near the figure for the C–Cl bond energy (2.9 eV).

VI. Irradiation effect in the case of polystyrene and comparison with electrical discharge treatment

Polystyrene sheets (0.14 mm thick), after irradiation, yielded light pulses when dissolved in an organic liquid scintillator (NE213, cf. III:2 above). The magnitude was low. Other samples were treated with an A.C. glow electrical discharge at the ASEA Company (by Dr. A. Kelén). The voltage used was 5 kV r.m.s. and the treatment was extended for 50 h. The sheets were then put in a Dewar flask and transferred to our laboratory where they were stored for 3 months at $-22°$C. It was then found that these samples gave the same kind of light pulses and that the magnitude was about the same.

VII. Discussion

A simplified model is discussed in the following paper and it will only be recalled here that electrons trapped in F-centers represent a potential energy which is released in some unknown way upon dissolution. The energy levels for sodium chloride, for instance, are sufficiently large to excite fluorescent solutes. The findings presented above are in qualitative accord with this view. The positive results for Tl^+, PPO and Belloid show that these entities certainly have been excited electronically. In the quantitative evaluation of the stored energy (Section VI), one has to assume that the excitation efficiencies in the dissolution and calibration are equal, an assumption which at present is unproved. It is gratifying to see, however, that the estimate of energy storage is of the same order as that found by chemical methods.

It seems to be indicated that surface chemical aspects have to be considered. The negative results for organic solids may be real but may also be caused by other surface phenomena (e.g. low concentration of the fluorescent solutes in the dissolution zone). No conclusion can, however, be drawn. Surface tension measurements indicated a decreasing tension with increasing TlCl concentration. This indicates that the thallium salt might be enriched near the surface of the solid during dissolution. If this is proved correct, it may show that the η_r-value given (Section V) is a high estimate.

The results with hydrophilic organic substances, although not very numerous, indicate that storage under humid conditions destroys this type of irradiation effect. This would have some application to the problems involved in the wholesomeness of irradiated foods [1].

The analogy between the actions of radiation and electrical discharges in gases has already been put forward by Lind [17]. The results for polystyrene constitute a further qualitative indication of this analogy. It was not possible to study it quantitatively, however.

It might be added that some experiments [5] performed by irradiating solid polystyrene and polymethylmethacrylate with U.V. light (2527 Å) indicate stored energy effects. After switching off the lamps, the material was placed in contact with tritium gas and a labelling result was obtained which was higher than that in a blank experiment without U.V. irradiation. This result, which is so far preliminary, is in accord with the fact that energy storage (perhaps in the form of free radicals) can give rise to graft polymerization (ref [1], No. 17).

ACKNOWLEDGEMENTS

The authors are indebted to H. Lindroth for performing some of the initial experiments and for contributions to the design of the apparatus. Thanks are also due to Mr P. Pedersen and Mr I. Ingefjäll for constructional and laboratory assistance. They thank, in addition, Dr G. Ahnström and Dr L. Ehrenberg for valuable discussions and the carrying out of numerous Co^{60} irradiations. Dr E. von Sydow, Svenska Konserveringsinstitutet, Gothenburg, also kindly performed Co^{60} irradiations. L. Westfelt is thanked for taking the surface tension data.

Division of Physical Chemistry, Royal Institute of Technology, Stockholm 70, Sweden.

REFERENCES

1. Westermark, T., *Risö Report 16*, p. 28–36, 1960 (papers presented at the First Nordic Meeting on Food Preservation by Ionizing Radiations, held at Risö, April 25–26, 1960).
2. Westermark, T., Biesèrt, N., and Grapengiesser, B., Observations by means of radiation chemical dosimetry liquid systems of irradiation effects in solid sodium chloride and some organic solids. *Arkiv kemi 17*, 151 (1960).
3. Westermark, T., and Grapengiesser, B., Observations of the emission of light on dissolution of irradiated solids in certain liquids. Short communication in *Nature 188*, No. 4748, 395 (1960).
4. Sangster, R. C., and Irvine, J. W., Jr., *J. Chem. Phys. 24*, 670–715 (1956).
5. Ghanem, N., and Westermark, T., Addendum to the paper "Extensions in the techniques for the accelerated unspecific isotopic labelling of organic compounds" (paper RIC/224 read before the I.A.E.A. conference on the use of Radioisotopes in the Physical Sciences and Industry, Copenhagen, 6–17 Sept., 1960).
6. Kallman, H., Furst, M., and Brown, F., *Nucleonics 14*, 48 (April 1956).
7. Weiss, J., *Nature 186*, 751 (1960).
8. Pringsheim, Ch. G. P., Fluorescence and Phosphorescence. Interscience Publishers Inc., New York 1949.
9. Swank, R. K., Back, W. L., Hayes, F. N., and Ott, D. G., *Rev. Sci. Instr. 29*, 279–284 (1958).
10. Moorehead, F. F., and Daniels, F., *J. Chem. Phys. 27*, 1318 (1957).
11. Ahnström, G., and Ehrenstein, G. v., *Acta Chem. Scand. 13*, 855 (1959).
12. Lind, S. C., The chemical effects of alpha particles and electrons. *Am. Chem. Soc. Monograph*, Series No. 2, New York 1928.

Tryckt den 14 mars 1961

Uppsala 1961. Almqvist & Wiksells Boktryckeri AB

ARKIV FÖR KEMI Band 17 nr 12

Communicated 26 October 1960 by Arne Ölander and Ole Lamm

Observations by means of radiation chemical dosimeter liquid systems of irradiation effects in solid sodium chloride and some organic solids

By T. Westermark, N. Biesèrt and B. Grapengiesser

With 12 figures in the text

SUMMARY

The dissolution of irradiated solid substances, e.g. sodium chloride and some organic solids, in a liquid measurement system used in radiation chemistry gives an easily measurable response. The effect increases with dose and possesses a similar saturation tendency to that found for F-center formation. An attempt was made to interpret the results in terms of the radiation-equivalent part of the stored energy.

I. Introduction

It has been observed that solids treated with ionizing radiation produce effects, similar to those given by the direct action of ionizing radiation, upon dissolution in certain liquids [1]. The present paper will describe some introductory studies on such effects, mainly involving the dissolution of irradiated solids in acid ferrous sulphate solutions and aqueous solutions of chloroform. These experiments might have some relevance to problems concerning the wholesomeness of food preserved by irradiation. An attempt was made, after calibration with gamma radiation doses, to calculate that fraction of the stored energy which behaves like radiation (the radiomimetic efficiency [1]).

II. Materials, irradiation and storage

The solid materials used in these investigations are listed in Table 1. They were irradiated with fast electrons or gamma rays in the manner recorded in the table. Normally all materials were procured and used in the form of powders (grain size 0.1–0.5 mm) with the highest available purity. The water content was 0.1–0.6 % (found by heating at 105°C to constant weight).

The chemicals irradiated were wrapped in plastic bags by the irradiation workers and mailed to this laboratory. Normally the samples were transferred here to closed glass vessels which were then kept dry in a refrigerator at −22°C (in darkness). In some cases, storage was made in darkness at room temperature or under some special conditions to be specified below.

Table 1. List of solids and irradiation treatments.

No.	Material	Irradiated at	Radiation source	Doses Mrad	Date of irradiation
1.	Sodium chloride	Risø, Denmark	Co^{60} γ-source	0.5, 2.0, 5.0	Dec. 1958
2.	Sodium chloride (denoted Leybold I)	Leybold Co., Cologne, Germany	2 MeV electrons from v.d. Graaff machine	10, 20, 50, 70, 100, 200	April 1959
3.	Sodium chloride (denoted Leybold II)	Leybold Co., Cologne, Germany	2 MeV electrons from v.d. Graaff machine	5, 10, 20, 50, 100, 200	July 1959
4.	Sodium chloride, glucose, sucrose, glycine	Wantage, England	Co^{60} γ-rays	5, 20, 100, 200	May 1959
5.	Sodium chloride, potassium iodide	Gothenburg, Sweden	Co^{60} γ-rays	5, 20	March 1960
6.	Glucose, sucrose, alginic acid, polystyrene, LiF, NaCl	Stockholm University Sweden	Co^{60} γ-rays	2, 5, 20, 50	April 1960 Aug. 1960

The doses recorded are those given by the laboratory performing the irradiation. The γ-sources are of modern design and have, in general, rather uniform radiation fields. The dose-rates are known to $\pm 5\,\%$ in most cases. The dose figures for the fast electron irradiations may be a little more uncertain. As will be seen, these uncertainties are of small concern in this investigation. The dose-rate in the γ-irradiations is of the order of 100000 rads/h whereas the electron irradiation is of the order of 10–100 Mrads/h.

III. Methods

1. *General*

As described in an earlier paper [1], an attempt was made to choose liquid systems typical for radiation chemistry for the dissolution of the irradiated solids. Care has been taken to emphasize radiation-like effects. To this end, each sample was studied twice, firstly, in the dosimeter liquid and, secondly, in the pure solvent to which, after complete dissolution, the dosimeter solute was then added (the latter is termed the blank test). The difference will be a measure of the stored energy which acts radiation-like (radiomimetic) during dissolution. It will be discussed below whether trivial explanations can be applied or not. We shall consider there the breaking of chemical bonds as an important criterion of radiation-like effects.

2. *The Fricke system*

The acid ferrous sulphate solution (or Fricke dosimeter) is one of the best known in chemical radiation dosimetry (Minder [2]). Decomposition products of water, viz. OH radicals and dissolved oxygen in combination with H radicals, are supposed to play an important part in the oxidation mechanism. Thus, a breaking of the H–OH bond, which requires 5.1 eV, is supposed to occur. These statements might, however, have to be reinvestigated in view of Weiss' recent theory concerning the decomposition of water by radiation [7]. The solution was prepared according to Weiss *et al.* [3]. In these experiments, 1 g samples were dissolved in 3 ml of the main solution diluted with 3 ml distilled water. The Fe^{3+} concentrations were measured by means of the colour of the SCN complex.

Details

The main solution had the composition: 1.17 g $FeSO_4 \cdot (NH_4)_2SO_4 \cdot 6\ H_2O$, 0.15 g NaCl, 55 ml 97 % H_2SO_4, distilled water to 1255 ml.

Blank test. Dissolution in 3 ml distilled water, thereafter 3 ml of the main Fe^{2+} solution.

Fe^{3+} measurements. 0.5 ml 20 % NH_4SCN solution added to samples followed by extinction measurement at 4800 Å in a Beckman B Spectrophotometer using 1 cm cells. Distilled water was used as the blank in the spectrophotometer. All samples were measured within 20 min after dissolution, since some instability was obtained with longer times.

3. *Chloroform–water system*

It is well known that radiation produces both hydrochloric acid, Minder [2] and oxidizing entities (presumably free chlorine) in water–chloroform mixtures. A breaking of the C–Cl bond and resultant destruction of the $CHCl_3$ molecule is supposed to occur in this case (Minder [2]). A rough estimate of the C–Cl bond energy is given by Pauling [8], viz. 2.9 eV.

The acid formation, due to radiation, in water nearly saturated with chloroform was found to yield colour changes with the neutral-red indicator. However, especially for the organic solids, acidity is formed [9] already in the blank tests and, for this reason, the method was abandoned.

The detection of the oxidizing entities formed in the chloroform–water mixtures was carried out in two ways. The first method involved the addition of potassium iodide and an excess of chloroform. The pink colour of the chloroform phase was used as a measure of the free iodine concentration [10] and it was measured photometrically at 5100 Å. However, the sensitivity of this method is not very high and so it was abandoned.

The method finally adopted was the classical detection of liberated iodine by starch [11] followed by spectrophotometry at 5100 Å. This method is very sensitive but, unfortunately, it requires a recalibration for different starch batches.

The use of potassium iodide as a solute is very practical and has been used frequently in this work. However, the presence of free iodine after the dissolution of the irradiated solids does not prove with certainty a destruction of the chloroform but can be thought to be a trivial oxidation effect requiring, in fact, only a very low energy [1] (a few tenths of an eV). Therefore, the experiments were repeated with

only chloroform as the solute and with the addition of KI after the dissolution. In this case, the argument for assuming C–Cl bond breaking is much stronger.

Details

Analytical reagent chloroform was shaken five times with distilled water to free it from alcohol and chlorine. The final water phase was used as the detector. In some experiments, it was made 0.001 C in KI. The blank test was made by dissolving 1 g of the irradiated solid in 3.6 ml water. Thereafter, 4 ml water saturated with chloroform and 0.4 ml 0.02 C KI were added. In both cases, 0.15 ml of an analytical grade starch solution was added and the spectrophotometric reading at 5100 Å was obtained with a Beckman B instrument using 1 cm cells. Pure water was used for matching in the twin cell.

4. *Experimental*

The radiation chemical measuring systems employed were the ferrous and chloroform ones described above. The latter was used both with and without the addition of potassium iodide. No care was taken to eliminate dissolved air and so all results apply to aerated solutions.

A weighed amount of the irradiated solid was taken and (after thawing, if taken from the refrigerator) dissolved by gentle shaking in an ordinary test tube with a glass stopper. After complete dissolution and possible addition of certain liquids (see above), samples were transferred to the spectrophotometer cells and measured. Each experiment was performed within 10 min and the colours produced were easily followed.

5. *Calibration*

The liquid measuring systems were calibrated using a 100 mC Ra^{226} source. Thus, information was obtained about the relationship between the dose received and the Fe^{3+} and iodine concentrations. This information was used to state to a first approximation the equivalent doses obtained upon dissolution of irradiated solids and to express them in the form of energy stored (for method, see [1]).

IV. Results

1. *Sodium chloride*

Sodium chloride was the main object of study during the introductory stage. The irradiated powder showed the characteristic colours [12]; they were, however, not always similar (at a given dose) but seemed to depend on the source of the material.

The ferrous system was found to respond to the dissolution of irradiated sodium chloride. The Fe^{3+} concentration of the samples, as found from the recorded extinction data, could be reproduced to within 10 % when repeated many times—a satisfactory reproducibility (cf. Table 2). An experiment, made to verify the linearity between amount oxidized and mass of sample, also gave satisfactory results.

The amount oxidized increased steadily with the dose received (cf. Fig. 1). The increase was slower than linear and tended gradually to an apparent but never reached saturation.

Table 2 a. Examples of dissolution of irradiated NaCl (at Wantage) in water–cloroform, 0.002 C in KI.

The figures listed are optical extinctions using the starch system described (readings at 5100 Å). The table indicates a good reproducibility and gives together with Table 2*b* an idea of the actual figures obtained.

Radiation dose Mrad	Experiment 1	Experiment 2	Experiment 3
0	0.000	0.000	0.000
5	0.177	0.186	0.175
20	0.272	0.280	0.270
100	0.429	0.428	0.414
200	0.541	0.548	0.522

Table 2 b. Blank test experiments for the two first series of Table 2 *a*.

Radiation dose Mrad	Experiment 1	Experiment 2
0	0.000	0.000
5	0.003	0.002
20	0.000	0.002
100	0.028	0.044
200	0.022	0.034

This type of curve for the chemical yield as a function of the dose absorbed by the solid was obtained in nearly all of the experimental series. The level of the curve does not seem to possess any clear relation to the irradiation parameters as far as is known. The different curves in Fig. 1, for example, apply to chemicals of different origin and this seems to explain simply the differences obtained.

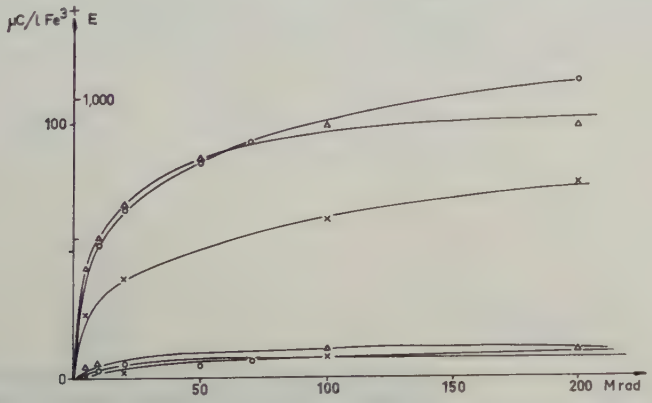

Fig. 1. Extinction data and concentration of Fe^{3+} obtained upon dissolution of irradiated sodium chloride. The lower three curves are blanks obtained by dissolution of the sodium chloride in water and subsequent addition of the dosimeter solute. Circles: material irradiated at Leybolds with fast electrons from a van de Graaff machine. Triangles: material irradiated at Wantage by Co^{60} γ-rays. Crosses: material irradiated at Leybolds as above but at a later date. The differences may be due to the different sources of the materials. Note that the blank test never exceeded 20 % of the main test.

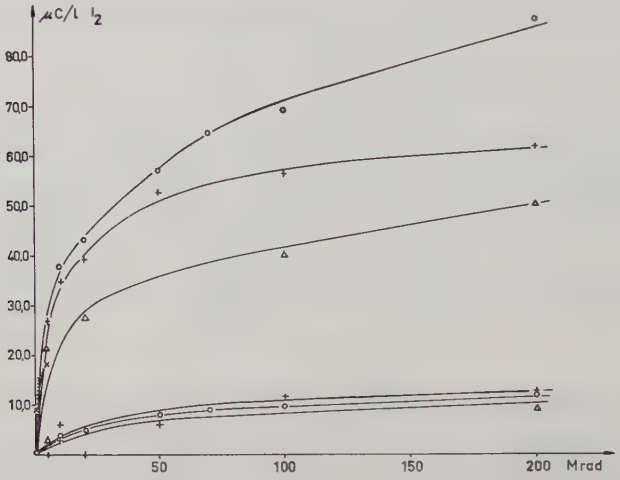

Fig. 2. Iodine liberated from a chloroform–KI solution upon dissolution of irradiated NaCl (dose on X-axis). Open circles: Leybold irradiation (cf. text for Fig. 1). Crosses: second Leybold irradiation. Triangles: Wantage irradiation. Bottom curves: blank tests.

The blank tests given by dissolution in water first and then adding the ferrous solution showed Fe^{3+} yields which were 5–20 % of those of the main tests. The form of the curve was roughly the same. (The term blank test should not be confused with measurements on non-irradiated solids. Such experiments give the small amount of Fe^{3+} present in the main solution which is then easily corrected for.)

Fig. 2 presents results obtained by dissolving irradiated sodium chloride in the water–chloroform system, the solution being 0.002 C in KI. The measurements were

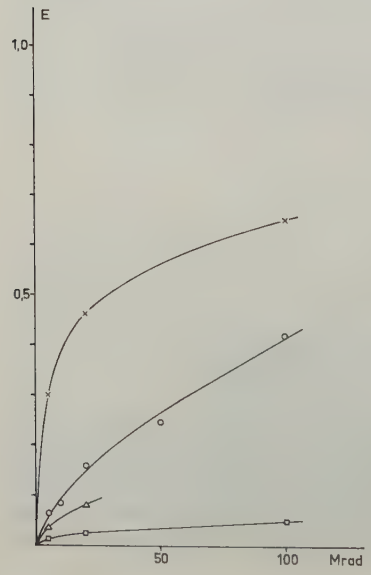

Fig. 3. Extinction data due to iodine–starch after dissolution of irradiated sodium chloride. Crosses: equal amount of 0.002 C KI and chloroform-saturated water. Circles: chloroform-saturated water. The other reagents were added after the complete dissolution of the sodium chloride. Triangles: 0.002C KI. (The other reagents added afterwards.) Squares: water. (The other reagents added afterwards.)

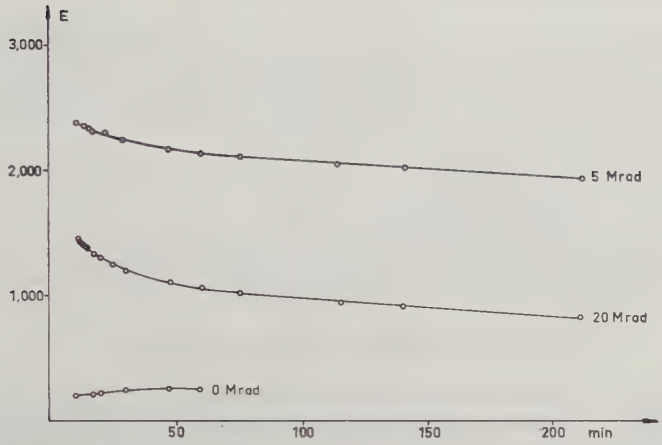

Fig. 4. Fe^{3+} (as extinctions) from sucrose irradiated with different doses. Note the reduction action which apparently reverses the order of the samples.

made after the addition of starch. In Fig. 2, the concentrations of iodine liberated are given (obtained from the extinction data and a calibration curve).

Once again, the shape of the curves is the characteristic one described above and the blank tests give yields of roughly the same relation to the main ones as for the iron system.

For the reasons discussed above, the experiments were repeated to include the case where no KI was added before dissolution. Fig. 3 shows the results obtained. It is seen that the yield is reduced but not drastically and that the blank test is still low.

2. *Organic solids*

The dissolution of irradiated sucrose yielded large Fe^{3+} amounts. However, a short time after dissolution the extinction dropped, apparently due to a reducing action. This action was stronger the larger the radiation dose received by the sucrose

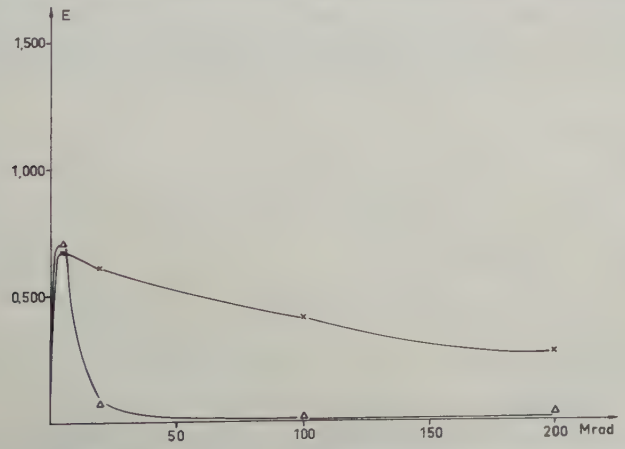

Fig. 5. Oxidation of the Fricke system by irradiated glycine. A reducing action was observed here as for sucrose (cf. Fig. 4).

powder. At moderate doses, the reaction rate was low enough to permit extrapolation back to the time of dissolution (cf. Fig. 4) but, at higher doses, the half-time of the reaction decreased to a few minutes and any extrapolation therefore became uncertain. The blank test (by dissolving in distilled water) gave negligible extinctions.

It was impossible to study glucose by the iron method because a strong red colour developed immediately upon dissolution in water.

Irradiated glycine oxidized the iron system but, as is seen from Fig. 5, the results did not follow the characteristic curve found previously. The blank test yielded a high figure at 5 Mrad but was more normal for higher doses.

V. Attempts to calculate the stored energy

From the results described and the irradiation of liquids with known Ra^{226} gamma doses, it is possible to calculate the equivalent doses. Now, this equivalent dose, corrected for dilution, divided by the original dose has been termed the radiomimetic efficiency η_r [1]:

$$\eta_r = \frac{E_r}{E_0} = \frac{D}{D_0}\left(1 + \frac{m_2}{m_1}\right), \tag{1}$$

where E_0 is the energy originally absorbed (D_0 the corresponding dose) and E_r the radiation-equivalent stored energy (D the corresponding dose). The solution studied is supposed to be formed by the dissolution of m_1 g of an irradiated solid in m_2 g of the measuring liquid.

If the G-value is well known (e.g. 15.6 for the iron system [3]) the calculation of energy is made straightforwardly. It should be stressed, however, that this conversion to radiation dosimetry units rests upon the assumption that part of the stored energy behaves like radiation during dissolution. This important point will be discussed further in Section VII of this paper.

Before equivalent doses are evaluated, the result for the blank test at each dose must be subtracted. Fig. 6 shows the energy storage in sodium chloride found using the procedure described. The results orginate from the data given in Fig. 1, i.e. using the iron system. Fig. 7 gives the corresponding radiomimetic efficiency. This property, of course, drops steadily because of the saturation tendency in the irradiation effect itself (cf. Figs. 1, 2 and 6). At 10 Mrad η_r was found to be about 0.2 %.

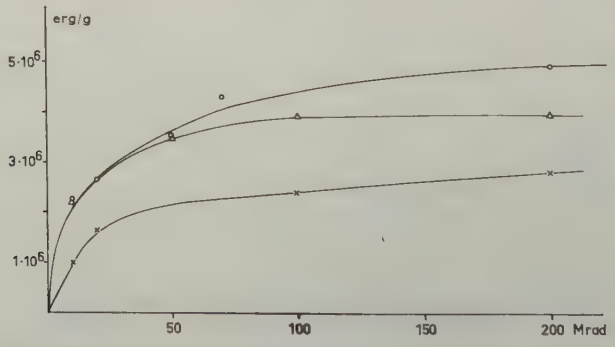

Fig. 6. Stored energy in irradiated NaCl as found by the Fricke dosimeter. (Symbols, see Fig. 1.)

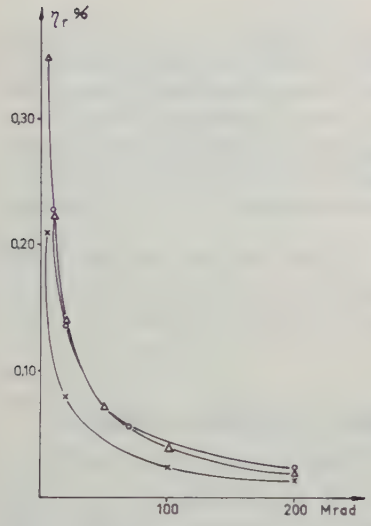

Fig. 7.

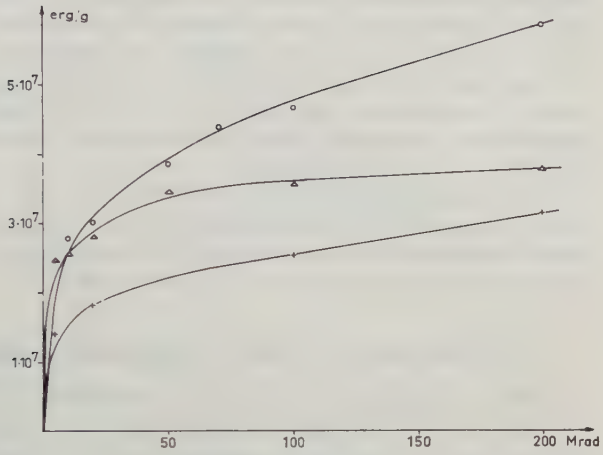

Fig. 8.

Fig. 7. Radiomimetic efficiency η_r for NaCl as found by the Fricke system (cf. Fig. 6).

Fig. 8. Stored energy for NaCl as found by the water–chloroform–KI method.

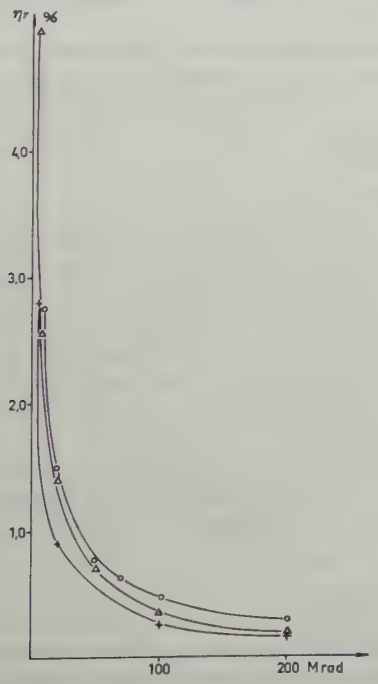

Fig. 9.

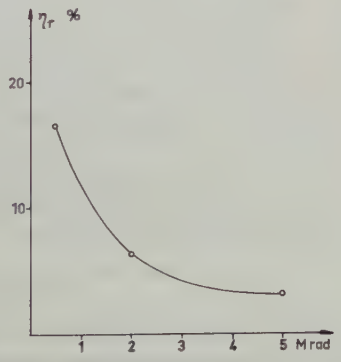

Fig. 10.

Fig. 9. Radiomimetic efficiency η_r as found for NaCl from data in Fig. 8.

Fig. 10. η_r for NaCl for small doses as measured by the chloroform method (irradiation at Risø).

Figs. 8 and 9 give the energy stored and radiomimetic efficiency for sodium chloride using the chloroform-potassium iodide system. (The G-value for the formation of iodine atoms was found to be 1.1 when KI was present.) The behaviour of the curves is seen to be very similar to that for the Fricke measuring system (cf. Figs. 6, 7). An important difference exists, however, in the fact that the energies are about a factor of 10 higher (for example, η_r is ~ 3 % at 10 Mrad). The results from the irradiations at Risø, Denmark, yielded the highest η_r figures obtained, cf. Fig. 10 (highest η_r figure is ~ 15 % at 0.5 Mrad).

As was described above, the results with the organic solids were not unambiguous, except perhaps for sucrose and glycine. The extrapolation of the Fe^{3+} amounts back to the time of dissolution yielded an η_r value of the order of 1 % for sucrose. A further discussion of these data will be given in Section VII.

VI. Experiments to remove irradiation effects in solid sodium chloride

A series of experiments were made to see whether the irradiation effect, as detected with the chemical systems described, could be removed by heating. It was found that keeping the irradiated material at 175°C gradually decreased the effect (cf. Fig. 11). After 24 hours' heating, it was no longer possible to detect it. The blank tests at each dose did not follow the same downward path as the main samples but showed a peculiar maximum. After this, the values, however, decreased to zero.

In another experiment, it was found that at 210°C the effect disappeared within less than 4 h.

The fact that samples have been kept for one year at room temperature without more than a 10 % reduction in the effect stands in good agreement with these findings.

VII. Discussion

1. *General*

An exact discussion of the mechanisms of the chemical reactions reported would presume (*a*) an exact knowledge of the physical changes due to irradiation in ionic crystals and organic covalent solids and (*b*) an exact knowledge of the nature of the process of interaction between the entities and of the structural changes induced by radiation occurring in the solvent and the solute. The latter may *a priori* consist of several kinetic steps linked together. Concerning the former, many physical investigations, e.g. those using electron spin resonance techniques, have been published and many more are likely forthcoming in the near future.

In our studies, the aim is to produce such basic information. At present, the information is however not ample enough to permit far-reaching conclusions. Some points can be put forward but, in other aspects of the problem, the discussion must necessarily be superficial at present.

2. *Ionic crystals*

The residual effect of irradiation on ionic crystals (such as NaCl) seems to be dominated by F-center formation, i.e. electrons being trapped in anion vacancies [12]. The electron set free is assumed to reach the conduction band and may then be trapped in a vacancy of this type. Fig. 12 gives a crude picture of the energetic conditions.

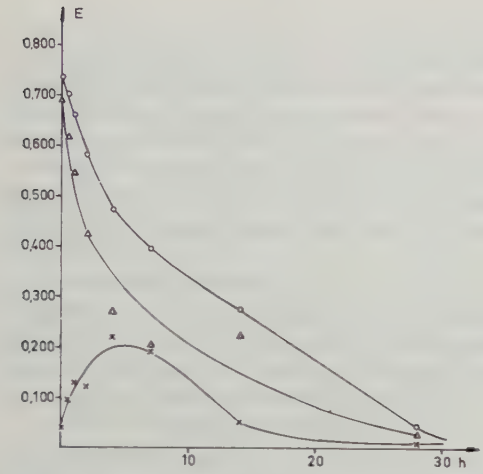

Fig. 11.

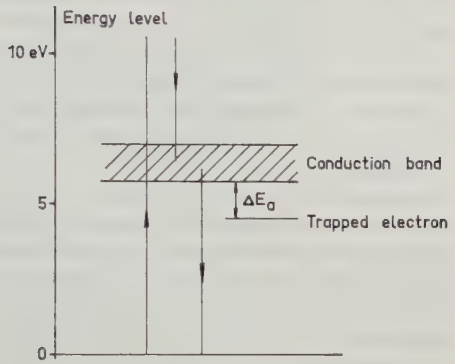

Fig. 12.

Fig. 11. Destruction of irradiation effect in NaCl at 175°C. Upper curve (circles) is main test, crosses are blank tests and triangles net effect. It is seen that the effect disappears almost completely after 30 h.

Fig. 12. Simplified model of trapped electron effect in sodium chloride. ΔE_a is trap depth or activation energy for thermoluminescence.

It is known that F-centers are produced not only by ionizing radiations but also by U.V. light [5, 12] (provided absorption bands are present).

These effects are responsible for the colours and the concentration of F-centers can be measured optically by means of transmission experiments [12]. Detection is also possible using electron spin magnetic resonance measurements (see, for instance, ref. 10 in [1]). There are various types of centers corresponding to different types of structural changes [12]. However, the F-centers might be the most important ones and so only these will be considered at this stage.

The minimum energy needed to produce an F-center is known from optical studies [12] (from the quantum energy of the exciting absorption bands). The figure is ~ 6 eV for NaCl. Heating provides the activation energy necessary to raise the electron to the conduction band where de-excitation may occur. The order of magnitude is 0.3–1 eV [19]. The energy release can be measured calorimetrically or by the thermoluminescence [19]. It should be noted that the light emitted is of longer wavelength than the exciting light. The kinetics of these processes would provide the activation energy data described.

The dissolution of ionic crystals in water solutions must in some way destroy the structural defects. The resultant energy release may be assumed to be of the same order as that shown in Fig. 12. This energy may *a priori* excite the solvent electronically (H_2O^* for instance), after which chemical changes may take place. Provided the energy release in the process is larger than the bond energies of the solvent, it is possible that bond rupture and free radical formation may take place. In water, H and OH radicals might be formed. The dissociation energy needed is 5.1 eV [6]. The fate of the free electron must also be considered. It may be captured by the solvent and thus, in water, form a polaron in the sense of Weiss [7]. This entity might then eventually yield hydrogen or hydrogen radicals and hydroxyl ions.

It is thus seen that these very simplified pictures provide some favourable arguments for linking, with radiation chemistry, the effects produced upon dissolving irradiated ionic crystals. It might be added that the existence, after irradiation, of multiply ionized entities such as Cl^+ provide conditions of very high potential energy [4] (12–15 eV). The dissolution reactions of such species are likely to bring about radiation-like effects, although their occurrence may be smaller than that of F-centers. Interaction of the primary particles will also yield Cl-atoms and these have actually been detected [13]. (The presence of free sodium has also been stated by the same authors.)

Turning now to the experiments reported here, we note that the blank test *a priori* eliminates chemical changes interfering with the measuring system which is designed to respond only to radiation-equivalent doses. For instance, halogen atoms should react similarly in the main and blank tests. It should then be possible, after calibration, to express the difference in radiation-like doses, provided no halogen evaporation takes place (this is unlikely at the concentrations used).

If our views are correct, we would expect a production of luminescence upon dissolution in suitable liquid systems containing fluorescent solutes. Such an observation should, qualitatively, confirm the chemical experiments. In fact, we have observed such effects and the results obtained are described in another paper [14].

The experiments with chloroform in water might be taken as an indication that an actual release of at least the dissociation energy (C–Cl) takes place. The experiments with the same system plus iodide ions and with the ferrous dosimeter could be criticized and stated to be a trivial oxidation effect requiring very little energy [1] in relation to that needed in general for the indiscriminate covalent bond breaking characteristic for ionizing radiation. But, together with the evidence of the chloroform–water system and the luminescence experiments, we have additional evidence against such an interpretation.

The fact that the energy release measured with the chloroform system is higher than that with the Fricke system may be related to the difference in bond energies of C–Cl and H–OH (2.9 and 5.1 eV, respectively) but surface chemical effects [1], which escape the calibration using the γ-source, may also enter in the case of the chloroform–water system. (If so, the very high η_r-figures are not real.)

The energies found are roughly of the same order as those given by Przibram as the energies required for F-center formation [12] (p. 64, Tables 9 and 10). These figures (as η-values) range from 0.115 to 0.041 for beta rays, are lower for alpha particles (0.027–0.00025) and show the same behaviour as the radiomimetic efficiencies found here. This qualitative tendency towards saturation is very similar to that found in electron spin resonance experiments. The dependence of the yield [12] on dose rate is not unambiguous in our experiments. It is known that the occurrence of vacancies before irradiation has a strong influence on the yield of F-centers [20]. This may explain why different chemical yields were obtained with materials of different origin.

The results of the heating experiments and the fact that the irradiated materials can be stored at room temperature apparently for years is in good agreement with the data from thermoluminescence.

It would be a natural step to extend these studies to other alkali halides and ionic crystals and also to extend the measuring methods to oxygen-free solutions and other systems. The interrelationships with electron spin resonance experiments will also be investigated. Irradiations with other kinds of particles would also be of interest.

3. *Organic solids*

The results for sucrose (and perhaps glycine) with the ferrous system are quite clear but, on the other hand, no response at all was found with the chloroform–iodide water system. Apparently we are faced here with much more complicated systems than for ionic crystals and, as is seen, complicated after-effects occur.

Even if the organic solids are quite different from ionic crystals, F-centers have nevertheless been observed [15]. The energy levels are not known with any accuracy. Numerous electron spin resonance investigations have revealed the existence of unpaired electrons (see [1], refs. 13–16). These are termed free radicals and have sometimes been identified but less attention seems to have been paid to the energetic considerations involved. It seems that free radicals, when set free by dissolution, do not in general possess the same high potential energies as is the case for ionic species of radical character. On the other hand, oxygen and the formation of peroxides seem to be important for the subsequent chemical reactions.

The fact that no iodine could be detected, whereas iron oxidation took place and was thereafter followed by reduction, might be compared with a statement [16] that iodine is reduced by freshly prepared solutions of irradiated organic solids. The presence of oxygen also complicates the interpretation. We shall not pursue the discussion further.

The radiomimetic effects observed in biological systems [17, 18] (see further [1], refs. 1–2) seem to apply for very wet conditions and may be explained by peroxide effects [16] rather than energy storage of the type described in this paper for solid substances. The experiments described in this paper may, however, indicate the necessity of further investigations about whether the energy stored in irradiated foods in the dry state involves hazards or not for human consumption. (Some observations on the influence of moisture will be given in our paper on luminescence effects [14].)

ACKNOWLEDGEMENTS

The authors are indebted to all the organizations mentioned in Table 1 for performing the irradiations and furnishing the dose data.

Division of Physical Chemistry, Royal Institute of Technology, Stockholm 70, Sweden.

REFERENCES

1. Westermark, T., Some points of view on stored energy in irradiated food, p. 28–36 in *Risø Report 16*, 1960 (papers presented at the first Nordic Meeting on Food Preservation by Ionizing Radiations, held at Risø, April 25–26, 1960).
2. Mohler, K. (Ed.), Chemische Reaktionen ionisierender Strahlen. Frankfurt a. M., 1958.
3. Weiss, J., Allen, A. O., and Schwarz, A., Inter. Conf. on Peaceful Uses of Atomic Energy (U.N.), Vol. *14*, 179 (1956).
4. Howard, R. E., and Schmoluchowski, R., *Phys. Rev. 116*, 314 (1959).
5. Mott, N. F., and Gurney, R. W., Electronic Processes in Ionic Crystals. Oxford, Clarendon Press 1948 (Ch. IV).
6. Coulson, C. A., Valence. Oxford, Clarendon Press 1958.
7. Weiss, J., *Nature 186*, 751 (1960).
8. Pauling, L., Nature of the Chemical Bond, 1945, p. 53 (Table 10–1).
9. Moody, G. J., and Philips, G. O., *Chemistry and Industry 40*, 1247 (1959).
10. Westermark, T., Report to F.O.A. 2, April 1951 (unpublished).
11. Boltz, D. F. (Ed.), Colorimetric Determination of Non-metals, 1958, p. 215.
12. Przibram, K., Verfärbung und Luminiscenz. Wien, 1953.
13. Hacskaylo, M. *et al.*, *J. Chem. Phys. 21*, 552 (1953); *Ibid. 21*, 1434 (1953).

14. WESTERMARK, T., and GRAPENGIESSER, B., Observations of light emitted upon dissolution in luminescent liquids of irradiated NaCl, LiF, KI and some organic solids. *Arkiv Kemi 17*, 139 (1960). See also by same authors: Observations of the emission of light on dissolution of irradiated solids in certain liquids. Short communication in *Nature 188*, No. 4748, 395 (1960).
15. ALGER, R. S., ANDERSON, T. H., and WEBB, L. A., *J. Chem. Phys. 30*, 695 (1959).
16. LÖFROTH, G., and EHRENBERG, L., *Risø Report 16*, p. 37, 1960, quoted in ref. 1.
17. NATARAJAN, A. T., *Risø Report 16*, p. 39, 1960, quoted in ref. 1.
18. STONE, W. S., *Proc. Nat. Acad. Sci. U.S. 33*, 59 (1947). See also Brookhaven Symposium on Biology *8*, 171, (1955).
19. HALPERIN, A., KRISTIANPOLLER, N., and BEN ZVI, A., *Phys. Rev. 116*, 1081 (1959); see also BONFIGLIOLI, G. *et al.*, *Phys. Rev. 114*, 151 (1959).
20. RØBIN, H., and KLICK, C. C., *Phys. Rev. 117*, 1005 (1960).

Note added in proof: The ordinates of Figs. 2 and 5 of ref. [1] should be raised by a factor of about ten because of a calculation error. These figures correspond to Figs. 6 and 8 in this paper, where correct data are given. Fig. 3 of ref. [1] corresponds to Fig. 7 in this paper. In this case, the ordinates in ref. [1] should be raised by a factor of about two.

Tryckt den 14 mars 1961

Uppsala 1961. Almqvist & Wiksells Boktryckeri AB

ARKIV FÖR KEMI Band 17 nr 13

Communicated 12 October 1960 by Karl Myrbäck and Arne Fredga

Substituent interactions in thiophenes

I. Preparation of disubstituted thiophenes

By Salo Gronowitz, Pinchas Moses,[1] Anna-Britta Hörnfeldt and Rolf Håkansson

With 2 figures in the text

Introduction

The extent of conjugation in some monosubstituted thiophenes has been studied earlier from the UV-spectra of these compounds [1] and from the C=O stretching frequencies in their IR-spectra [2]. Information about the electron-densities at the various ring hydrogens of these compounds has been obtained from a study of the chemical shifts in the NMR-spectra of monosubstituted thiophenes [3, 4].

By studying the disubstituted thiophenes from certain physico-chemical aspects, such as IR-, UV- and NMR-spectroscopy, polarography, dissociation constants, etc. much can be learned about the electronic and steric interactions of the substituents with each other and with the ring hydrogens. The non-equivalence of the two ortho-positions in 3-substituted thiophenes [5] makes a comparative study of 2,3- and 3,4-similarly substituted thiophenes particularly interesting.

Under the present project, disubstituted thiophenes have been prepared in connection with a general NMR-investigation of the thiophenes. From the NMR-spectra of disubstituted thiophenes, it is possible to establish the ranges of variation of the ring-coupling constants of these compounds, such information making NMR-spectroscopy an extremely useful tool for structure determination of disubstituted thiophenes [6, 7]. Special emphasis has been placed on the preparation of such compounds containing the aldehyde, methyl or thiol groups, since these compounds also lend themselves to an investigation of the side-chain couplings to the ring hydrogens [8] and intercoupling between two side-chains [9]. Such a study should facilitate the understanding of the mechanism of spin-spin coupling in general.

Preparation of disubstituted thiophenes

A dominating feature in the chemistry of thiophene is the much greater reactivity of the α-positions over the β-positions with respect to most substitution reactions (for review, cf. [5]). In such reactions involving β-substituted thiophenes, the entering group will occupy either one or the other of the free α-positions and the product will consist either of pure 2,3- or 3,5-disubstituted thiophenes or of a mixture of these two isomers. In the case of the α-substituted thiophenes, the product will consist

[1] On leave of absence from the Hebrew University of Jerusalem, Israel.

either of pure 2,5-disubstituted thiophene or more generally of mixtures containing the 2,3- or 2,4-isomers as well. The product actually obtained will depend upon the type of substituent already present and the reagent used.

We shall first consider reactions involving a $\pm I + M$ 2-substituted thiophene. If the substituent is deactivating, e.g. halogen, the product will consist exclusively of the 2,5-isomer as illustrated by the halogenation [10] and nitration [11] of the 2-halothiophenes. With activating substituents, e.g. methyl [12] or methoxy [13], the product will in general consist of mixtures of the 2,5- and 2,3-isomers. For example, nitration of 2-methylthiophene [14] gave ca. 70 % of the 2,5-isomer and 30 % of the 2,3-isomer in contrast with the findings of an earlier worker [15].

The reagent used often has a decisive influence on the orientation. Bromination of 2-methylthiophene with N-bromosuccinimide gave isomer-free 5-bromo-2-methylthiophene [16, 17] and metalation with organolithium compounds results exclusively in the 2,5-isomer. Thus Sicé [13] has prepared 5-methyl-2-methoxythiophene and 2-methoxy-5-thiophenealdehyde by reacting the corresponding organolithium compound with methyl sulphate and *N*,*N*-dimethyl formamide respectively, and the present authors have prepared 2-*t*-butyl-5-thiophenecarboxylic acid and 5-methylthio-2-methylthiophene by reacting the corresponding organolithium compound with carbon dioxide and dimethyl disulphide respectively.

The commercial availability of 3-methylthiophene and the easy preparation of 3-bromothiophene [18] and other 3-substituted thiophenes from it [5] make the use of 3-substituted thiophenes as starting materials for disubstituted thiophenes practicable. Electrophilic substitution reactions with $\pm I + M$ 3-substituted thiophenes lead in some cases to mixtures of 2,3- and 3,5-isomers, the former predominating (for review, cf. [5, 19]). For example, acylation [20] and formylation of 3-methylthiophene lead to mixtures containing 80–85 % of the 2,3- and 15–20 % of the 3,5-isomer. Bromination, however, seems to lead exclusively to the 2,3-isomer, as illustrated by the bromination of 3-methyl- [21], 3-bromo- [22] and 3-acetaminothiophene [23]. Thus isomer-free 3-methyl-2-thiophenealdehyde could not be prepared directly by the Vielsmeyer formylation [24, 25] but could be obtained by a sequence involving bromination of 3-methylthiophene, formation of the Grignard reagent from it followed by reaction with *N*,*N*-dimethyl formamide. Wolf-Kishner reduction gave pure 2,3-dimethylthiophene.

Metalation of 3-methoxy- [26], 3-*t*-butoxy- [7] and 3-methylthio-thiophene [6] leads exclusively to the 2,3-isomer, whilst with 3-methylthiophene [cf. [27]) a mixture containing ca. 85 % of the 3,5- and 15 % of the 2,3-isomer is obtained.

Considering $-I - M$ 2-substituted thiophenes, mixtures of the 2,4- and 2,5-isomers are generally obtained, the composition of which varies with the deactivating strength of the substituent [28].

These reactions are generally impracticable, as the isolation of a pure isomer is often tedious and difficult. In some cases, however, separation of the components can be achieved without any great difficulties [29, 30]. In the bromination of 2-thiophenealdehyde only the 2,5-isomer is obtained [31, 32].

Substitution reactions involving $-I - M$ 3-substituted thiophenes lead exclusively to the 3,5-isomers. Campaigne & Bourgeois [33] have prepared 5-nitro-, 5-chloro- and 5-bromo-3-thiophenecarboxylic acid[1] by direct substitution of 3-thiophene-

[1] The present authors found that this compound melted at 141–142°, which differs from the m.p. found by Campaigne & Bourgeois [33] and later by Lawesson [34], who report an m.p. of 117–118°.

carboxylic acid and the present authors have prepared 5-nitro-3-thiophenealdehyde by direct nitration of 3-thiophenealdehyde. Bromination of 3-thiophenealdehyde under the conditions used for 2-thiophenealdehyde [31] resulted in ill-defined products only.

As in the benzene series, it is possible to obtain an otherwise difficultly accessible isomer by blocking reactive positions with easily removable groups. The carboxyl group in particular has served as such a blocking agent in the thiophene series, as exemplified by the preparation of 2-bromo-3-nitrothiophene [35] and the now outdated preparation of 2,3-dibromothiophene [36]. Decarboxylation is effected with mercuric acetate, or with copper and quinoline. Bromine has also been used as a protective group [17, 18, 37]. A further example is the alternative preparation of 2-methyl-3-bromothiophene [cf. [17]) given in this paper. It can conveniently be removed by zinc [17, 18] or copper [37] reduction or with hypophosphorous acid [37].

Sometimes a desired disubstituted thiophene can be prepared by a sequence of reactions involving modification of a substituent already present. Thus we prepared 2-bromo-3-thiophenealdehyde through the Sommelet reaction with 2-bromo-3-bromomethylthiophene. Although we followed the conditions recommended by Angyal [38] for better yields, we found that this was not much better than that given by Campaigne & LeSuer [39] in their original synthesis. Oxidation of the aldehyde group to the corresponding acid [39] or reduction of nitrothiophenecarboxylic acid to the amino compound [40] are further examples of this approach.

Nucleophilic substitution of activated halothiophenes has been used to some extent for the preparation of disubstituted thiophenes [40, 41] as exemplified by the preparation of 5-nitro-2-cyanothiophene from 5-nitro-2-iodothiophene.

The four isomeric dibromothiophenes have proved extremely useful starting materials for a great variety of disubstituted thiophenes. Most of the disubstituted thiophenes described in this paper have been prepared from them. Through halogen-metal interconversion, one of the bromine atoms can be selectively exchanged for a lithium atom, and the resulting organolithium compound can be made to react with suitable reagents to give a variety of substituted bromothiophenes. Bromo-substituted thiophenecarboxylic and boronic acids have been prepared by the reaction of bromothienyllithium with carbon dioxide [42, 43] and *n*-butyl borate [44] respectively, bromomethylthiothiophenes through the reaction with dimethyl disulphide [17] and bromothiophenethiols through the reaction with sulphur [45].

The current paper describes the preparation of 3- and 4-bromo-2-thiophenealdehyde and of 4-bromo-3-thiophenealdehyde by this method. 3-Bromo-2-thiophenealdehyde has recently been obtained by the Vielsmeyer formylation using phosphorous oxybromide as the condensing agent [35]. With phosphorous oxychloride, halogen exchange occurs, and a mixture of 3-bromo- and 3-chloro-2-thiophenealdehyde is obtained [46].

The substituted bromothiophenes may be subjected to further halogen-metal interconversion, and a second substituent may thus be introduced, providing that the first substituent does not interfere in the interconversion reaction. Thus 4-methylthio-3-thiophenealdehyde has been prepared from 3,4-dibromothiophene by stepwise conversion via 3-bromo-4-thienyllithium, 3-bromo-4-methylthio-thiophene, and 4-methylthio-3-thienyllithium, the appropriate reagents being *n*-butyllithium, dimethyl disulphide and *N*,*N*-dimethylformamide. Details are given in the experimental section.

Table 1. Physical constants of substituted thiophenealdehydes.

Compound	B.p.	M.p.	n_D^{20}	Semicarbazone m.p.
3-Methyl-2-thiophenealdehyde	100–101°/15 mm Hg		1.5882	194.5–195°
3-Bromo-2-thiophenealdehyde	114–116°/12 mm Hg	24–25°	1.6377	195–196°
4-Bromo-2-thiophenealdehyde	114–115°/11 mm Hg	44–45°		206–207°
2-Methyl-3-thiophenealdehyde	86–88°/12 mm Hg		1.5758	190–191°
2-Methylthio-3-thiophenealdehyde	119–121°/1.0 mm Hg		1.6506	180–182°
4-Methyl-3-thiophenealdehyde	82–84°/13 mm Hg		1.5765	194–195°
4-Methylthio-3-thiophenealdehyde	98–105°/0.3 mm Hg	53–55°		191–192°
4-Bromo-3-thiophenealdehyde	108–111.5°/11 mm Hg		1.6340	184–185°
5-Methylthio-3-thiophenealdehyde	83–85°/0.10 mm Hg		1.6300	173–174°
5-Nitro-3-thiophenealdehyde	137–141°/2 mm Hg	82.5–83.5°		215–216°

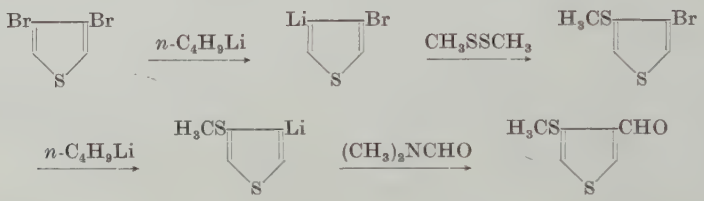

In a similar way, we have prepared 4-methylthio-3-thiophenecarboxylic acid, 2-methylthio-3-thiophenealdehyde and acid, and 2-methyl-3-thiophenealdehyde and some derivatives of these compounds. Table 1 gives some data about the aldehydes prepared. The thiols prepared under the present project are described elsewhere [45].

In the reactions involving organolithium reagents, it is of the utmost importance to adhere to rigid experimental conditions. It has often been necessary to prepare a substituted thienyllithium intermediate which tends to rearrange[1] to a more stable

Table 2. Physical constants of substituted thiophenecarboxylic acids and their methyl esters.

Acid	M.p.	Methyl ester b.p.	Methyl ester m.p.	Methyl ester n_D^{20}
4-Bromo-2-thiophenecarboxylic acid	122–123.5°	113–115°/9 mm Hg		1.5802
5-*t*-Butyl-2-thiophenecarboxylic acid	126.5–128°			
4-Bromo-3-thiophenecarboxylic acid	158–159°	126–128°/10 mm Hg	48.5–50°	
4-Methylthio-3-thiophenecarboxylic acid	159.5–160°	158°/11 mm Hg	76.5–78°	
4-Methylsulphonyl-3-thiophenecarboxylic acid	217–219°			
5-Methylthio-3-thiophenecarboxylic acid	78–80°	134–136°/9 mm Hg		1.5816

[1] Provisional experiments have shown that 3-bromo-4-thienyllithium rearranges under certain conditions to 3-bromo-2-thienyllithium [47]. We hope to study this further.

isomeric form, hence halogen metal interconversion has to be carried out at −70°. Further complications arise at higher temperature due to metalation taking place concurrently with halogen-metal interconversion [27, 42, 43].

However, IR- and NMR-spectroscopy showed that pure isomer-free compounds have been obtained in the reactions carried out under the correct experimental conditions, hence the substituted thienyllithium reagents serve as extremely useful intermediates for the preparation of hitherto only difficultly accessible compounds.

A detailed discussion of the proton spin-couplings in these and other disubstituted thiophenes is given elsewhere [14].

Some physical constants of the disubstituted thiophenes prepared in this study are collected in Tables 1 and 2.

Experimental

The preparations utilizing metalorganic compounds were carried out under nitrogen in a four-necked flask equipped with stirrer, dropping funnel and condenser.

Unless otherwise stated, the compounds prepared were isomerically pure, the purity being determined by IR- and NMR-spectroscopy. Melting points were determined with a hot-stage microscope.

2-t-Butyl-5-thiophenecarboxylic acid. 260 ml of 1.25-*N* *n*-butyllithium was added dropwise to 45.0 g (0.32 moles) of 2-*t*-butylthiophene [48] in 100 ml of ether and the solution refluxed for 45 min. The solution was poured onto solid carbon dioxide in ether and after the temperature had risen to −10°, the mixture was hydrolyzed with water. The ether phase was extracted with sodium carbonate solution and the combined aqueous phases acidified with 1:1 hydrochloric acid, giving 40 g (68 %) of crude acid. After one recrystallization from 450 ml of ligroin (b.p. 80–100°) 32.6 g (55 %) of pure acid, crystallizing in colourless needles of m.p. 126.5–128°, was obtained. (Literature value [49, 50] 124–125°.)

5-Methylthio-2-methylthiophene. 380 ml of 1.15-*N* *n*-butyllithium was added at refluxing rate to 42.8 g (0.437 moles) of 2-methylthiophene [51] in 100 ml of ether. After refluxing for half an hour, the reaction mixture was cooled to −40°, whereupon 41.0 g (0.437 moles) of dimethyl disulphide in 50 ml of ether was added in a slow stream. After 2 hours at room temperature the mixture was decomposed with water, the ether phase washed with dilute sodium hydroxide and water, dried over calcium chloride and fractionated. 47.0 g (75 %) of pure 5-methylthio-2-methylthiophene, b.p. 76–77°/10 mm Hg, $n_D^{20} = 1.5785$ was obtained.

Anal. $C_6H_8S_2$ (144.2)			
Calc.	C 49.96	H 5.58	S 44.45
Found	C 50.06	H 5.49	S 44.23

5-Methoxy-2-methylthiophene. 110 ml of 0.90-*N* *n*-butyllithium was added dropwise to 10.0 g (0.088 moles) of 2-methoxythiophene [13, 52] in 50 ml of ether. The solution was refluxed for half an hour and then pressed with nitrogen into a stirred solution of 22.3 g (0.12 moles) of methyl *p*-toluenesulphonate in 100 ml of ether. After being stirred for 3 hours at room temperature, the reaction mixture was poured into water. The ether phase was washed with water, dried over sodium sulphate and fractionated, yielding 8.8 g (78 %) of 5-methoxy-2-methylthiophene, b.p. 59.5–60.5°/15 mm Hg, $n_D^{20} = 1.5202$. (Literature values [13], b.p. 51–52°/10 mm Hg, $n_D^{18} = 1.5216$.)

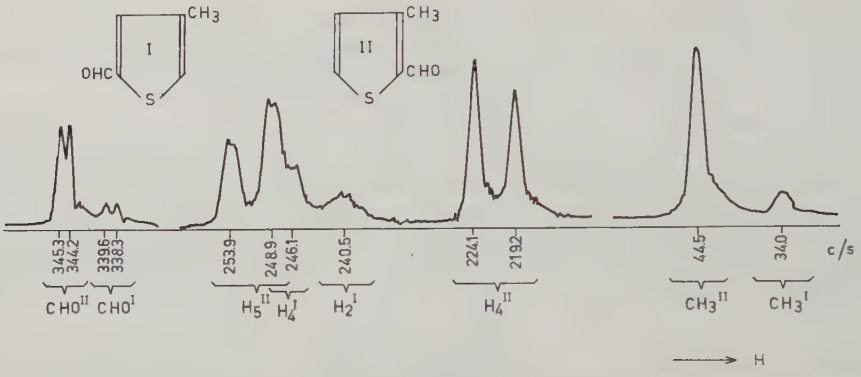

Fig. 1. NMR-spectrum at 40 Mc/s of the aldehyde mixture, obtained in the Vielsmeyer formylation of 3-methylthiophene, containing about 20 % of *cyclo*hexane as internal reference. The shifts are given in c/s relative to this reference. H_2^I denotes the resonance of hydrogen 2 in compound I, etc.

Formylation of 3-methylthiophene. This was carried out according to the description given in ref. [24]. From 25.0 g (0.255 moles) of 3-methylthiophene, 30 g (0.41 moles) of *N*,*N*-dimethyl formamide and 48 g (0.32 moles) of phosphorous oxychloride was obtained 20.0 g (62 %) of a product, b.p. 92°/10 mm Hg, n_D^{20} –1.5878. The product consisted of a mixture of 3-methyl-2-thiophenealdehyde and 3-methyl-5-thiophenealdehyde. NMR-spectral analyses showed the mixture to consist of 85 ± 3 % of the former and 15 ± 3 % of the latter.

The NMR-spectrum is shown in Fig. 1. The assignments of the different hydrogens were based on the characteristic ring-coupling constants ($J_{45} \approx 5.0$ c/s in a 2,3-disubstituted thiophene and $J_{35} \approx 1.5$ c/s in a 2,4-disubstituted thiophene) and on the characteristic side-chain couplings. The quantitative analysis was based on the areas of the methyl and aldehyde bands. (For a detailed discussion on the interpretation of the NMR-spectra of thiophenes, see [8, 14, 53, 54].)

3-Methyl-2-thiophenealdehyde. The Grignard reagent, prepared in the usual manner from 22.0 g (0.12 moles) of 3-methyl-2-bromothiophene [21] in 150 ml of ether and 4.1 g (0.17 moles) of magnesium, was pressed with nitrogen into a stirred solution of 19.7 g (0.27 moles) of *N*,*N*-dimethyl formamide in 100 ml of ether. The reaction mixture was refluxed for 2 hours and decomposed with excess dilute hydrochloric acid. The ether phase was washed with bicarbonate solution and water, dried over magnesium sulphate and distilled. 10.7 g (69 %) of pure 3-methyl-2-thiophenealdehyde, b.p. 100–101°/15 mm Hg, $n_D^{20} = 1.5882$ was obtained.

Semicarbazone. M.p. 194.5–195°.

Anal. $C_7H_9N_3OS$ (183.2)

Calc.	N 22.94
Found	N 22.80

2,3-Dimethylthiophene. 9.55 g (0.076 moles) of 3-methyl-2-thiophenealdehyde was reduced with a mixture of 28 ml of hydrazine hydrate (100 %), 67 ml of ethylene glycol and 17 g of potassium hydroxide, according to the description given by King & Nord for the preparation of 2-methylthiophene [51] from 2-thiophenealde-

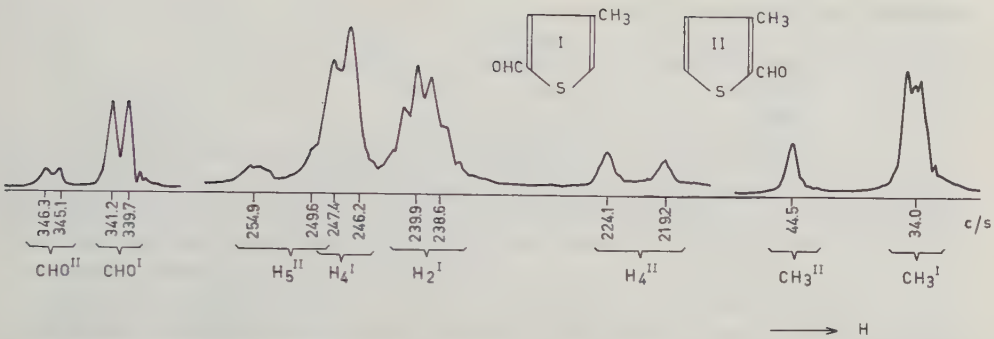

Fig. 2. NMR-spectrum at 40 Mc s of the aldehyde mixture, obtained in the reaction of 3-methylthiophene, *n*-butyllithium and *N*,*N*-dimethyl formamide, containing about 20 % of *cyclo*hexane as internal reference. The shifts are given in c s relative to this reference. H_2^I denotes the resonance of hydrogen 2 in compound I, etc.

hyde. 6.6 g (77 %) of 2,3-dimethylthiophene, b.p. 141–142°, $n_D^{20} = 1.5163$ was obtained. (Literature values [55], b.p. 140.2–141.2°, $n_D^{20} = 1.5188$.)

Metalation of 3-methylthiophene [56]. 170 ml of 1.47-*N* *n*-butyllithium was added dropwise to 25 g (0.255 moles) of 3-methylthiophene in 100 ml of ether and the mixture refluxed for half an hour. The reaction mixture was pressed with nitrogen into a stirred solution of 25 g (0.34 moles) of *N*,*N*-dimethyl formamide in 100 ml of ether. After standing at room temperature overnight, the reaction mixture was hydrolyzed with water. The ethereal layer was extracted twice with dilute hydrochloric acid, washed with dilute bicarbonate and water, dried over magnesium sulphate and fractionated *in vacuo*. 19.0 g (59 %) of an aldehyde mixture, b.p. 95–96°/11 mm Hg, $n_D^{20} = 1.5796$ was obtained. NMR-spectral analysis (Fig. 2) showed the mixture to consist of 83 ± 3 % of 3-methyl-5-thiophenealdehyde and 17 ± 3 % of 3-methyl-2-thiophenealdehyde, the assignments being determined as outlined above.

5-Nitro-3-thiophenealdehyde. To 55 g (0.57 moles) of sulphuric acid at −10° was added dropwise with stirring 22.5 g (0.20 moles) of 3-thiophenealdehyde [57], followed by the dropwise addition of a pre-cooled (−10°) mixture of 47 g (0.78 moles) of fuming nitric acid and 37 g (0.37 moles) of concentrated sulphuric acid. The temperature was kept at −10° throughout the addition. The reaction mixture was stirred at −10° for a further half hour, after which the temperature was allowed to rise to 0°. The reaction mixture was then poured into ice-water, the nitroaldehyde taken up in ether and the aqueous phase extracted several times with ether. The combined ether phases were washed with bicarbonate solution and water, dried over magnesium sulphate and distilled. 20.5 g (65 %) of crude 5-nitro-3-thiophenealdehyde, b.p. 137–141°/2 mm Hg, m.p. 70–78° was obtained. Two recrystallizations from 50 % aqueous ethanol yielded pure aldehyde, m.p. 82.5–83.5°.

Anal. $C_5H_3NO_3S$ (157.2)

Calc.	C 38.21	H 1.91	N 8.92	S 20.34
Found	C 38.16	H 1.87	N 8.87	S 20.25

Semicarbazone. M.p. 215–216°.

Anal. $C_6H_6N_4O_3S$ (214.2)

Calc.	N 26.16
Found	N 26.03

2-Bromo-3-thiophenealdehyde. A mixture of 40 g (0.15 moles) of crude 2-bromo-3-bromomethylthiophene [57], 44 g (0.31 moles) of hexamine and 130 ml of 50% acetic acid was refluxed for 4 hours. 60 ml of conc. hydrochloric acid was added and refluxing continued for 5 min. After cooling, the mixture was extracted with ether and the ether phase dried and distilled, yielding 7.3 g (25%) of crude 2-bromo-3-thiophenealdehyde, b.p. 105–110°/10 mm Hg. After one recrystallization from ligroin (b.p. 80–100°) the pure compound, melting at 34–35°, was obtained. (Literature value [39], m.p. 34°.)

3-Bromo-2-thiophenealdehyde. 170 ml of 0.82-*N* *n*-butyllithium was added dropwise to 29 g (0.12 moles) of 2,3-dibromothiophene [22] in 35 ml of absolute ether at −70°. After 5 min, the solution was pressed with nitrogen into a stirred solution of 13 g (0.18 moles) of *N*,*N*-dimethyl formamide in 67 ml of ether and the reaction mixture worked up as described above, yielding 16 g (70%) of crude aldehyde, b.p. 114–116°/12 mm Hg. Redistillation yielded pure aldehyde, b.p. 113–115°/10 mm Hg, m.p. 24–25°, $n_D^{20} = 1.6377$ (supercooled liquid). (Literature value [35], b.p. 91–92°/3 mm Hg.)

Anal. C_5H_3BrOS (191.1)

Calc.	C 31.43	H 1.58
Found	C 31.74	H 1.71

Semicarbazone. M.p. 195–196°.

Anal. $C_6H_6BrN_3OS$ (248.1)

Calc.	N 16.94
Found	N 16.92

4-Bromo-2-thiophenealdehyde. This was prepared from 12.1 g (0.050 moles) of 2,4-dibromothiophene [42] in 25 ml of ether, 200 ml of 0.25-*N* *n*-butyllithium and 8.0 g (0.11 moles) of *N*,*N*-dimethyl formamide in 50 ml of ether, as described above. 5.3 g (55%) of 4-bromo-2-thiophenealdehyde, b.p. 114–115°/11 mm Hg, m.p. 41–44° was obtained. Recrystallization from aqueous ethanol raised the m.p. to 44–45°.

Anal. C_5H_3BrOS (191.1)

Calc.	C 31.43	H 1.58
Found	C 31.44	H 1.59

Semicarbazone. M.p. 206–207°.

Anal. $C_6H_6BrN_3OS$ (248.1)

Calc.	N 16.94
Found	N 16.84

Methyl 4-bromo-2-thiophenecarboxylate. An ethereal solution of diazomethane was added dropwise to an ice-cold solution of 24.0 g (0.116 moles) of 4-bromo-2-thiophenecarboxylic acid [31, 42] in 150 ml of ether until the yellow diazomethane colour

persisted. Distillation yielded 20.7 g (81 %) of methyl 4-bromo-2-thiophenecarboxylate, b.p. 113–115°/9 mm Hg, $n_D^{20}=1.5802$.

4-Bromo-3-thiophenealdehyde. This was prepared in a similar manner to 3-bromo-2-thiophene aldehyde from 72.6 g (0.30 moles) of 3,4-dibromothiophene [17] in 75 ml of ether, 206 ml of 1.60-*N* *n*-butyllithium, and 33 g (0.47 moles) of *N*,*N*-dimethyl formamide. The dibromothiophene was added rapidly to the *n*-butyllithium at −70°. 44 g (77 %) of crude 4-bromo-3-thiophenealdehyde, b.p. 114–125°/14 mm Hg was obtained. Refractionation gave 27.2 g (47 %) of pure 4-bromo-3-thiophenealdehyde, b.p. 108–111.5°/11 mm Hg, $n_D^{20}=1.6340$.

Anal. C_5H_3BrOS (191.1)

Calc.	C 31.43	H 1.58
Found	C 31.40	H 1.66

Semicarbazone. M.p. 184–185°.

Anal. $C_6H_6BrN_3OS$ (248.1)

Calc.	N 16.94
Found	N 16.94

Methyl-4-bromo-3-thiophenecarboxylate. An ethereal solution of diazomethane was added dropwise to 23 g (0.11 moles) of 4-bromo-3-thiophenecarboxylic acid [43] in 100 ml of ether until the yellow diazomethane colour persisted. Distillation yielded 20.5 g (84 %) of methyl 4-bromo-2-thiophenecarboxylate, b.p. 126–128°/10 mm Hg, m.p. 48.5–50°.

4-Methylthio-3-thiophenealdehyde. This was prepared as described above from 20.9 g (0.10 moles) of 4-methylthio-3-bromothiophene [17] in 75 ml of ether, 127 ml of 0.83-*N* *n*-butyllithium and 11 g (0.15 moles) of *N*,*N*-dimethyl formamide, yielding 7.2 g (46 %) of 4-methylthio-3-thiophenealdehyde, b.p. 98–105°/0.3 mm Hg, m.p. 53–55°.

Anal. $C_6H_6OS_2$ (158.2)

Calc.	C 45.54	H 3.82	S 40.52
Found	C 45.74	H 3.86	S 40.18

Semicarbazone. M.p. 191–192°.

Anal. $C_7H_9N_3OS_2$ (215.3)

Calc.	N 19.52
Found	N 19.52

4-Methylthio-3-thiophenecarboxylic acid. A solution of 4-methylthio-3-thienyllithium, prepared at −70° from 39.7 g (0.19 moles) of 4-methylthio-3-bromothiophene [17] and 110 ml of 1.9-*N* *n*-butyllithium, was poured after 5 min onto solid carbon dioxide covered with ether. The reaction mixture was hydrolyzed with water and the ether phase extracted with 2-*N* sodium hydroxide. On acidification with hydrochloric acid, the combined aqueous phases yielded 28.8 g (87 %) of crude acid. Upon recrystallization from ethanol 19.5 g (60 %) of pure 4-methylthio-3-thiophenecarboxylic acid, m.p. 159.5–160°, crystallizing in fine needles, was obtained.

Anal. $C_6H_6O_2S_2$ (174.2)

Calc.	C 44.66	H 4.28	S 34.06
Found	C 44.67	H 4.28	S 34.07

Methyl 4-methylthio-3-thiophenecarboxylate. 8.7 g of 4-methylthio-3-thiophenecarboxylic acid was esterified with diazomethane. Distillation yielded 7.8 g (83 %) of methyl 4-methylthio-3-thiophenecarboxylate, b.p. 158°/11 mm Hg, m.p. 76.5–78°.

Anal. $C_7H_8O_2S_2$ (188.3)

Calc.	C 41.36	H 3.47	S 36.80
Found	C 41.42	H 3.48	S 36.75

4-Methylsulphonyl-3-thiophenecarboxylic acid. 8.7 g (0.05 moles) of 4-methylthio-3-thiophenecarboxylic acid in 80 ml of acetic acid was heated with 25 ml of 30 % hydrogen peroxide for 90 min on a steam-bath. After cooling somewhat, an equal volume of water was added and the mixture chilled in an ice-salt mixture. 8.4 g (81 %) of 4-methylsulphonyl-3-thiophenecarboxylic acid, m.p. 217–220° was collected. Recrystallization from ethanol yielded 7.3 g of pure crystals, m.p. 217–219°.

Anal. $C_6H_6O_4S_2$ (206.2)

Calc.	C 34.98	H 2.93	S 31.09
Found	C 34.88	H 2.97	S 30.94

2-Methylthio-4-thiophenealdehyde. This was obtained from 39.7 g (0.19 moles) of 2-methylthio-4-bromothiophene [17] in 75 ml of ether, 185 ml of 1.15-*N* *n*-butyllithium and 21.4 g (0.29 moles) of *N*,*N*-dimethyl formamide in 100 ml of ether. Fractionation yielded 17.5 g (58 %) of 2-methylthio-4-thiophenealdehyde, b.p. 83–85°/0.1 mm Hg, $n_D^{20} = 1.6300$.

Anal. $C_6H_6OS_2$ (158.2)

Calc.	C 45.54	H 3.82	S 40.52
Found	C 44.78	H 3.83	S 39.97

This compound gave persistently somewhat low carbon and sulphur values, although no impurity was detected in its NMR-spectrum.

Semicarbazone. M.p. 173–174°.

Anal. $C_7H_9N_3OS_2$ (215.3)

Calc.	N 19.52
Found	N 19.49

5-Methylthio-3-thiophenecarboxylic acid. A solution of 5-methylthio-3-thienyllithium, prepared from 10.5 g (0.050 moles) of 5-methylthio-3-bromothiophene [17] in 40 ml of ether and 44 ml of 1.25-*N* *n*-butyllithium, was poured onto carbon dioxide and the mixture worked up as before. 7.3 g (84 %) of crude acid, m.p. 76–79°, was obtained. Recrystallization from 50 % ethanol yielded 6.0 g (69 %) of pure acid, m.p. 78–80°.

Anal. $C_6H_6O_2S_2$ (174.2)

Calc.	C 41.36	H 3.47	S 36.80
Found	C 41.05	H 3.45	S 36.50

Methyl 5-methylthio-3-thiophenecarboxylate. This was prepared in the usual manner with diazomethane. B.p. 134–136°/9 mm Hg, $n_D^{20} = 1.5816$.

2-Methylthio-3-thiophenealdehyde. This was prepared from 20.9 g (0.10 moles) of 2-methylthio-3-bromothiophene [17] in 75 ml of ether, 85 ml of 1.30-*N* *n*-butyllithium

and 11.0 g (0.15 moles) of *N*,*N*-dimethyl formamide in 75 ml of ether. Fractionation yielded 10.7 g (68 %) of pure compound, b.p. 119–121°/1.0 mm Hg, $n_D^{20} = 1.6506$.

Anal. $C_6H_6OS_2$ (158.2)

Calc.	C 45.54	H 3.82	S 40.52
Found	C 45.65	H 4.06	S 40.11

Semicarbazone. M.p. 180–182°.

Anal. $C_7H_9N_3OS_2$ (215.3)

Calc.	N 19.52
Found	N 19.47

3,5-Dibromo-2-methylthiophene. A solution of 60 ml (1.10 moles) of bromine in 80 ml of chloroform was added dropwise during 3 hours to a solution of 50.0 g (0.51 moles) of 2-methylthiophene [51] in 200 ml of chloroform at 0°. After standing at room temperature overnight, the chloroform was distilled off and the residue refluxed for 5 hours with 100 ml of 30 % alcoholic potassium hydroxide. The organic phase was separated, washed with water, dilute hydrochloric acid and water, dried over calcium chloride and distilled, yielding 94.5 g (72 %) of crude product, b.p. 98–108° (mainly 98–102°)/11 mm Hg. Refractionation yielded 81 g (62 %) of pure compound, b.p. 98.5–100°/10 mm Hg, n_D^{20} 1,6080. (Literature value [12], b.p. 227.5–230°.)

3-Bromo-2-methylthiophene. 47 g (0.18 moles) of 3,5-dibromo-2-methylthiophene was added to a refluxing mixture of 60 ml of water, 20 g of zinc powder and 25 ml of acetic acid. The reaction mixture was refluxed for 20 hours and then distilled from the reaction flask. The aqueous layer of the distillate was separated from time to time from the organic phase and returned to the reaction vessel. The organic phase was washed with sodium carbonate solution and water, dried over calcium chloride and fractionated yielding 22 g (69 %) of pure compound, b.p. 174–177°, $n_D^{20} = 1.5735$. Its IR-spectrum was identical with that of authentic 3-bromo-2-methylthiophene [17], b.p. 173–174°, $n_D^{20} = 1.5752$.

2-Methyl-3-thiophenealdehyde. 122 ml of 1.07-*N* *n*-butyllithium was added rapidly to 22 g (0.125 moles) of 2-methyl-3-bromothiophene in 100 ml of ether at −70°. After 5 min, the solution was pressed over into 18.3 g (0.25 moles) of *N*,*N*-dimethylformamide in 50 ml of ether (Mixture A). A large amount of solid crystallized out in the first flask, which could not be pressed over into the dimethyl formamide solution. This was treated with 50 ml of ether followed by a solution of 18 g (0.25 moles) of *N*,*N*-dimethyl formamide in 50 ml of ether (Mixture B). Both mixtures were allowed to stand overnight at room temperature, then hydrolyzed and worked up as usual. Upon fractionation, A yielded 6.5 g (41 %) of crude aldehyde, b.p. 92–105°/17 mm Hg, $n_D^{20} = 1.5638$, and B yielded 4.4 g (27 %) of a purer product, b.p. 86–88°/12 mm Hg, $n_D^{20} = 1.5758$. The two fractions were combined and refractionated, giving 7.0 g (44 %) of pure 2-methyl-3-thiophenealdehyde, b.p. 80.5–82°/10 mm Hg, $n_D^{20} = 1.5741$, which solidified when stored at −15°.

Anal. C_6H_6OS (126.2)

Calc.	C 57.06	H 4.79	S 25.39
Found	C 57.03	H 4.98	S 25.09

Semicarbazone. M.p. 190–191°.

Anal. $C_7H_9N_3OS$ (183.2)

Calc.	N 22.94
Found	N 22.94

4-Methyl-3-thiophenealdehyde. To 85 ml of 1.60-*N* *n*-butyllithium was added 21.7 g (0.123 moles) of 4-methyl-3-bromothiophene [17] in 50 ml of ether at −70° and the mixture pressed after 5 min into 15 g (0.21 moles) of *N*,*N*-dimethyl formamide in 50 ml of ether. After the usual work-up, 8.9 g (57 %) of crude 4-methyl-3-thiophenealdehyde, b.p. 80–105°/11 mm Hg was obtained. Refactionation yielded 4.1 g of pure 4-methyl-3-thiophenealdehyde, b.p. 82–84°/13 mm Hg, $n_D^{20} = 1.5765$.

Anal. C_6H_6OS (126.2)

Calc.	C 57.06	H 4.79	S 25.39
Found	C 56.23	H 4.86	S 25.24

Semicarbazone. M.p. 194–195°.

Anal. $C_7H_9N_3OS$ (183.2)

Calc.	N 22.94
Found	N 22.91

A Perkin Elmer model 21 spectrometer equipped with a sodium chloride prism was used for the IR-measurements. The NMR-spectra were obtained at 40 Mc/s with a Varian Associates model V-4300B high resolution NMR-spectrometer and a flux stabilized 12″ electromagnet from the same company.

SUMMARY

Disubstituted thiophenes have been prepared for a study of their NMR-spectra.

A discussion of the available methods for the preparation of such compounds is given. Most of the compounds prepared have been obtained through the reaction of substituted thienyllithium intermediates with *N*,*N*-dimethyl formamide or carbon dioxide. The preparation of some new substituted 2-and 3-thiophenealdehydes is given.

ACKNOWLEDGEMENTS

The authors wish to express their thanks to Prof. Arne Fredga for his interest in this work and for all facilities put at their disposal. Thanks are also due to Dr. R. Hoffman for recording and discussing the NMR-spectra and to Mr. S. Johansson for recording the IR-spectra. The elementary analyses were carried out at the Analytical Department of the Chemical Institute. Grants from the *Swedish Natural Science Research Council* to S.G. are gratefully acknowledged.

Chemical Institute, University of Uppsala, Sweden, October 1960.

REFERENCES

1. GRONOWITZ, S., *Arkiv Kemi 13*, 239 (1958).
2. GRONOWITZ, S., and ROSENBERG, A., *Arkiv Kemi 8*, 23 (1955).
3. GRONOWITZ, S., and HOFFMAN, R. A., *Arkiv Kemi 13*, 279 (1958).
4. —— ibid. *16*, 539 (1960).
5. GRONOWITZ, S., *Arkiv Kemi 13*, 295 (1958).
6. —— ibid. *13*, 269 (1958).
7. —— ibid. *16*, 363 (1960).
8. GRONOWITZ, S., and HOFFMAN, R. A., *Acta Chem. Scand. 13*, 1687 (1959).
9. —— *Arkiv Kemi 15*, 499 (1960).

10. Coonradt, H. L., Hartough, H. D., and Johnson, G., *J. Am. Chem. Soc. 70*, 2564 (1948).
11. Babasinian, V. S., *J. Am. Chem. Soc. 57*, 1763 (1935).
12. Steinkopf, W., *Ann. 513*, 281 (1934).
13. Sicé, J., *J. Am. Chem. Soc. 75*, 3697 (1953).
14. Hoffman, R. A., and Gronowitz, S., *Arkiv Kemi 16*, 563 (1960).
15. Rinkes, I. J., *Rec. trav. chim. 51*, 1134 (1932).
16. Dittmer, K., Martin, R. P., Herz, W., and Cristol, S. J., *J. Am. Chem. Soc. 71*, 1201 (1949).
17. Gronowitz, S., Moses, P., and Håkansson, R., *Arkiv Kemi 16*, 267 (1960).
18. Gronowitz, S., *Acta Chem. Scand. 13*, 1045 (1959).
19. Hartough, H. D., Thiophene and its Derivatives. New York, 1952, pp. 145 ff.
20. Hartough, H. D., and Kosak, A. I., *J. Am. Chem. Soc. 69*, 3093 (1947).
21. Steinkopf, W., and Penz, H., *Ann. 515*, 273 (1935).
22. Lawesson, S.-O., *Arkiv Kemi 11*, 373 (1957).
23. Campaigne, E., and Monroe, P. A., *J. Am. Chem. Soc. 76*, 2447 (1954).
24. Campaigne, E., and Archer, W. L., *J. Am. Chem. Soc. 75*, 989 (1953).
25. Lamy, J., Lavit, D., and Buu-Hoi, Ng. Ph., *J. Chem. Soc. 1958*, 4202.
26. Gronowitz, S., *Arkiv Kemi 12*, 239 (1958).
27. —— ibid. *7*, 361 (1954).
28. Tirouflet, J., and Fournari, P., *Compt. rend. 246*, 2003 (1958).
29. Reynaud, P., and Delaby, R., *Bull. chim. France 1955*, 1614.
30. Blatt, A. H., Bach, S., and Kresch, L. W., *J. Org. Chem. 22*, 1693 (1957).
31. Gronowitz, S., *Arkiv Kemi 8*, 87 (1955).
32. Buu-Hoi, Ng. Ph., and Lavit, D., *J. Chem. Soc. 1958*, 1721.
33. Campaigne, E., and Bourgeois, R. C., *J. Am. Chem. Soc. 76*, 2445 (1954).
34. Lawesson, S.-O., *Arkiv Kemi 11*, 345 (1957).
35. Nishimura, S., Motoyama, R., and Imoto, E., *Bull. Univ. Osaka Prefect.* Ser. *A 6*, 127 (1958).
36. Steinkopf, W., and Köhler, W., *Ann. 532*, 250 (1937).
37. Blatt, A. H., Gross, N., and Tristiam, H. W., *J. Org. Chem. 22*, 1588 (1957).
38. Angyal, S. J., *Organic Reactions, 8*, 197 (1954).
39. Campaigne, E., and LeSuer, W. M. J., *J. Am. Chem. Soc. 71*, 333 (1949).
40. Dann, O., *Ber. 76*, 419 (1943).
41. Hurd, C. D., and Kreuz, K. L., *J. Am. Chem. Soc. 74*, 2965 (1952).
42. Lawesson, S.-O., *Arkiv Kemi 11*, 317 (1957).
43. —— ibid. *11*, 325 (1957).
44. —— ibid. *11*, 387 (1957).
45. Gronowitz, S., Moses, P., and Hörnfeldt, A.-B., *Arkiv Kemi*, in print.
46. Gronowitz, S., and Hoffman, R. A. Unpublished results.
47. Gronowitz, S., and Moses, P. To be published.
48. Ref. 19, p. 497.
49. Hartough, H. D., and Conley, L. G., *J. Am. Chem. Soc. 69*, 3096 (1947).
50. Schick, J. W., and Hartough, H. D., *J. Am. Chem. Soc. 70*, 1645 (1948).
51. King, W. J., and Nord, F. F., *J. Org. Chem. 14*, 638 (1949).
52. Profft, E., *Ann. 622*, 196 (1959).
53. Hoffman, R. A., and Gronowitz, S., *Arkiv Kemi 16*, 501 (1960).
54. —— ibid. *16*, 515 (1960).
55. Ref. 19, p. 68.
56. Sicé, J., *J. Org. Chem. 19*, 70 (1954).
57. Gronowitz, S., *Arkiv Kemi 8*, 441 (1955).

Tryckt den 30 januari 1961

Uppsala 1961. Almqvist & Wiksells Boktryckeri AB

ARKIV FÖR KEMI Band 17 nr 14

Communicated 12 October 1960 by Arne Fredga

Synthetic estrogenic isoflavonoids

II. The synthesis of $C^{14}_{(4)}$–labelled biochanin A[1]

By Anna Nilsson, Salo Gronowitz and Rolf Ekman

The interest in the plant estrogens has increased in recent years for several reasons. Excessive ingestion of forage rich in estrogens has resulted in breeding disorders similar to those which occurred in sheep grazing on subterranean clover pastures in Australia [1]. Later there have been from different parts of the world reports of similar disturbances in the reproductive system in cattle [2], wethers [3] and lambs [4] grazing on red clover pastures.

The demonstration of improved feed efficiency and rate of growth in cattle and sheep fed synthetic estrogens, suggests that the natural estrogens may have a similar beneficial effect. Recent work has also shown that animals fed a basic diet rich in plant estrogens are less responsive to synthetic estrogens [5, 6]. Only in a few cases is the chemical nature of the plant estrogens known. Genistein [7] has been isolated as the principal estrogen in *Trifolium subterraneum* and genistein-4′-methylether, biochanin A [8], in *Trifolium pratense*. More recently coumestrol has been found to be the estrogenic factor in *Trifolium repens* [9].

The estrogenic potency of the isoflavones, genistein and biochanin A is low, the activity being only 10^{-5} times that of diethyl stilbestrol when orally administered to mice. The amount in red clover is, however, of the level of 0.5–8 mg per gram dry matter, hence the quantity the animals ingest with the forage is not insignificant [10, 11].

Although a considerable amount of knowledge has been accumulated concerning the level of estrogenic activity in different forage species and at various stages in the harvesting and processing procedures, little is known so far about the metabolism of these compounds in the animal body.

Labelled genistein-4′-methylether has therefore been synthesised to enable the metabolic pattern of one of the estrogens to be followed, the C^{14} isotope being introduced into the $C_{(4)}$-position.

Genistein-4′-methylether has been synthesised by Yoder *et al.* [12] through a route involving condensation of anisaldehyde with rhodanine, alkaline cleavage of the condensation product to *p*-methoxyphenyl thiopyruvic acid, oximation, and dehydratization and decarboxylation of the oximino *p*-methoxyphenyl pyruvic acid to *p*-methoxybenzyl cyanide. This route cannot be used to prepare C^{14}-labelled *p*-methoxybenzyl cyanide when it is required to introduce the isotopic carbon into the cyano group by means of $KC^{14}N$, hence in our synthesis of $C^{14}_{(4)}$-labelled biochanin A, we prepared the radioactive nitrile by reacting *p*-methoxybenzyl

[1] Part I, Arkiv Kemi in press.

chloride with potassium cyanide in dry acetone, according to the recent description in Organic Syntheses [13].

As *p*-methoxybenzyl alcohol required for the preparation of *p*-methoxybenzyl chloride was not available, we investigated the reduction of anisaldehyde to the alcohol. Although reduction with $LiAlH_4$ in absolute ether gave a 60 % yield of the alcohol and with $NaBH_4$ in methanol a 30 % yield, the most convenient method giving very high yields was the crossed Cannizzaro reaction with formaldehyde [14] analogous to the preparation of *p*-methylbenzyl alcohol described in Organic Synthesis [15].

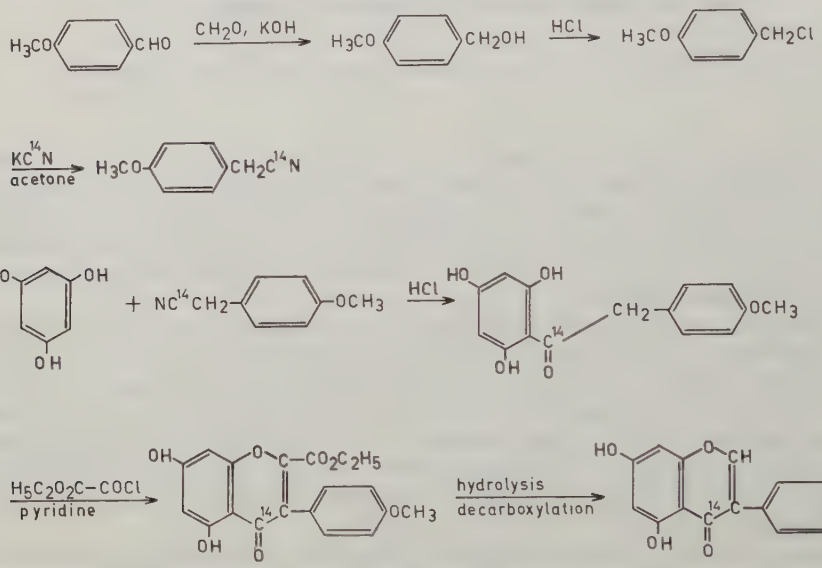

The further steps in the preparation of biochanin A were carried out according to [12, 16]. (C.f. reaction scheme.) We found that commercial phloroglucinol of good quality (colourless) only is to be used in order to obtain reproducible yields in the Hoesch synthesis, and anhydrous conditions are imperative; yields of 60–80 % of the desoxybenzoin can then be obtained. Ethyl oxalyl chloride [17] was used in the cyclization of the labelled ketone to the carbethoxy isoflavone, which was hydrolyzed to the carboxy acid without previous purification. This was decarboxylated by heating it to its m.p., giving $C^{14}_{(4)}$-labelled biochanin A.

The labelled isoflavone was purified by chromatography on a cellulose column, using 5 % potassium carbonate as the eluent. Its UV and IR spectra were identical with unlabelled biochanin A. The specific activity was 116 $\mu c/g$.

We consider the preparation of *p*-methoxybenzyl cyanide via the chloride to be the best method even for the synthesis of unlabelled biochanin A.

Experimental

p-Methoxybenzyl alcohol, Method I

119 g (0.88 moles) of anisaldehyde in 100 ml absolute ether was added at refluxing rate to a slurry of 9.5 g (0.25 moles) of lithium aluminium hydride in 300 ml of absolute ether. After refluxing for an additional 15 min, excess hydride was decomposed

with ethyl acetate and the reaction mixture poured into 250 ml of 2-*N* hydrochloric acid. The ether phase was separated, washed with water, dried over magnesium sulphate and fractionated. 71 g (60 %) of *p*-methoxybenzyl alcohol, b.p. 132–134°/12 mm Hg was obtained.

p-Methoxybenzyl alcohol, Method II

A solution made up from 204 g (1.50 moles) of anisaldehyde, 150 ml of 40 % formalin and 150 ml of methyl alcohol was added to 250 g of potassium hydroxide in 375 ml of methanol according to the description in [15]. 175 g (85 %) of *p*-methoxybenzyl alcohol b.p. 115–117° 6 mm Hg, which crystallized when stored in the refrigerator, was obtained.

p-Methoxybenzyl cyanide-C^{14}

4.3 g (0.028 moles) of *p*-methoxybenzyl chloride [14], 1.5 g of sodium iodide and 2.0 g (0.037 moles) of potassium cyanide containing 4 mg (1 mC) of C^{14}-marked potassium cyanide (from the Radiochemical Center, Amersham) was refluxed in 50 ml of dry acetone for 20 h. The mixture was then filtered, the precipitated salts washed with a little acetone and the acetone distilled off. The residual oil was taken up in benzene, washed with hot water, dried over sodium sulphate and distilled. 2.7 g (67 %) of labelled *p*-methoxybenzyl cyanide, b.p. 97°/0.3 mm Hg was obtained.

2,4,6-Trihydroxyphenyl p-methoxybenzyl ketone-C^{14}

The Hoesch synthesis was carried out according to [12] using 2.7 g (0.018 moles) of labelled *p*-methoxybenzyl cyanide, 2.4 g (0.018 moles) of anhydrous phloroglucinol in 20 ml of dry ether. 2.05 g (42 %) of crude ketone was obtained which gave a m.p. of 192–194° after one recrystallization from aqueous methanol.

2-Carboxy-5,7-dihydroxy-4'-methoxyisoflavone-4-C^{14}

0.75 g (0.0027 moles) of the labelled desoxybenzoin was dissolved in 3.8 ml of dry pyridine and 1.5 ml of ethyl oxalyl chloride [17] was added drop-wise, the temperature being maintained below 25°. After heating at 65° for 20 min, the mixture was cooled and poured into dilute hydrochloric acid. The aqueous phase was extracted with chloroform, the combined organic phases washed with 10 % hydrochloric acid, dried over magnesium sulphate and the chloroform distilled off *in vacuo*. The crystalline residue was hydrolyzed by refluxing it for four hours with 4 ml of 5 % aqueous sodium carbonate solution and 10 ml of acetone. The acetone was removed *in vacuo*, the solution cooled and carefully acidified with 2-*N* hydrochloric acid to pH 3, yielding 0.62 g (69 %) of the crude labelled acid, m.p. 270–276°.

5,7-Dihydroxy-4'-methoxyisoflavone-4-C^{14}

0.62 g of the acid was heated in a Pyrex test tube to 275° in an oil bath for 10 min, until the evolution of carbon dioxide had ceased. After cooling, the melt was dissolved in the minimum amount of boiling methanol and discoloured with charcoal. After adding an equal volume of water, 0.50 g (93 %) of labelled biochanin A crystallized out in pale yellow needles, m.p. 207–210°. It was further purified through

chromatography on a cellulose column using 5 % potassium carbonate as an eluent, m.p. 210–211°. Its IR and UV spectra (λ_{max} = 263 mμ, log λ = 4.56) and chromatography behaviour was the same as that of unlabelled biochanin A. The specific activity was 116 μC/g and was determined in a Ekco scintillation counter cooled to −20°.

SUMMARY

Biochanin A (5,7-dihydroxy-4′-methoxyisoflavone) labelled in the 4-position with C^{14} has been prepared in order to study the metabolism of the naturally occurring estrogenic isoflavones in the animal body.

ACKNOWLEDGEMENTS

The authors are indebted to Professor Sam Nordfeldt, Professor Nils Hellström and to Professor Arne Fredga, for all facilities put at their disposal.

Grants from "Reservationsanslaget till biträdeshjälp m.m. åt docent" to S. G. and from the *N.J.F. Committee on Forage Quality* to A. N. is gratefully acknowledged.

Institute of Animal Husbandry, Royal Agricultural College, and Chemical Institute, University of Uppsala, Uppsala. September 1960.

REFERENCES

1. Bennetts, H. W., Underwood, E., J. and Shier, F. L., Australian Vet. J. *22*, 2 (1946).
2. Schoop, G., and Klette, H., Fortpflanzung und Besammung der Haustiere *2*, 73 (1952).
3. New Zealand Dep. Agr. Rep. 37 (1950).
4. Ch'ang, T. S., *Nature 182*, 1175 (1958).
5. Hammond, J., Outlook on Agriculture *I*, 6 (1957).
6. Cheng, E. W., Yoder, L., Story, C. D., and Burroughs, W., Ann. N.Y. Acad. Sci. *61*, 652 (1955).
7. Bradbury, R. B., and White, D. E., J. Chem. Soc. *1951*, 3447.
8. Pope, G. S., Elcoate, P. V., Simpson, S. A., and Andrews, D. G., Chemistry & Industry *1953*, 1092.
9. Bickoff, E. M., Booth, A. N., Lyman, R. L., Livingston, A. L., Thompson, C. R., and DeEds, F., Science *126*, 969 (1957).
10. Pope, G. S., Dairy Sci. Abstr. *16*, 334 (1954).
11. Nilsson A., Kgl. Lantbrukshögskol. Ann. *26*, 19 (1959).
12. Yoder, L., Cheng, E. W., and Burroughs, W., Proc. Iowa Acad. Sci. *61*, 271 (1954).
13. Rorig, K., Johnston, J. D. P., Hamilton, R. W. and Telinski, T. J., Org. Syntheses *36*, 50 (1956).
14. Dankova, T. F., Evdomikova, L. G., Stepanov, I. I., and Preobrazhenskii, N. A., Zhur. Obshchii Khim. *18*, 1724 (1958).
15. Davidson, D., and Weiss, M., Org. Syntheses Coll. Vol. II, p. 590. New York 1943.
16. Baker, W., Chadderton, J., Harborne, J. B. and Ollis, W. D., J. Chem. Soc. *1953*, 1852.
17. Adickes, F., Brunnert, W., and Lücker, O., J. prakt. Chem. *130*, 163 (1931).

Tryckt den 30 januari 1961

Uppsala 1961. Almqvist & Wiksells Boktryckeri AB

ARKIV FÖR KEMI Band 17 nr 15

Communicated 1 June 1960 by Arne Fredga and Gunnar Blix

On the formation of racemic compounds in monomolecular films on water

I. 2-Hydroxyalkanes and certain derivatives

By Monica Lundquist

With 14 figures in the text

A monolayer study of racemic and optically active forms of *n*-eicosanol-2 and *n*-tetracosanol-2 and their acetates indicates that racemic compounds between enantiomeric molecules do exist in "two-dimensional" films. The results also show that an orderly arrangement of the molecules can exist within a compressible monolayer phase.

The study of the arrangement of molecules within monomolecular layers on water is difficult because no methods are at present available for direct crystallographic studies. Conclusions about the crystalline arrangement in condensed, solid films must therefore be drawn from indirect evidence. Condensed films of normal chain compounds with small polar groups show three different phases which all exist at areas per molecule so small that there is little doubt that the chains must be vertically oriented. It has been suggested [1] that the chain-packing in the so-called CS and S phases corresponds closely to that of the normal orthorhombic and the hexagonal high-temperature forms respectively of *n*-hydrocarbons in the three-dimensional state. The third form, LS, may be perhaps considered as a two-dimensional analogue of a liquid crystal [2].

However, the orientation or configuration of the chain in the case of compressible, condensed films is difficult to determine and has been the subject of much speculation. One view is that the long carbon chains are inclined with respect to the normal to the water surface and are successively brought into a more upright position as the area per molecule is diminished. Dervichian [3] has suggested the alternative explanation that the chains are helically coiled. Joly [4] has interpreted monolayer phase transitions in the following manner. He considers that over each compressible region (except the gas phase) the pressure-area (π–A) curve corresponds to a mixture of two phases whose composition is continuously altered. In regions of constant pressure (first-order transitions) the phases are immiscible. Abrupt changes in the compressibility occurs at points where only one phase is present.

Provided the chains are long enough, the compressible phases L_2 and L_2' observed for normal chain fatty acids [5] are solid. We must conclude, therefore, that the chains are fairly tightly packed. The question is then to determine whether we have a regular "crystalline" arrangement of tilted molecules or not in regions of

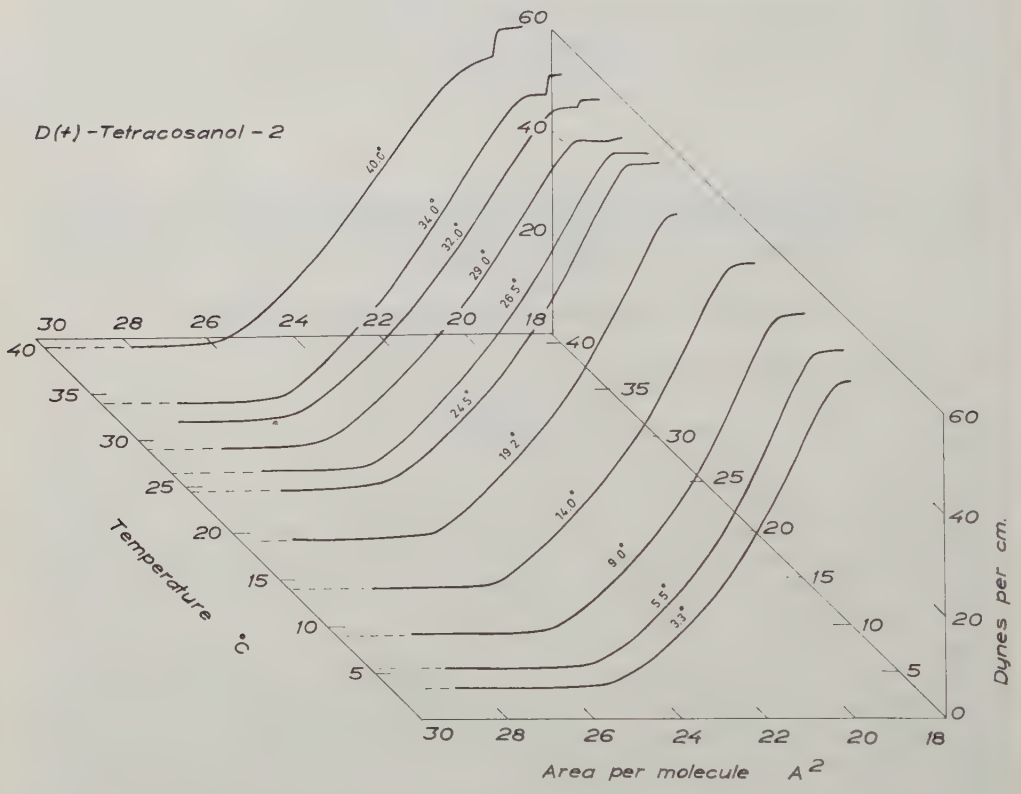

Fig. 1. π–A curves for D(+)-tetracosanol-2 at different temperatures.

high compressibility of the monolayers. It was thought possible to study this matter using suitable optically active long-chain molecules and the corresponding racemates. In the three-dimensional liquid state, racemic substances behave as mixtures (at least at temperatures above the freezing points). In the three-dimensional solid state, the enantiomers form racemic compounds which possess crystalline structures different from those of the enantiomers themselves [6]. If formation of racemic compounds is observed in the compressible region of a monolayer, this would suggest that the molecules in the compressible states are not necessarily oriented at random.

The monolayer data of the racemic and the optically active forms of *n*-eicosanol-2 and *n*-tetracosanol-2 and the derived acetates are compared in the present communication. An earlier monolayer study of *n*-eicosanol-2 has been reported [7], but it was subsequently found that part of the material used was impure [8].

Materials

The synthesis of the compounds studied has been described previously [8, 9].

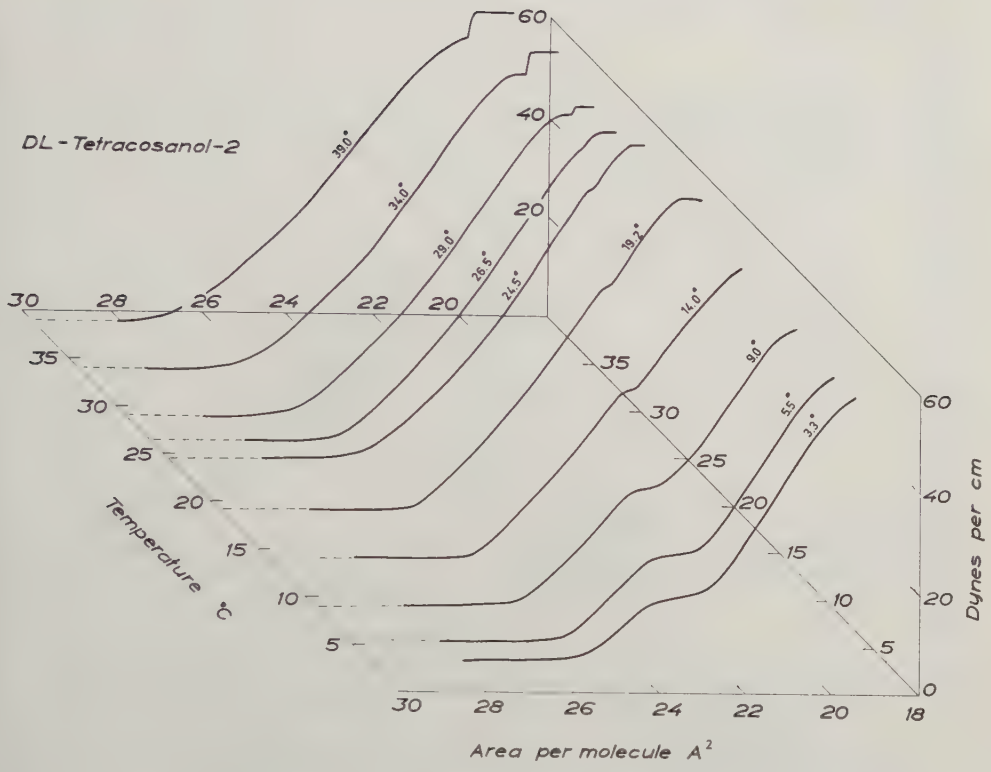

Fig. 2. π–A curves for DL-tetracosanol-2 at different temperatures.

Experimental

A recording surface balance of the horizontal type employing the "Mikrokator" principle [10] was used. Spreading was effected on a substrate of 0.01-N hydrochloric acid by an "Agla" micrometer syringe. Freshly distilled solvents were used.

A peculiar phenomenon was observed when spreading DL-tetracosanol-2 from a mixture of benzene and chloroform (9 : 1 by volume) at temperatures above 30°. During the compression, the solid monolayer was pressed out over the paraffined edges of the trough, causing an erroneous kink in the recording. This phenomenon was not observed when the spreading was performed from a solution of the DL-alcohol in light petroleum (b.p. 40–60°): ethanol (9 : 1 by volume). This solvent mixture was therefore employed in experiments at higher temperatures. Benzene was used as solvent for the alcohols in most of the experiments at lower temperatures.

Results

The enantiomers of tetracosanol-2 showed an identical behaviour (Fig. 1). The films are solid condensed over the whole temperature region studied (3.3°–40.0°). At 3.3°, the limiting area is 24.8 A^2/molecule and the monolayer collapses

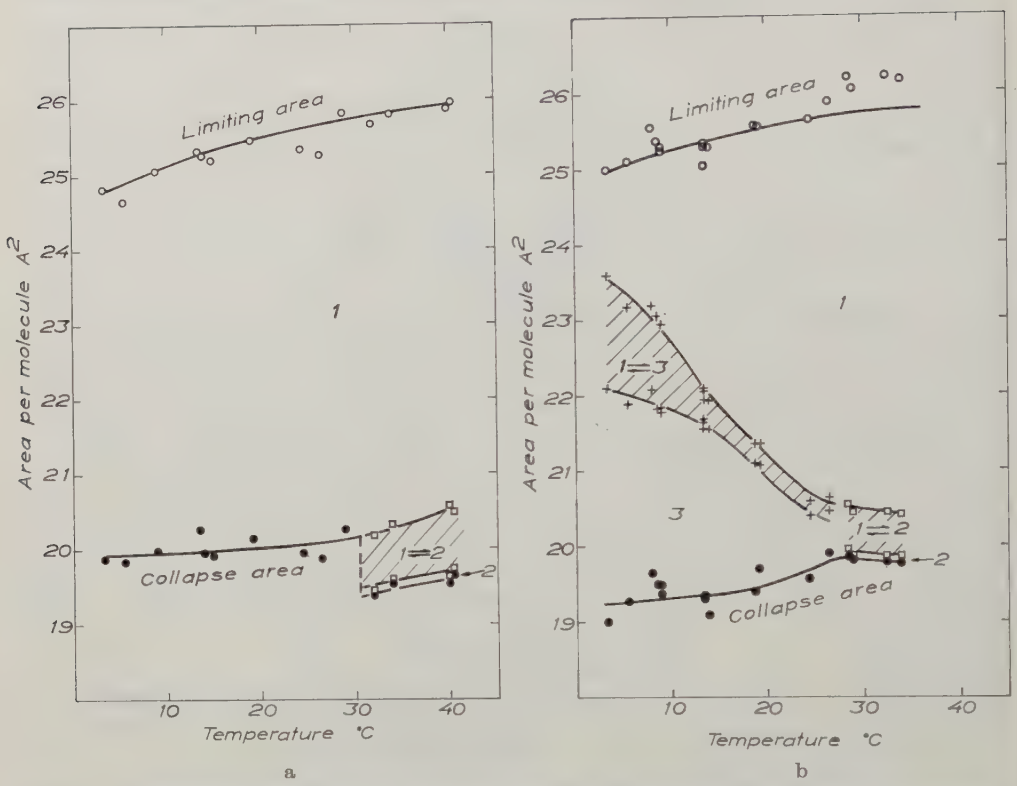

Fig. 3. Variation of certain characteristic areas with temperature for (*a*) D(+)-tetracosanol-2, and (*b*) DL-tetracosanol-2.

at about 60 dynes/cm and 19.9 A^2/molecule. The monolayer is comparatively compressible, but no phase transitions are observed.

The limiting area increases with rising temperature and is about 26 A^2/M at 40°. At 32°, a phase transition—apparently of the first order—to an incompressible S phase is observed at an area of 19.5 A^2/M and a pressure of 61 dynes/cm. The pressure at which the phase transition occurs decreases slightly with increasing temperature (Fig. 4 *a*).

A corresponding series of π–A curves for DL-tetracosanol-2 is shown in Fig. 2. The limiting areas for the DL-form are not significantly different from those of the enantiomers. The DL-compound shows a plateau in the π–A curve over the temperature range 3.3°–27.5°. The length of the plateau (see Fig. 3) becomes smaller and the pressure at which it occurs increases linearly with temperature as shown by the phase diagram reproduced in Fig. 4*b*.

The variation of the compressibility with temperature at a pressure of 23.4 dynes/cm is compared with that of the enantiomers in Fig. 5. The high-temperature, high-pressure phase (phase 2; the different phases are identified by numbers in Figs. 3 and 4) appears at a slightly lower temperature for the DL-form than for the enantiomers. The area at the point of collapse is about one A^2 lower

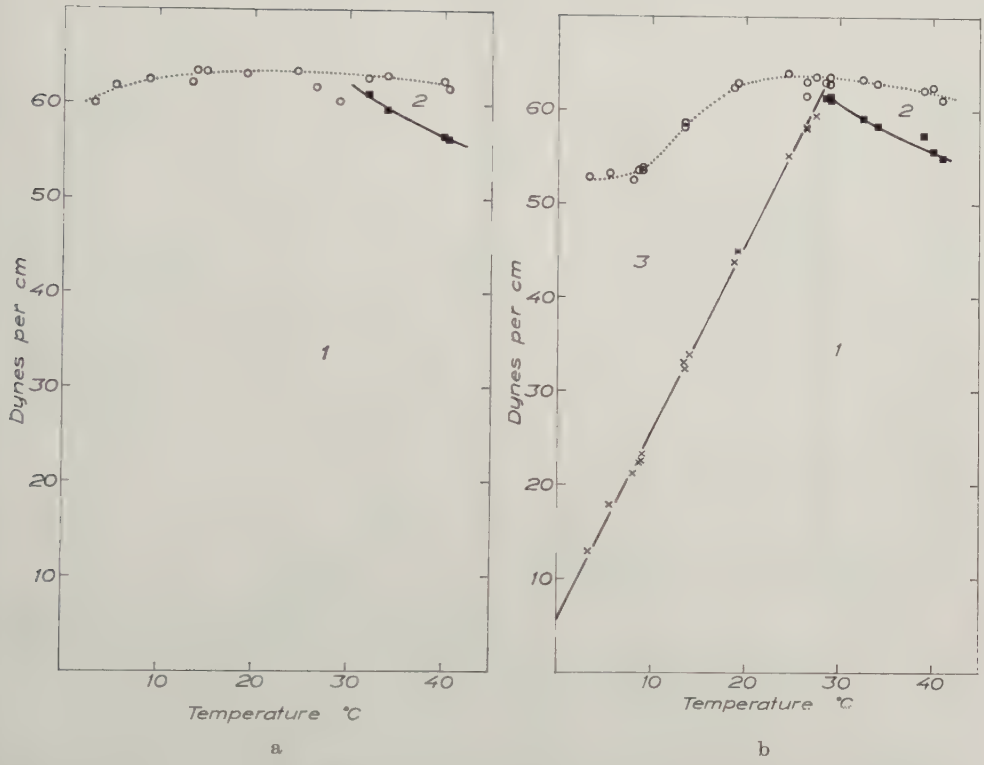

Fig. 4. π–t diagram for (*a*) D(+)-tetracosanol-2, and (*b*) DL-tetracosanol-2.

than for the enantiomers at temperatures below 26°. At temperatures of 32° and above, the π–A curves of the DL-compound are very similar in form to those of the enantiomers at corresponding temperatures.

Fig. 6 shows the phase boundary lines between phases 1 and 3 in monolayers of mixtures of the enantiomers of different composition. The transition $1 \rightleftharpoons 3$ is observed in mixtures containing from 10 to 50 % of one enantiomer. The area change involved becomes smaller as the ratio between the components deviates from 1:1.

Fig. 7 shows the $1 \rightleftharpoons 3$ transition temperature at a pressure of 38 dynes/cm as a function of the composition of the binary system of enantiomers. The relation appears linear from 10 to 45 % of one enantiomer. The temperature then falls about 1.5° for 47.5 % and rises again slightly for the 1 : 1 mixture. This finding seems real as the 45 % mixture at any rate has a higher transition temperature than the DL-alcohol synthesized from inactive starting material.

The phase diagrams for the racemic and enantiomeric forms of the lower homologue, eicosanol-2, are shown in Fig. 8. The $1 \rightleftharpoons 3$ phase transition for the racemic compounds involves only a small area change in the region available for study. A distinct $1 \rightleftharpoons 2$ transition is found for the racemic alcohol over the whole temperature range studied.

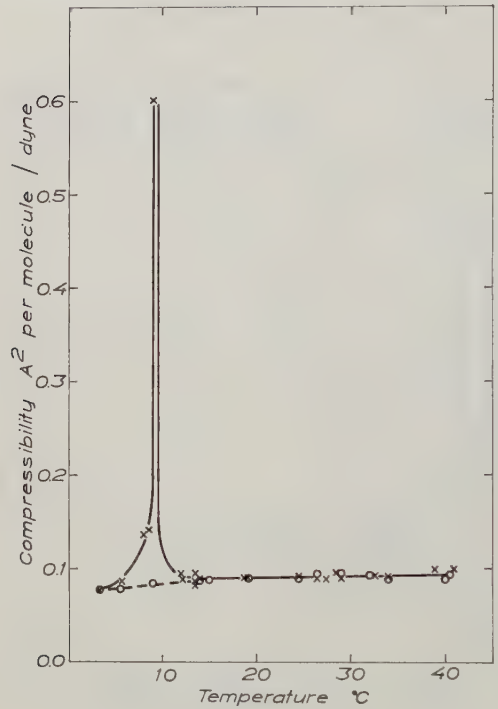

Fig. 5. Compressibility at a pressure of 23.4 dynes/cm of monolayers of D-(+)-tetracosanol-2 (O) and DL-tetracosanol-2 (×).

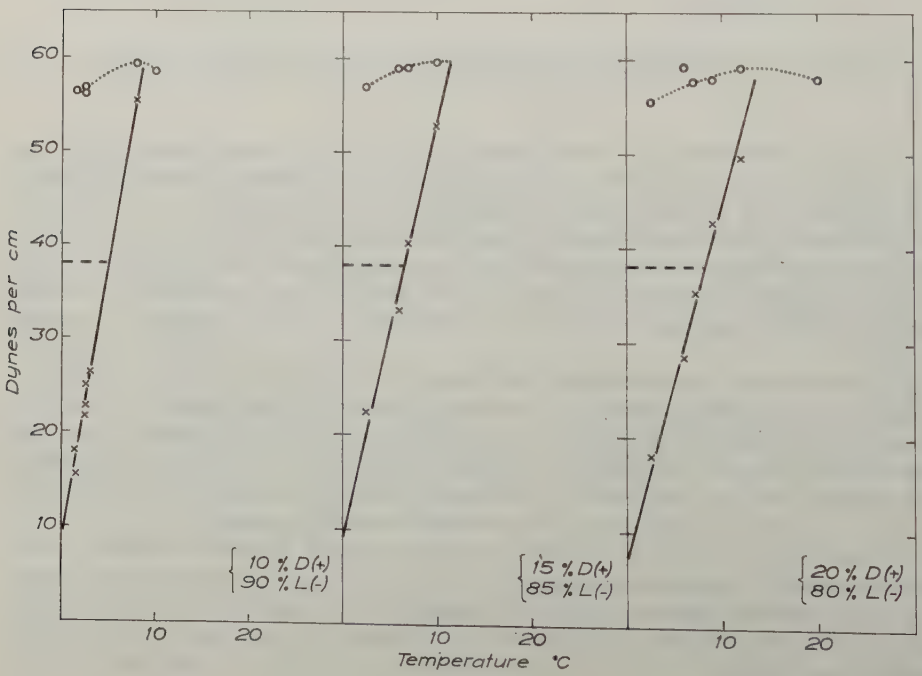

Fig. 6. Transition line 1⇄3 for different binary mixtures of D(+)- and L(−)-tetracosanol-2.

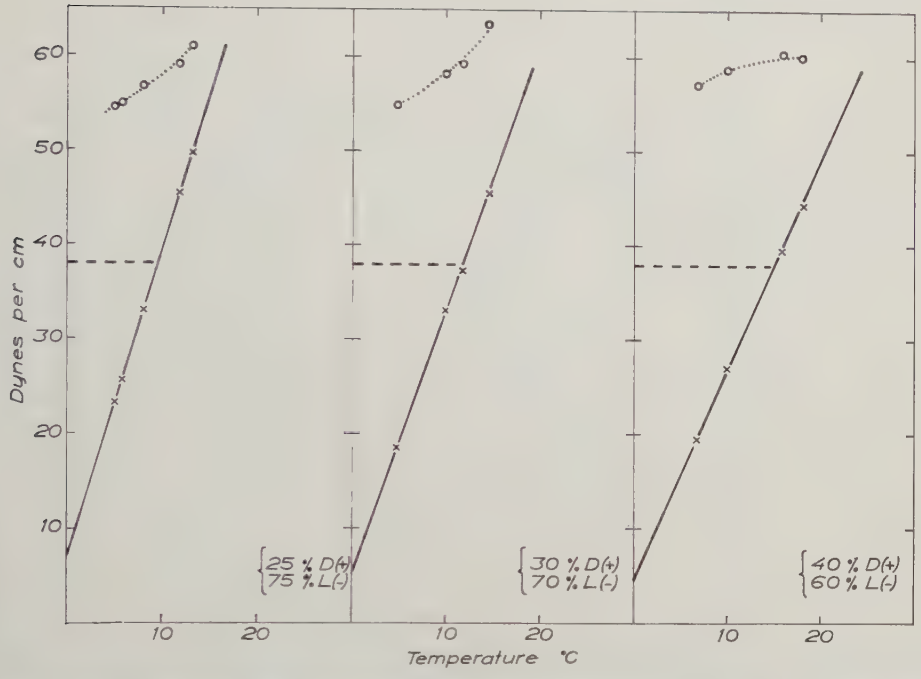

Fig. 6 (cont.). Transition line 1⇌3 for different binary mixtures of D (+)- and L (−)-tetracosanol-2.

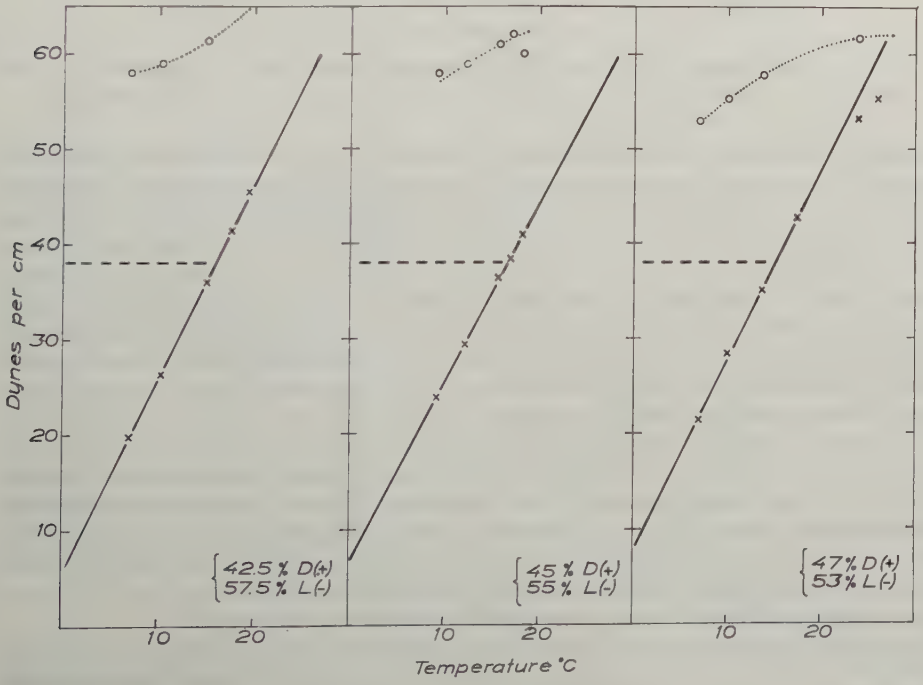

Fig. 6 (cont.). Transition line 1⇌3 for different binary mixtures of D (+)- and L (−)-tetracosanol-2.

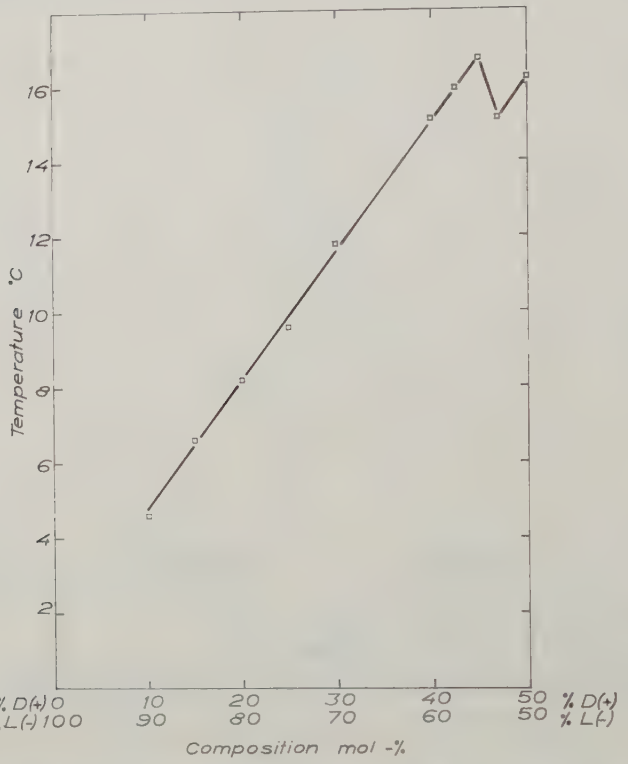

Fig. 7. The $1 \rightleftarrows 3$ transition temperature at a pressure of 38 dynes/cm as a function of the composition of the mixture for the binary system D(+)- and L(−)-tetracosanol-2.

The film behaviour of the acetates is shown in Figs. 9 and 10. The area per molecule at characteristic points in the π–A curves are plotted against temperature in Fig. 11, and the pressure-temperature relations are presented in the phase diagrams of Fig. 12. The enantiomers differ from the racemic form at temperatures below 27°. Above this temperature, monolayers of the enantiomers cannot be distinguished from those of the inactive form. The high temperature-small area form appears at a much lower temperature for the inactive form than for the enantiomers. The curves of the optically active forms also show a decrease in pressure immediately after the onset of the transition which is not observed in the rather diffuse transition of the DL-form.

The curves recorded with a barrier speed of 5 cm per minute do not represent the equilibrium pressures of the transition. If the barrier movement is stopped shortly after the transition region has been reached, the pressure will fall along an exponential curve to the equilibrium pressure (Fig. 13). After restarting the barrier movement, the pressure increases rapidly, however, until the dynamic equilibrium curve for the compression rate employed is reached.

Approximately five minutes is needed to attain equilibrium.

Figs. 13 *c* and *d* show that the same equilibrium pressure is reached both on compression and expansion of the monolayer of the D(+)-enantiomer over the

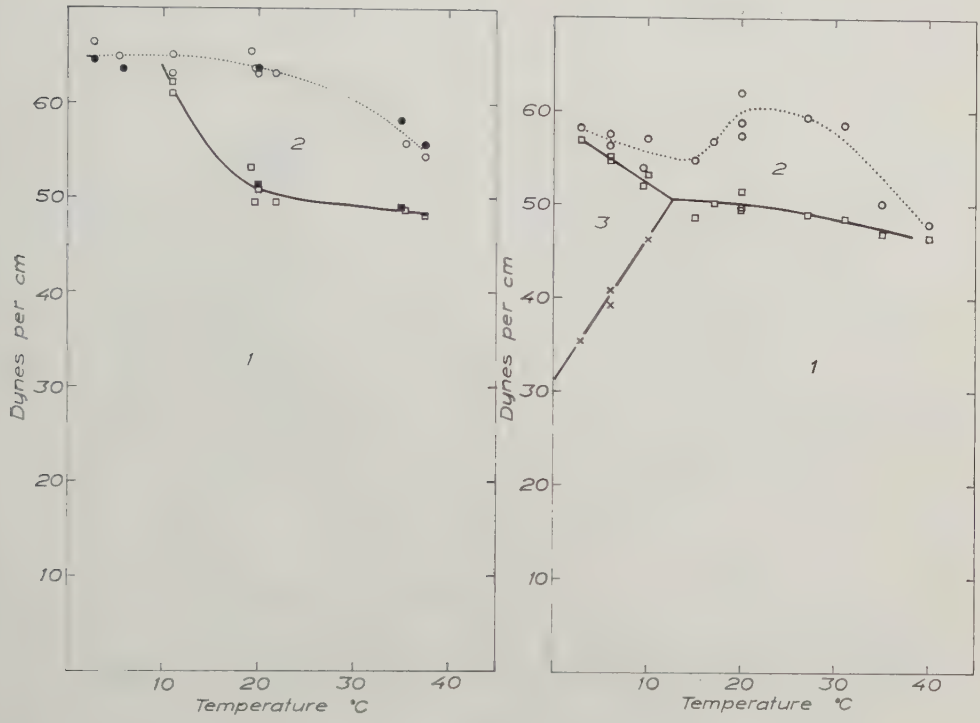

Fig. 8. π–t diagram for (*a*) D(+)-eicosanol-2 (○–□) and L(−)-eicosanol-2 (●–■), and (*b*), DL-eicosanol-2.

transition region. The curves shown were obtained at 18° when the equilibrium pressure is 17.5 dynes/cm. No change in pressure was recorded when the film was kept overnight at constant temperature.

The lowest area at which the monolayers of the DL-acetate is stable is 18.5 A^2 at 9.0°.

The phase diagram for the racemic acetate is very similar to those of long chain compounds with a small polar group at the end of the chain. CS and S phases and a typical CS⇌S transition thus occurs, and phases corresponding to the L_2 and LS types are also found. No distinct CS⇌S transition is observed for the enantiomeric acetates, but the collapse pressure of the film shows a maximum at 17°. A stability maximum is usually found at or near the upper end of a CS⇌S phase boundary line. The enantiomers show L_2 and LS phases over limited pressure regions at temperatures above 23°. A large-area, low-pressure condensed phase exists at low temperatures. The phase diagram of the enantiomeric acetates shows a much extended region of existence for this phase. The dashed phase-boundary line in the diagram marks the onset of the transition at a compression rate of 5 cm/min. As already pointed out, the transition is accompanied by considerable hysteresis, and the true equilibrium lines are shown full drawn in Figs. 12 *a* and *b*.

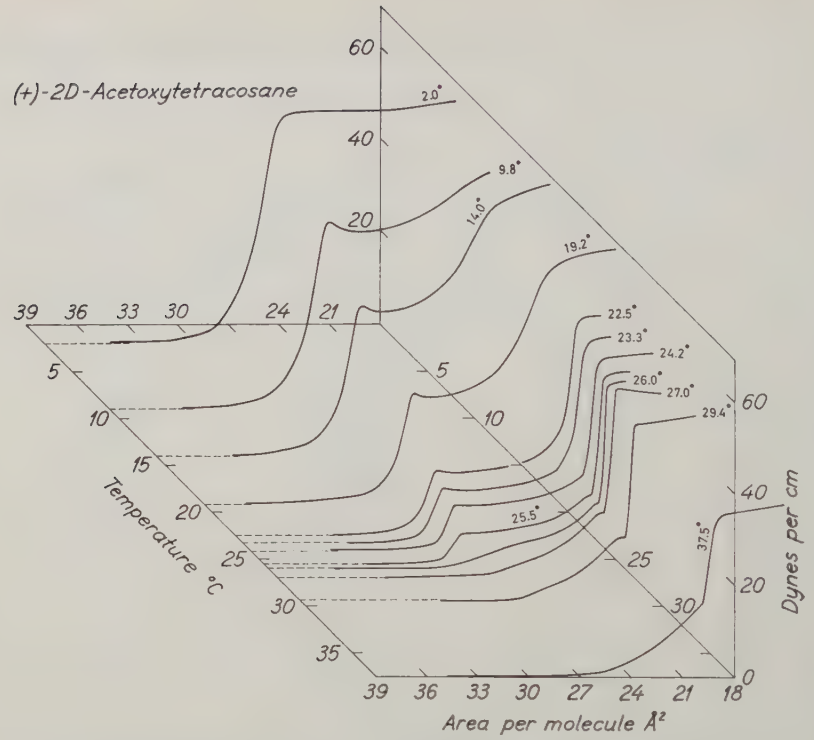

Fig. 9. π–A curves for acetate of D(+)-tetracosanol-2 at different temperatures.

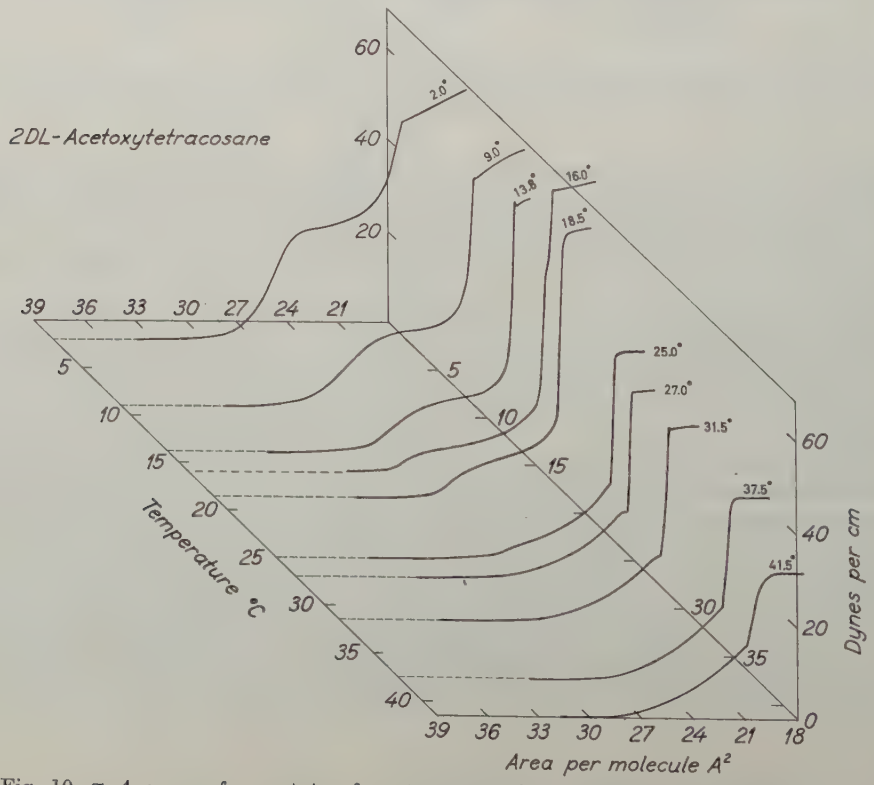

Fig. 10. π–A curves for acetate of DL-tetracosanol-2 at different temperatures.

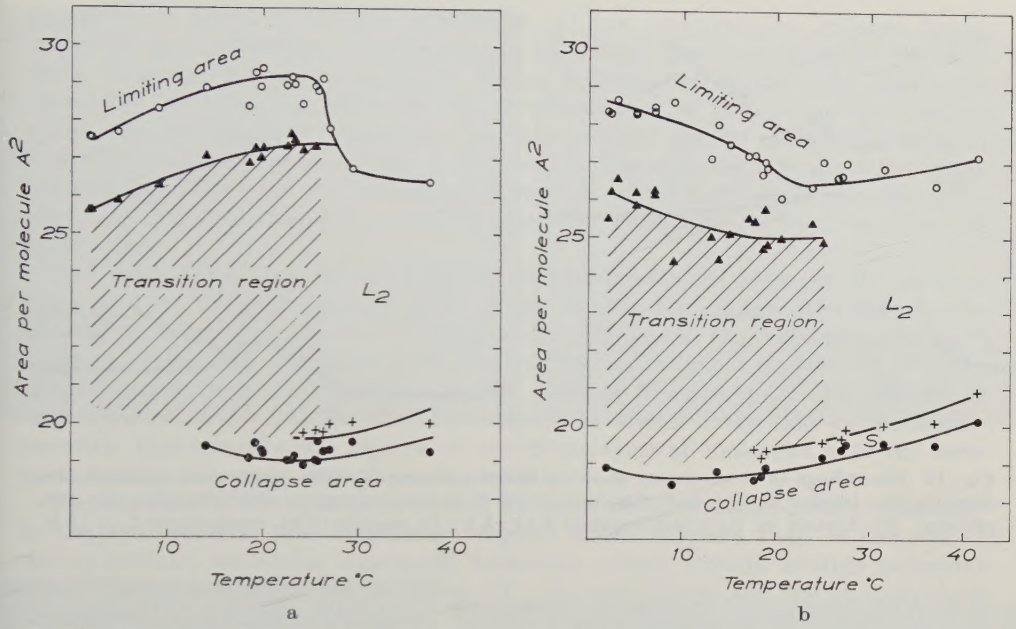

Fig. 11. Variation of certain characteristic areas with temperature for (*a*) acetate of D(+)-tetracosanol-2, and (*b*) acetate of DL-tetracosanol-2.

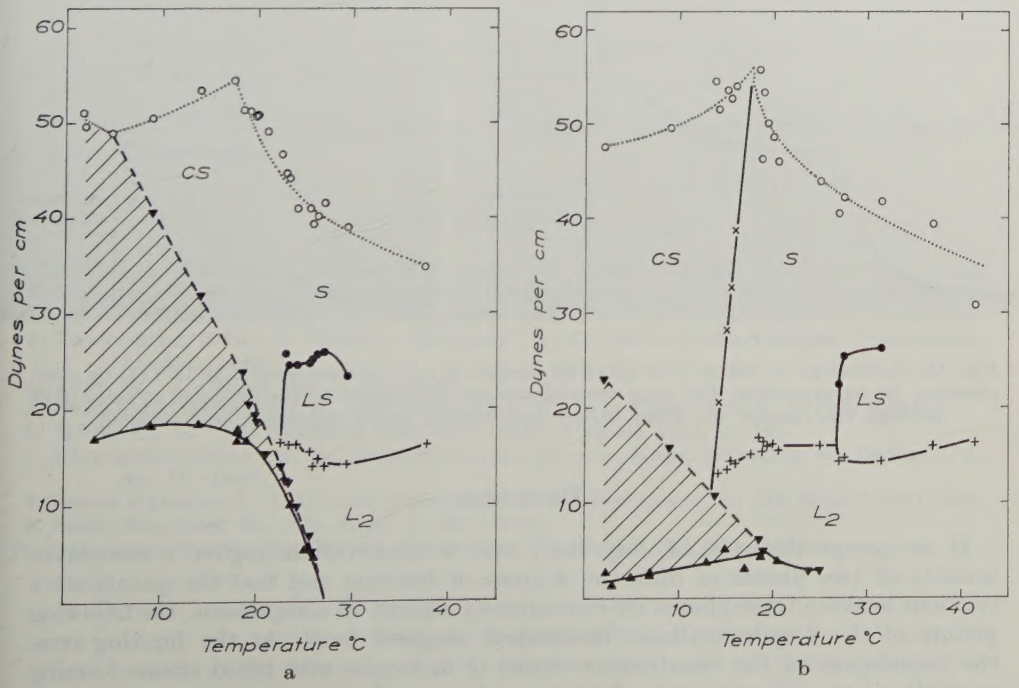

Fig. 12. π–t diagram for (*a*) acetate of D(+)-tetracosanol-2, and (*b*) acetate of DL-tetracosanol-2.

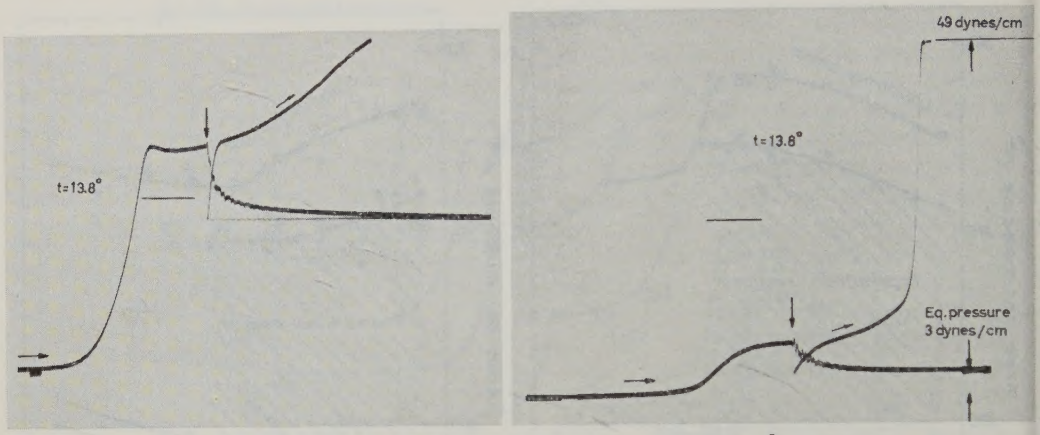

a b

Fig. 13. Recordings of π–A curves showing the attainment of static equilibrium pressure after stopping the barrier motion and the resumption of dynamic pressure after restarting the compression. (*a*) Acetate of D(+)-tetracosanol-2 at 13.8°; (*b*) acetate of DL-tetracosanol-2 at 13.8°.

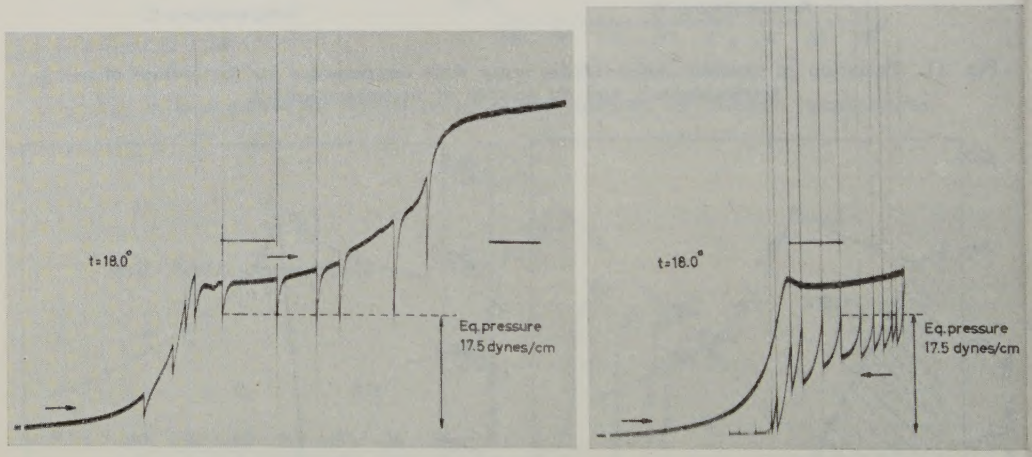

a b

Fig. 14. Recordings of static π–A curve for acetate of D(+)-tetracosanol-2 at 18°: (*a*) on compression; (*b*) on expansion. The long vertical streaks are caused by the exposure to stray light through the camera slit when barrier and camera drum movement was arrested.

Discussion

If we accept the view of Joly that, over a compressible region, a monolayer consists of two phases of different degrees of freedom and that the quantitative relations between these phases are continuously altered on compression, the following picture of the 2-hydroxyalkane monolayers suggests itself. At the limiting area, the monolayers of the enantiomers consist of molecules with tilted chains forming a single phase. Compression of the monolayer causes an increasing number of

molecules to adapt a vertical orientation. At low temperatures, collapse occurs before all molecules have been brought to an upright position. At higher temperatures, however, complete conversion occurs as indicated by the final first order transition. The limiting area and the compressibility of the low-pressure regions of the monolayers of the enantiomers and the DL-form are the same which suggests a similar molecular arrangement in this region. The simplest interpretation of the transition between the two compressible regions is that it is due to pair-wise combination; i.e., formation of a racemic molecular compound between enantiomeric molecules.

The diagrams of Figs. 6 and 7 appear consistent with the existence of a racemic compound in the high-pressure part of the compressible region. The enantiomers and the DL-tetracosanol-2 are not significantly different in the incompressible high-pressure region. On the other hand, the incompressible phase is observed over the whole temperature region studied in the case of DL-eicosanol-2 (Fig. 8), but it only appears above 10° for the enantiomers. It seems likely that in the incompressible high-temperature regions of the monolayers all molecules have the same arrangement; i.e., only one phase is present.

The acetates of the enantiomeric and DL-forms of tetracosanol-2 differ markedly in the low-pressure, low-temperature regions which suggests that, in the case of the DL-acetate, molecular compound formation occurs already at large molecular areas. Above a temperature of about 27°, the enantiomers and the DL-form show an identical monolayer behaviour.

ACKNOWLEDGEMENTS

The author is indebted to Mr. Klaus Serck-Hanssen for the supply of material used in this study and to Mrs. Karin Nilsson for skilled assistance.

Institute of Medical Chemistry, University of Uppsala, and Institute of Medical Biochemistry, University of Gothenburg.

REFERENCES

1. STÄLLBERG-STENHAGEN, S., and STENHAGEN, E., Nature *156*, 239 (1947).
2. HARKINS, W. D., The surfaces of solids and liquids and the films that form upon them, *in* "Colloid Chemistry" (J. ALEXANDER, ed.), Vol. V, p. 12. Reinhold, New York 1944.
3. DERVICHIAN, D. G., *in* "Surface Chemistry", p. 47. Butterworths Scientific Publications, London, 1949.
4. JOLY, M., J. Colloid Sci. *5*, 49 (1950).
5. STÄLLBERG-STENHAGEN, S., and STENHAGEN, E., Acta Chem. Scand. *3*, 1035 (1949).
6. HÄGG, G., *in* "The Svedberg 1884 30/8 1944", Uppsala 1944, p. 140.
7. STÄLLBERG-STENHAGEN, S., and STENHAGEN, E., Ark. Kemi, Mineralogi och Geologi *18A*, No. 19 (1944).
8. SERCK-HANSSEN, K., STÄLLBERG-STENHAGEN, S., and STENHAGEN, E., Ark. Kemi *5*, 203 (1953).
9. SERCK-HANSSEN, K., Ark. Kemi *8*, 401 (1955).
10. STÄLLBERG-STENHAGEN, S., and STENHAGEN, E., Nature *159*, 814 (1947).

Tryckt den 30 januari 1961

Uppsala 1961. Almqvist & Wiksells Boktryckeri AB